Technical Report

TR-06-15

Development of Landscape Dose Factors for dose assessments in SR-Can

Rodolfo Avila, Per-Anders Ekström
Facilia AB

Ulrik Kautsky, Svensk Kärnbränslehantering AB

August 2006

Svensk Kärnbränslehantering AB
Swedish Nuclear Fuel
and Waste Management Co
Box 5864
SE-102 40 Stockholm Sweden
Tel 08-459 84 00
+46 8 459 84 00
Fax 08-661 57 19
+46 8 661 57 19

Development of Landscape Dose Factors for dose assessments in SR-Can

Rodolfo Avila, Per-Anders Ekström
Facilia AB

Ulrik Kautsky, Svensk Kärnbränslehantering AB

August 2006

Keywords: Modeling, Radionuclides, Landscape, Dose, SR-Can, Safety assessment, Biosphere, Forsmark, Laxemar.

A pdf version of this document can be downloaded from www.skb.se

Abstract

As a part of SKBs assignment to provide safety assessments for a potential future release of radionuclides from a deep repository, SKB has analysed several possible ways to calculate to dose to human. In previous safety assessments Ecosystem Dose Factors (EDFs), were derived from estimates of doses to the most exposed group resulting from constant unit radionuclide release rates over 10,000 years to various ecosystem types, e.g. mires, agricultural lands, lakes and marine ecosystems. A number of limitations of the EDF approach have been identified. The objectives of this report is to further develop the EDF approach, in order to resolve the identified limitations, and to use the improved approach for deriving Dose Conversion Factors for use in the SR-Can risk assessments. The Dose Conversion Factors derived in this report are named Landscape Dose Factors (LDFs). It involves modelling the fate of the radionuclides in the whole landscape, which develops from a sea to a inland situation during 20,000 years. Both candidate sites studies in SR-Can, Forsmark and Laxemar, are included in the study.

As a basis for the modelling, the period starting at the beginning of the last interglacial (8,000 BC) is used, over which releases from a hypothetical repository were assumed to take place. For the present temperate period, the overall development of the biosphere at each site is outlined in a 1,000 year perspective and beyond, essentially based on the ongoing shoreline displacement and the understanding on the impact this has on the biosphere. The past development, i.e. from deglaciation to the present time, is inferred from geological records and associated reconstructions of the shore-line. For each time step of 1,000 years, the landscape at the site is described as a number of interconnected biosphere objects constituting an integrated landscape model of each site. The water fluxes through the objects were estimated from the average run-off at the site, the areas of the objects and their associated catchment areas. Radionuclides in both dissolved and particulate forms were considered in the transport calculations. The transformation between ecosystems (every 1,000 years) was modelled as discrete events, by substituting one model by another.

All radionuclides of relevance for safety assessments, except for C-14, are included in the study. For radionuclides with decay chains, the contribution of the daughter nuclides is also considered in the dose assessments. Predictions of the long-term distribution in the landscape resulting from unit continuous release rates with groundwater discharges are presented for each studied radionuclide. In the main calculation variant, the releases are assumed to start at the beginning of the simulation period; and distributed between the landscape objects according to release fractions obtained from analyses of the results of the hydrological modelling. Additionally, to study the effect of the start time and location of the releases, a series of complementary simulation variants are carried out in different environmental media, comprising soils, waters and sediments. The predictions of the distribution of the radionuclides in the landscape per unit release rates are used to derive time-dependent dose conversion factors for each landscape object and for the whole landscape.

To ensure that the dose to a representative member of the public in the population is identified, calculations of the dose rate are made for population groups taken to occupying a single landscape object and obtain all their resources from that object. The number of individuals that can be sustained by a landscape object is calculated for each time period by dividing the potential food production by the yearly food demand of a reference adult person. The average Dose Conversion Factors, i.e. the LDFs, for different groups in the landscape, including the most exposed group are derived, which take into account the distribution of radionuclides in the whole landscape. For each radionuclide derived maximum LDF values are given for the two studied sites, Forsmark and Laxemar. The derived maximum LDF values estimate effective dose rates to the most exposed population group per unit release of activity from a repository. By multiplying these factors by estimates of the release rates to the biosphere, it is possible to obtain conservative estimates of the doses to most exposed groups.

A summary of the sensitivity analysis and uncertainties of the models is also presented in the report. These preliminary studies show that the effect of the distribution coefficient (K_d) on the maximum values of the dose rates was different in different periods with practically no effect in some periods and pronounced effects in other periods, particularly in periods when ecosystem shifts occur. The maximum LDF values were obtained at different time periods for the different cases included in the sensitivity analyses, with values differing by a factor of 10 or more. The topography, which affects the drainage area, the hydrology, the sedimentation environment and the size of the biosphere objects, is also an important factor. During the sea period, the fraction of accumulation bottoms and the water velocity in the bottom sediments has the largest effect on the retained fraction of the releases.

A number of limitations of the previous EDF approach, have been overcome in deriving the LDFs in the study presented here. In particular, the connection of the different ecosystems within the landscape is considered and the fluxes of radionuclides through these interconnected ecosystems are taken into account. This also allows estimation of the significance of simultaneous exposures to several ecosystems and other relevant interactions between ecosystems, such as the use of a lake for irrigation of agricultural lands. A major improvement, as compared to previous approaches, relates to the fact that now temporal changes in the biosphere driven by land rise, ecosystem succession, climate change, etc are explicitly addressed. These changes usually are difficult to model when considering generic ecosystems in isolation, since the relevant processes act on a landscape scale. They can, however, be consistently taken into account based on the dynamic landscape model presented here using the data obtained from the site investigation programmes.A further benefit of the dynamic landscape model is that important exposure parameters, such as the size of exposed groups and drainage areas, can be consistently estimated within the landscape model and do not have to be treated as generic input parameters to the modelling, as in the case of considering isolated ecosystems.

Sammanfattning

Som ett led i säkerhetsanalysen kring djupförvar av högaktivt avfall, analyserar SKB olika möjligheter för beräkning av dos till människa vid ett eventuellt utsläpp av radionuklider. I tidigare säkerhetsanalyser (presenterat i SR 97 och SR-Can Interim), användes olika utsläppsscenarier för att beräkna årlig dos till människa samt identifiera den grupp som kan förväntas vara mest exponerad vid ett radioaktivt utsläpp, genom att multiplicera utsläppsmängder med tidigare framräknade doskonverteringsfaktorer. Dessa omvandlingsfaktorer har räknats fram genom att analysera utsläpp till enstaka biosfärsobjekt (ett homogent ekosystem av en given storlek) inom olika typer av ekosystem, t ex myrar, jordbruksmark. Det har dock visat sig att denna beräkning (EDF) har vissa begränsningar. Exempelvis tas liten hänsyn till de radionuklider som inte stannar i ett biosfärsobjekt, det är svårt att uppskatta exponering av nuklider som förekommer i flera biosfärsobjekt och relationen mellan objekt, och det är svårt att modellera spatiala och temporala förändringar i ekosystemen på grund av bland annat landhöjningen. Syftet med den här rapporten är att förbättra EDF-analysen genom att lösa dessa problem och därigenom kunna ge ett mer tillförlitligt underlag för att beräkna doskonverteringsfaktorer för säkerhetsanalysen som presenteras i SR-Can. I denna rapport beräknas doskonverteringsfaktorer för hela landskapet och kallas landskapsdosfaktorer (LDF). Båda kandidatområdena, Forsmark och Laxemar, är inkluderade i denna studie.

Rapporten presenterar en landskapsmodell med fokus på effekterna av utsläpp av radionuklider under en mellanistid. Perioden för modelleringen startar istiden dvs år 8,000 f kr, i nuvarande mellanistid och går framåt i tiden med tusen års intervaller till ca år 10,000 e kr. Tidsintervallet är valt med avseende på effekter av landhöjningen samt förändringar i enskilda biosfärsobjekt. Genom att använda denna typ av modellering kan påverkan av utsläppen även beräknas för framtida mellanistider, men fungerar även som riktlinjer för att beräkna effekter av utsläpp under perioder med andra typer av klimat. För vart tusende år beskrivs landskapet för Forsmark respektive Laxemar med hjälp av de olika biosfärsobjekten inom varje ekosystem. Transporten av radionuklider mellan biosfärsobjekt antas vara direkt proportionella mot vattentransporten genom uppströms belägna biosfärsobjekt. Både radionuklider i partikelform och upplösta är med i transportberäkningarna.

Alla radionuklider relevanta för säkerhetsanalysen, utom C-14, är inkluderade i studien. För radionuklider med sönderfallkedjor beräknas även dosen av dotternukliderna. För varje radionuklid görs framtida projektioner av dess utbredning i landskapet, baserat på beräkning av grundvattenflödet. I den centrala beräkningen antas utsläppet starta i början av simuleringsperioden och radionuklidernas fördelning i landskapet kommer följaktligen att vara ett resultat av den hydrologiska modelleringen. Som ett komplement till detta har även andra kompletterande simuleringar gjorts, där andra media har använts, t ex jord och sediment. Genom att göra säkrare uppskattningar av mängden radionuklider i landskapet baserat på utsläppsmängder, är det möjligt att konstruera tidsberoende dosekonvertingsfaktorer för varje enskilt biosfärsobjekt och för hela landskapet.

För att beräkningen av dos till människa ska vara representativ, är beräkningarna gjorda baserat på den gruppen människor som bor och tar sina resurser från det specifika biosfärsobjektet/ekosystemet. Detta gör det möjligt att uppskatta, inte bara dos till en person som nyttjar ett specifikt biosfärsobjekt, utan även antalet personer som ett objekt kan försörja. Detta beräknas genom att dela potentiell produktion av föda med den årliga förbrukningen av föda hos en referensperson (c 110 kg C/år). Detta gör det möjligt att beräkna LDFs för olika grupper av människor i landskapet genom att ta hänsyn till distributionen av radionuklider. I rapporten presenteras maximala LDFs för Forsmark och Laxemar.

En sammanställning av sensitivitetsanalyserna och osäkerheter presenteras också i rapporten. Slutvärdena av analyserna visar hur stor del av utsläppet som finns kvar i ekosystemet; koncentration i jord, vatten och sediment samt stråldosen. Parametrarna med störst påverkan på koncentrationen i de olika objekten samt stråldosen kan också identifieras. Preliminära resultat visar att distributionskoefficienten för maximalt LDF värde skiljde sig mycket mellan perioder, speciellt under perioder med ekosystemskiften. Det var också skillnader i distributionen mellan olika radionuklider, med faktor 10 eller mer. En vikig faktor som påverkar analyserna är topografin, vilket i sin tur påverkar avrinningsområdet, hydrologin, sedimentationen och biosfärsobjektets storlek. Ackumulation under vatten verkar dock ha liten effekt på maximala doser och LDF-värden.

Mycket av begränsningarna med EDF-analyserna för att bestämma doskonverteringsfaktorer kan elimineras vid användandet av LDFs. Detta beror främst på att förbindelsen mellan olika biosfärsobjekt beaktas och att flödet av radionuklider mellan dessa objekt kan beräknas. Det ger också möjligheter att uppskatta exponering i flera ekosystem samtidigt, t ex bevattning av jordbruksmark med kontaminerat sjövatten. LDFs gör det också möjligt att studera temporala förändringar i biosfären som drivs av exempelvis landhöjning, succession och klimatförändring, vilka normalt är svåra att studera över så stora ytor som ett landskap. Dessa förändringar i tiden kan läggas in i modellen kontinuerligt, vilket gör modellen dynamisk både i tid och rum. En annan fördel är att exponeringsparametrar, så som storleken på gruppen individer som exponeras eller avrinningsområde, tillåts förändras kontinuerligt i modellen beroende på aktuella data från platsundersökningsprogrammet.

Contents

1 Introduction

This report is subreport to the safety assessment SR-Can /SKB 2006d/, parts of this report are summarised in /SKB 2006ab/.

In previous safety assessments of the KBS-3 concept for geological disposal of HLW, SR 97 /SKB 1999/ and SR-Can Interim /SKB 2004/, annual doses to man resulting from different release scenarios were calculated by multiplying the release rates to the biosphere by pre-calculated Dose Conversion Factors. The Dose Conversion Factors, called Ecosystem Dose Factors (EDFs), were derived /Bergström et al. 1999/ from estimates of doses (the term dose is generally used in this report to mean annual effective dose, being the sum of annual effective dose from external exposure and annual committed effective dose from internal exposure) to the most exposed group resulting from constant unit radionuclide release rates over 10,000 years to single biosphere objects, i.e. single homogeneous ecosystems of a given size Various ecosystem types were considered, including mires, agricultural lands, lakes and marine ecosystems. Additionally, Dose Conversion Factors for releases to wells were also calculated. The highest EDF values were obtained for releases either to mires or wells, depending on the radionuclide. These EDF values were used for the dose calculations in the safety assessments. A number of limitations of the EDF approach have been identified in previous reviews of the safety assessments and by the authors of this report. These are summarised below:

- The fate of the radionuclides that are not retained in the ecosystem is not explicitly considered. This is despite the fact that generally only a small fraction of the radionuclides entering an ecosystem is retained in each ecosystem considered. It could be argued that the radionuclide fluxes from an ecosystem will be often lower than the fluxes entering this ecosystem and thus the corresponding release to downstream ecosystems will be lower. However, consideration has to be given for in-growth in the upstream ecosystem, e.g. Ra-226 from U-238. Also, accumulation of radionuclides in upstream ecosystems may lead, temporarily, to higher downstream releases. Moreover, downstream ecosystems may receive simultaneous radionuclide inputs from several upstream ecosystems. Furthermore, a lower flux does not necessarily corresponds to a lower dose, as the dose depends also on the bioaccumulation factors in the ecosystem and the degree of exposure of humans to environmental media.
- By considering each ecosystem in isolation, it is difficult to estimate simultaneous exposures to several ecosystems and other relevant interactions between ecosystems. For example, a lake can be used for irrigation of agricultural lands.
- The EDF approach does not address temporal changes in the surface biosphere driven by factors such as land rise, ecosystem succession and climate change. These changes usually are difficult to model when considering generic ecosystems in isolation, since the relevant processes act on the landscape scale, i.e. involving several biosphere objects.
- When considering generic isolated ecosystems, it is difficult to justify the values used for spatial dependent parameters. Examples are the area of the ecosystems and their drainage areas. It is also difficult to estimate the size of the exposed groups, which will depend on which ecosystems contribute to the exposure and their area.

The objective of the work described in this report was to further develop the EDF approach, in order to resolve the above mentioned limitations. Other approaches proposed in the literature are also based on generic biosphere models (as the BIOGEM model described in /Chen et al. 2004/), developed on the basis of the IAEA BIOMASS reference biosphere methodology /BIOMASS 2003/, and do not resolve these limitations, at least for situations with a transient biosphere, as it is the case for the situations considered here.It was decided that for the situations considered in this study, the above mentioned problems could be solved by modelling the fate of the radionuclides in the whole affected landscape, taking into consideration the temporal transformations in the ecosystems and the interactions between ecosystems.

Hence, a model of the long-term distribution and accumulation of radionuclides in the landscape, described in Chapter 2, was implemented. The model was derived from the landscape models developed in SR-Can for Forsmark /SKB 2006a/ and Laxemar /SKB 2006b/. Simulations using the radionuclide landscape model were then carried out for generating projections (Chapter 3) of the environmental concentrations resulting from unit radionuclide release rates with groundwater discharges. The predictions of radionuclide concentrations for unit release rates were used for estimating dose rates for unit release rates (Dose Factors) to different potentially exposed groups (Chapter 4). Finally, the Dose Factors to be used in SR-Can for evaluating compliance with the criteria established in the Swedish regulations /SSI 2005/ were selected (Chapter 5). The Dose Factors derived in this report are named Landscape Dose Factors (LDF), to reflect the difference in approach to that adopted in deriving the Ecosystem Dose Factors (EDFs) used in previous assessments.

The Landscape Dose Factors derived based on this approach are believed to provide conservative estimates for impacts from potential releases of radionuclides from a HLW repository at some point in the future. Thus, these dose factors can be used to assess compliance with regulatory dose criteria for a HLW disposal facility at the sites considered.

This report intends to provide a traceable and sufficiently detailed description of the work carried out in derivation of the LDFs, so that it can be evaluated by the reader. To achieve this, each section of the report starts with a description of the applied methods, including references, where needed, to other publications where more detailed descriptions of the methods are given. In each section, the results obtained for the two sites assessed in SR-Can, Forsmark and Laxemar, are presented. The report also contains a discussion on the parameter sensitivity of the models applied, the uncertainty of the derived LDFs and a comparison of the LDF values obtained for the studied sites and for different climatic conditions.

The report concludes with a summary of the results. The practical applicability of the LDF obtained is discussed and suggestions for the further development of adequate landscape models are discussed.

2 Modelling the long-term transport and accumulation of radionuclides in the landscape

In long-term assessments of the transport and accumulation of radionuclides potentially released to the biosphere, it is necessary to take into account that releases to the biosphere may occur thousands of years into the future, by which time today's biosphere will have undergone considerable changes. In the SR-Can assessments, a model reconstruction of the last glacial cycle, the Weichselian, from 120,000 years ago to the present is chosen as the reference evolution /SKB 2006c/. The evolution of the landscape is mainly affected by the evolution of climate-related conditions, such as shore-line migration, the development of permafrost and ice sheets, and by changes in the climatic conditions. On the basis of possible conditions and processes relevant for repository safety, three characteristic *climate domains* that can be expected to occur in Sweden in a 100,000-year time perspective have been identified: temperate, permafrost and glacial.

Regardless of the evolution of the repository, a realistic, site-specific handling of the biosphere is likely to yield very low doses during most of the assessment period for several reasons. Due to expected shore-line displacements over a glacial period, coastal sites are likely to be submerged for extended periods of time /SKB 2006c/ leading to both stagnant groundwater and potentially a considerable dilution of any releases from the geosphere. There is also a possibility of accumulation in bottom sediments, which, as long as the sediments are submerged, retards the release of radionuclides. Glacial conditions, meaning that the site is covered by ice, will, for obvious reasons, lead to very low, if any, doses. The highest doses are expected for the periods when the site is not submerged during the interglacial period (temperate domain). For this period, a model of the temporal evolution of the potentially affected landscape at Forsmark and Laxemar is presented in /SKB 2006ab/. On the basis of this model, a model of the long-term transport and accumulation of the radionuclides in the landscape, described in this section, was developed. The assessments for other climatic domains (permafrost and glacial periods) and for a variant pattern of climatic changes (greenhouse conditions leading to a protracted interglacial episode) were carried out as modifications of this model.

The developed model focuses on changes in the landscape and impacts of radionuclide releases during interglacial periods, since the highest annual doses to humans will arise during these periods. As a basis for the modelling, the period starting at the beginning of the last interglacial (8,000 BC) was used, over which releases from a hypothetical repository were assumed to take place. In the following, the references to times correspond to the current interglacial period, even though releases can potentially occur in future interglacial periods.

Modelling of radiological impact on this basis was assumed to be also applicable for estimation of the annual doses resulting from potential releases from a repository in future interglacial periods. It was further assumed that resulting annual doses for this basic calculation will provide conservative estimates of radiological impacts for the case that releases do not start at the beginning of an interglacial period, but that first releases occur at some point in time during such a period. This assumption is reasonable since, in this case, the accumulation period will be shorter. The above assumptions explain why the full period from deglaciation was studied.

2.1 Model of the temporal development of the biosphere during an interglacial period

The temporal development of the biosphere during an interglacial period is handled by setting up biosphere models for the succession of situations that was projected to occur. These are based on various sources of information. A digital elevation model (DEM) is a central source of information for predicting or retrodicting the locations, characteristics and evolution of past and future Running Waters, Lakes, Mires, Seas and surface hydrology. Information on the regolith (quaternary maps, marine geological maps, lake sediment characteristics and soil profiles) was used for predicting the potential for future agricultural land use or forestry /SKB 2006ab/.

For the present temperate period, the overall development of the biosphere at the site is outlined in a 1,000 year perspective and beyond, essentially based on the ongoing shore-line displacement and the understanding of the impact this has on the biosphere data /SKB 2006ab/. The past development, i.e. from de-glaciation to the present time, is estimated from geological records and associated reconstructions of the shore-line.

For each time step of 1,000 years, the landscape at the site is described as a number of connected biosphere objects constituting an integrated landscape model for each site. The choice of 1,000 years as time step for the modelling was motivated by the available time resolution of the maps used in the model development. The descriptions of the biosphere objects are based on the ecosystem models and on site data /SKB 2006ab/. The two main categories of ecosystems, aquatic and terrestrial, are further subdivided into a number of more specified ecosystem types. Aquatic ecosystems comprise marine systems, lakes and running water and the terrestrial ecosystems considered were agricultural land, mire and forest.

Through hydro-geological modelling /SKB 2006ab/, flow and transport pathways from different locations within the repository were analysed to estimate the locations at which discharges of radionuclides to the surface environment could occur (see example for Forsmark in Figure 2-1). This allowed to identify the potentially affected area of the landscape, which is defined by biosphere objects that can potentially receive direct releases and objects downstream of those, as determined by the topography of the sites.

The results show that discharge points are often coincident with low points in the landscape, e.g. shorelines, lakes and mires of each sub-catchment area /SKB 2006ab/. To identify all possible biosphere objects (at repository closure and forward in time), the potential discharge points were plotted on a map of identified future sub-catchment areas, lakes and running waters. Thus, a pattern with clusters of potential discharge points was used to identify distinct biosphere objects. Very few points were found isolated from the clusters. Such isolated points were transferred to the closest object downstream /SKB 2006ab/.

2.1.1 Model for Forsmark

At Forsmark, 23 objects and two running waters (objects 20 and 25) were identified in the affected area of the landscape (see Figure 2-1 and Table 2-1) /SKB 2006a/. Three time periods with different conditions can be identified during the interglacial period: the Sea Period from 8,000 BC to about 1,000 AD, a Coastal Period from 1,000 AD to about 5,000 AD, and a Terrestrial Period until 10,000 AD (see Figure 2-2). For the first 10,000 years after de-glaciation, the site is submerged under the sea. During this period, only three objects are included in the model: the basin above the repository (object 17), the entire Öregrundsgrepen (object 3) and the rest of the Baltic Sea (object 1). The Coastal Period starts with a situation similar to that prevailing today at the site, with 4 objects on land; a mire (object 21) and three lakes (objects 22, 23 and 24). There are two more Sea Objects (objects 11 and 18) appearing at the period corresponding to the present time, both of which receive radionuclide discharges during this period. Shoreline displacement gradually reveals more Terrestrial Objects and the

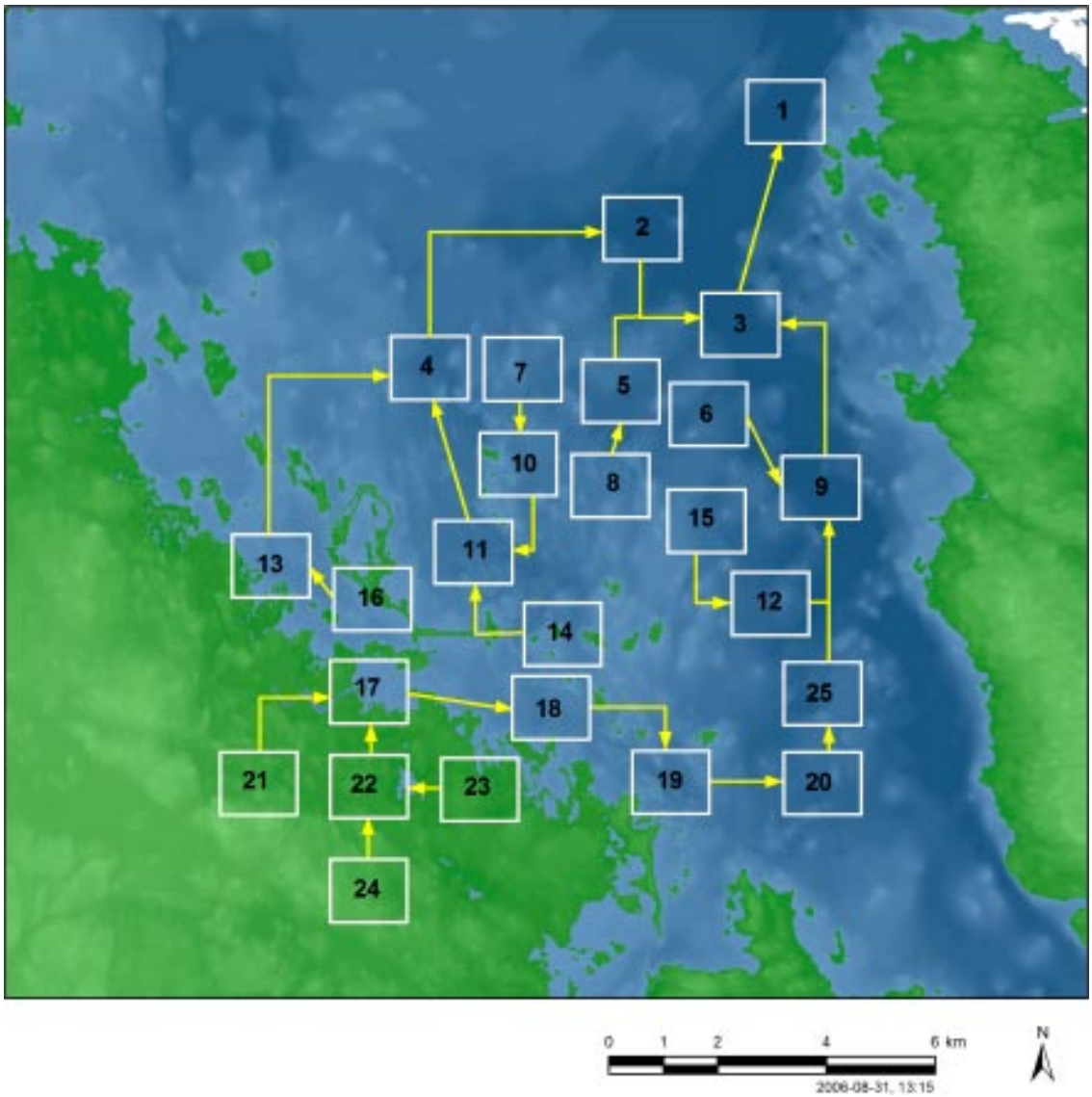

Figure 2-1. *The landscape model used for Forsmark. Boxes indicate objects that are interconnected by flows of radionuclides (arrows). Boxes 20 and 25 correspond to Running Waters. Hypothetical release points from the geosphere into the biosphere from 2,000 AD to 20,000 AD are indicated with dots. The underlying map shows today's shoreline /SKB 2006a/.*

ecosystem succession in these objects (see Table 2-1) generates the time dynamics of the landscape. At the start of the Coastal Period, a running water (object 20) appears in the landscape, which flows between objects 19 and 9 and merges with a second running water (object 25) at 5,000 AD. The diversity and spatial heterogeneity of objects is highest during this period. From 7,000 AD and onwards there are few Sea Objects (objects 1 and 3 remain) and few lakes (object 9 remains), the rest are forests and mires, some of which are transformed to agricultural lands. After 9,000 AD, the Sea Objects disappear, but object 9 persists as a lake until about 20,000 AD, assuming current climatic conditions /SKB 2006a/. The total area over all potentially affected objects (excluding object 1) at the start of the interglacial period is $3.98\ 10^8$ m^2. The overall affected area reduces with time and equals $1.90\ 10^7$ m^2 at 10,000 AD.

Table 2-1. Ecosystem types included in the Forsmark model at different times in an interglacial period. For each landscape object in the model the succession of ecosystem types is shown /SKB 2006a/.

Object	8,000 BC–2,000 AD	2,000–3,000 AD	3,000–4,000 AD	4,000–5,000 AD	5,000–6,000 AD	6,000–7,000 AD	7,000–8,000 AD	8,000–9,000 AD	9,000-10,000 AD
1	Sea	Sea	Sea	Sea	Sea	Sea	Sea	Sea	Sea
2					Sea	Sea	Sea	Mire	Mire
3	Sea	Sea	Sea	Sea	Sea	Sea	Sea	Sea	Sea
4					Lake	Lake	Mire	Mire	Agricultural Land
5						Lake	Lake	Mire	Mire
6							Lake	Lake	Mire
7					Forest	Forest	Forest	Forest	Forest
8					Lake	Mire	Mire	Mire	Mire
9					Sea	Sea	Sea	Sea	lake
10					Forest	Forest	Forest	Forest	Forest
11		Sea	Sea	Sea	Lake	Lake	Mire	Mire	Agricultural Land
12							Lake	Lake	Mire
13			Lake	Lake	Mire	Mire	Mire	Agricultural Land	Agricultural Land
14				Forest	Forest	Forest	Forest	Forest	Forest
15						Lake	Mire	Mire	Mire
16			Lake	Lake	Mire	Mire	Forest	Forest	Forest
17	Sea	Sea	Lake	Lake	Mire	Mire	Mire	Mire	Mire
18		Sea	Sea	Mire	Mire	Agricultural Land	Agricultural Land	Agricultural Land	Agricultural Land
19				Sea	Lake	Lake	Mire	Agricultural Land	Agricultural Land
20			Running Water	Running Water	Running Water	Running Water	Running Water	Running Water	Running Water
21		Sea	Mire	Mire	Agricultural Land	Agricultural Land	Forest	Forest	Forest
22		lake	Mire	Mire	Mire	Mire	Mire	Mire	Mire
23		Lake	Mire	Mire	Agricultural Land	Agricultural Land	Agricultural Land	Agricultural Land	Agricultural Land
24		Lake	Lake	Mire	Mire	Agricultural Land	Agricultural Land	Agricultural Land	Agricultural Land
25					Running Water	Running Water	Running Water	Running Water	Running Water

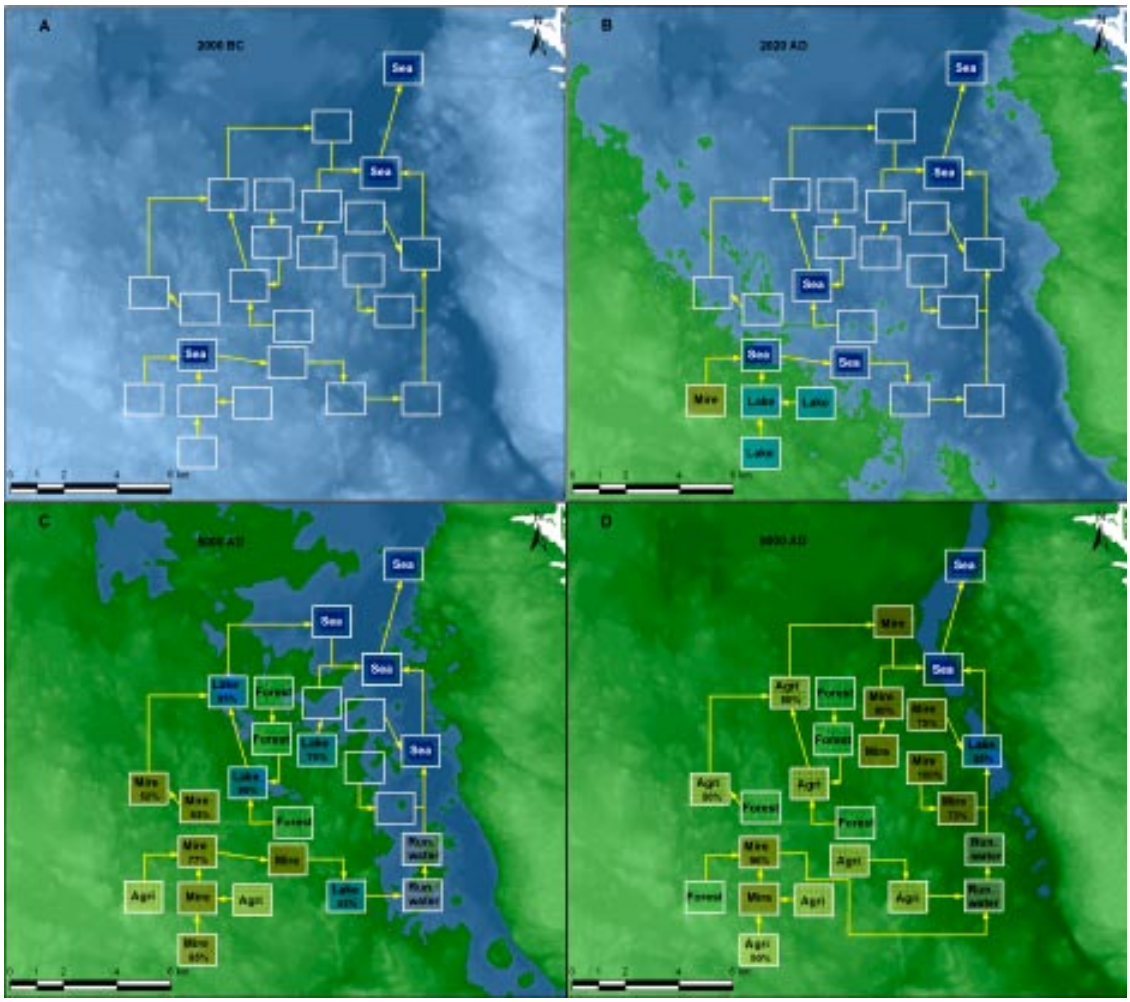

Figure 2-2. *Assumed succession of the landscape at Forsmark for the interglacial period. The maps represent different periods: Sea Period from 8,000 BC to 1,000 AD (top left), the Coastal Period (shown at 2,020 AD at the top right), the Terrestrial Period (shown at 5,000 AD at the bottom left and from 7,000 AD and onwards at the bottom right) /SKB 2006a/.*

2.1.2 Model for Laxemar

At Laxemar, 21 objects and five running waters (objects 22, 23, 24, 25 and 26) were identified in the landscape (see Figure 2-3 and Table 2-2) /SKB 2006b/. Three main periods of landscape development were also identified in the interglacial period (Figure 2-4). However, the duration and timing of these periods differs from that at Forsmark. Quite soon after the de-glaciation, at about 8,000 BC, parts of the hills closest to the repository are small islands. These are then re-submerged during a regression of the shoreline which occurs between 7,000 BC and 5,000 BC. All release points are located in the sea until 3,000 BC (Sea Period). Thereafter, a Coastal Period starts, during which mires and lakes are formed in narrow valleys around the repository footprint and already around 3,000 BC the first potential agricultural areas are formed. From 3,000 BC, release points occur also in terrestrial ecosystems. At around 0 AD, the landscape resembles the present conditions at Laxemar, with several small agricultural areas situated in long and deep valleys. Only a few of the lakes and mires that are formed from the sea objects have properties that preclude them from being transformed into agricultural lands. Mires are assumed to be transformed to agricultural lands unless factors such as size and boulder content make this unlikely. This overestimates the area of agricultural land, which in most cases is cautious for estimating radiological impact on humans /SKB 2006b/.

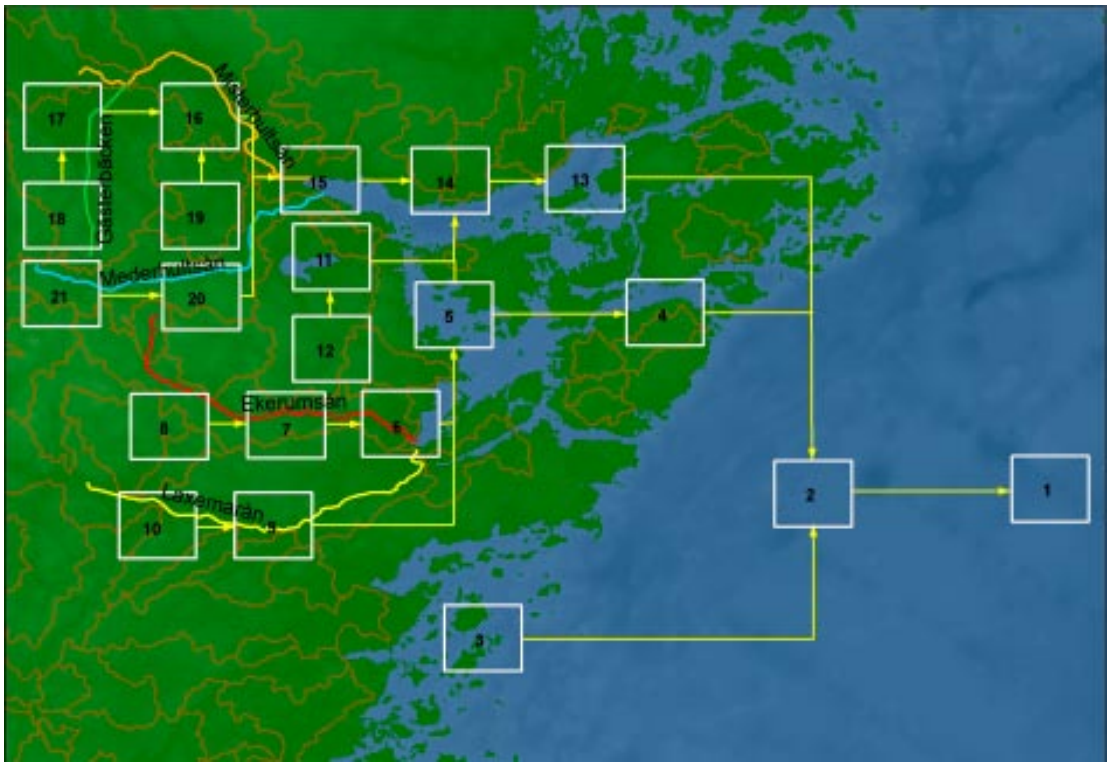

Figure 2-3. *The landscape model used for Laxemar. Boxes indicate objects that are interconnected by flows of radionuclides (arrows). The five Running Waters modelled are indicated with coloured lines. The underlying map shows today's shoreline /SKB 2006b/.*

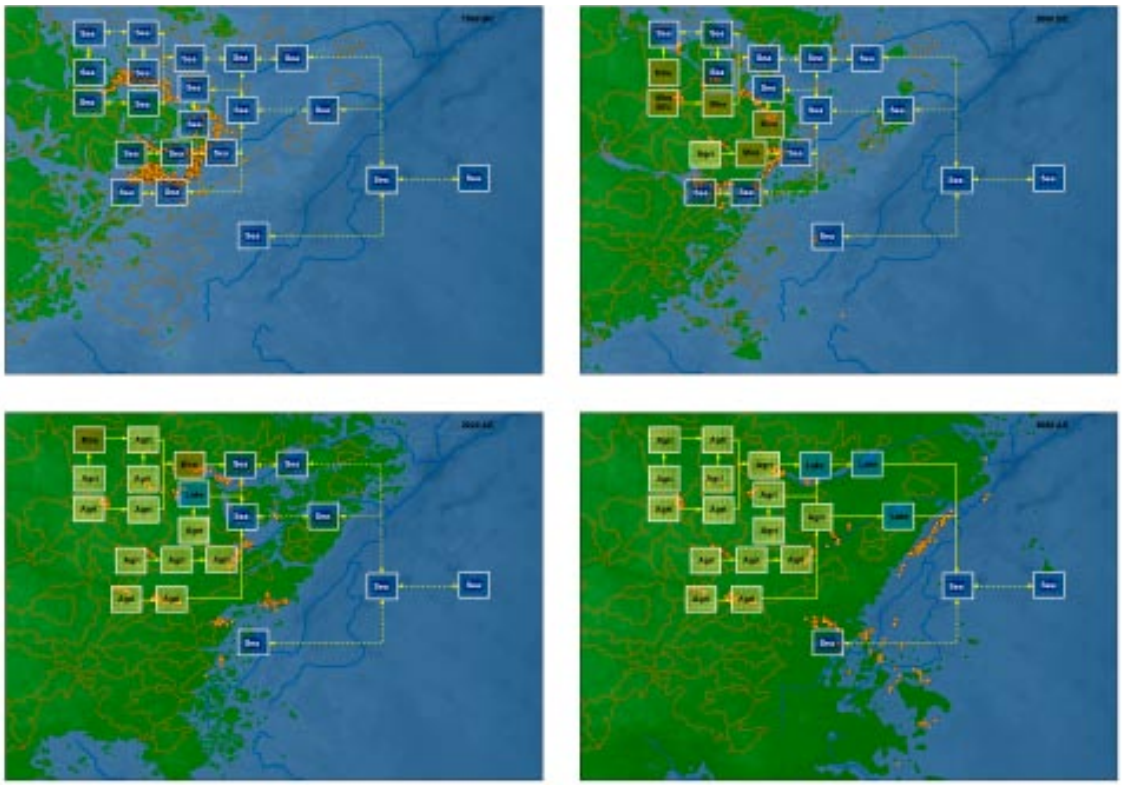

Figure 2-4. *Assumed succession of the landscape at Laxemar for the interglacial period. Modelled potential discharge points are indicated as dots. The maps represent different time periods: the Sea Period (top left), the Coastal Period (shown at the top right at 2,000 BC and at the bottom left at 2,020 AD) and the Terrestrial Period (shown at the bottom right at 8,000 AD) /SKB 2006b/.*

Table 2-2. Ecosystem types included in the Laxemar model at different times in an interglacial period. For each landscape object in the model the succession of ecosystem types is shown /SKB 2006b/.

Object	8,000–3,000 BC	3,000–2,000 BC	2,000–1,000 BC	1,000 BC–0 AD	0–1,000 AD	1,000–2,000 AD	2,000–3,000 AD	3,000–4,000 AD
2	Sea	Sea	Sea	Sea	Sea	Sea	Sea	Sea
3	Sea	Sea	Sea	Sea	Sea	Sea	Sea	Sea
4	Sea	Sea	Sea	Sea	Sea	Sea	Sea	Sea
5	Sea	Sea	Sea	Sea	Sea	Sea	Sea	Sea
6	Sea	Sea	Sea	Sea	Sea	Mire	Agricultural Land	Agricultural Land
7	Sea	Sea	Mire	Agricultural Land	Agricultural Land	Agricultural Land	Agricultural Land	Agricultural Land
8	Sea	Mire	Agricultural Land	Agricultural Land	Agricultural Land	Agricultural Land	Agricultural Land	Agricultural Land
9	Sea	Sea	Sea	Sea	Mire	Agricultural Land	Agricultural Land	Agricultural Land
10	Sea	Sea	Sea	Sea	Mire	Agricultural Land	Agricultural Land	Agricultural Land
11	Sea	Sea	Sea	Sea	Sea	Agricultural Land	Lake	Mire
12	Sea	Sea	Mire	Agricultural Land	Agricultural Land	Agricultural Land	Agricultural Land	Agricultural Land
13	Sea	Sea	Sea	Sea	Sea	Sea	Sea	Sea
14	Sea	Sea	Sea	Sea	Sea	Sea	Sea	Sea
15	Sea	Sea	Sea	Sea	Sea	Sea	Mire	Mire
16	Sea	Sea	Sea	Sea	Agricultural Land	Agricultural Land	Agricultural Land	Agricultural Land
17	Sea	Sea	Sea	Sea	Lake	Lake	Mire	Agricultural Land
18	Sea	Sea	Mire	Agricultural Land	Agricultural Land	Agricultural Land	Agricultural Land	Agricultural Land
19	Sea	Sea	Sea	Mire	Agricultural Land	Agricultural Land	Agricultural Land	Agricultural Land
20	Sea	Sea	Sea	Mire	Agricultural Land	Agricultural Land	Agricultural Land	Agricultural Land
21	Sea	Lake	Mire	Agricultural Land	Agricultural Land	Agricultural Land	Agricultural Land	Agricultural Land
22					Running Water	Running Water	Running Water	Running Water
23					Running Water	Running Water	Running Water	Running Water
24		Running Water	Running Water	Running Water	Running Water	Running Water	Running Water	Running Water
25		Running Water	Running Water	Running Water	Running Water	Running Water	Running Water	Running Water
26					Running Water	Running Water	Running Water	Running Water

Table 2-2 (cont). Ecosystem types included in the Laxemar model at different times in an interglacial period. For each landscape object in the model the succession of ecosystem types is shown /SKB 2006b/.

Object	4,000–5,000 AD	5,000–6,000 AD	6,000–7,000 AD	7,000–8,000 AD	8,000–10,000 AD
2	Sea	Sea	Sea	Sea	Sea
3	Sea	Sea	Sea	Sea	Sea
4	Sea	Sea	Sea	Lake	Lake
5	Lake	Mire	Mire	Mire	Agricultural Land
6	Agricultural Land	Agricultural Land	Agricultural Land	Agricultural Land	Agricultural Land
7	Agricultural Land	Agricultural Land	Agricultural Land	Agricultural Land	Agricultural Land
8	Agricultural Land	Agricultural Land	Agricultural Land	Agricultural Land	Agricultural Land
9	Agricultural Land	Agricultural Land	Agricultural Land	Agricultural Land	Agricultural Land
10	Agricultural Land	Agricultural Land	Agricultural Land	Agricultural Land	Agricultural Land
11	Mire	Agricultural Land	Agricultural Land	Agricultural Land	Agricultural Land
12	Sea	Agricultural Land	Agricultural Land	Agricultural Land	Agricultural Land
13	Lake	Sea	Lake	Lake	Lake
14	Agricultural Land	Mire	Lake	Lake	Lake
15	Agricultural Land	Agricultural Land	Agricultural Land	Agricultural Land	Agricultural Land
16	Agricultural Land	Agricultural Land	Agricultural Land	Agricultural Land	Agricultural Land
17	Agricultural Land	Agricultural Land	Agricultural Land	Agricultural Land	Agricultural Land
18	Agricultural Land	Agricultural Land	Agricultural Land	Agricultural Land	Agricultural Land
19	Agricultural Land	Agricultural Land	Agricultural Land	Agricultural Land	Agricultural Land
20	Agricultural Land	Agricultural Land	Agricultural Land	Agricultural Land	Agricultural Land
21	Agricultural Land	Agricultural Land	Agricultural Land	Agricultural Land	Agricultural Land
22	Running Water	Running Water	Running Water	Running Water	Running Water
23	Running Water	Running Water	Running Water	Running Water	Running Water
24	Running Water	Running Water	Running Water	Running Water	Running Water
25	Running Water	Running Water	Running Water	Running Water	Running Water
26	Running Water	Running Water	Running Water	Running Water	Running Water

At 4,000 AD the Coastal Period ends and terrestrial objects, mainly agricultural lands, dominate the surroundings of the repository (Terrestrial Period). Thereafter, the remaining bays and lakes are gradually filled, but Bornholmsfjärden (object 14) remains as a lake until 20,000 AD, due to its steep shores and depth. The coastline outside the Simpevarp peninsula changes only slightly up to 20,000 AD when an archipelago is formed /SKB 2006b/. The succession of ecosystems during the interglacial period predicted by the model is shown in Table 2-2. The total area over all potentially affected objects (excluding object 1) at the start of the interglacial period is 5.6 107 m^2. The overall affected area reduces with time and equals 1.8 107 m^2 at 10,000 AD.

2.2 Biosphere model for permafrost, glacial and greenhouse conditions

Permafrost period

Permafrost conditions occur in several episodes in the reference evolution covering the Weichselian glacial cycle /SKB 2006c/. At both sites, the first permafrost episode starts at about 10,000 AD following the current interglacial period. At this time, the coastline at both sites is at some distance from the repository and major discharge areas are located inshore /SKB 2006ab/. The situation is similar at the end of the interglacial period when global sea levels are falling. To simulate the permafrost conditions, it is assumed that the spatial distribution of landscape objects is similar to that at the end of the interglacial period /SKB 2006ab/, except that agricultural lands are replaced by forest or mires, reflecting the consideration that a significant degree of agriculture would not be tenable in such a context.

Glacial period

During the glacial period the repository will be either beneath the ice, or submerged under the sea at the ice margin. For this time period, it is assumed that conditions with the repository at the ice margin are associated with the higher radiological impact and therefore the same landscape model as for the beginning of the interglacial period was used /SKB 2006ab/.

Greenhouse conditions

In the greenhouse variant a protracted interglacial period is expected to occur. For this variant the landscape model at the end of the interglacial period was used, as after that the landscape does not experience substantial changes /SKB 2006ab/.

2.3 The landscape models for radionuclide transport and accumulation

The models of radionuclide transport and accumulation in the landscape for both sites were developed on the basis of the above described landscape models. For this purpose, an ecosystem model was assigned for each time period to the landscape objects according to the projected succession of ecosystems in the objects shown in Tables 2-1 and 2-2. The ecosystem models applied are described in the next section. All these models are compartment type (except in the case of running waters, see below). Hence, the landscape models can be described as a set of interconnected compartment models, and, in mathematical terms, as a system of ordinary differential equations (ODEs). The fluxes of radionuclides between objects were assumed to be directly proportional to the fluxes of water through upstream objects. The water fluxes were estimated from the average run-off at the site, the areas of the objects and their associated catchment areas. Radionuclides in both dissolved and particulate forms were considered in the transport calculations.

The transformations of the ecosystems were modelled as discrete events occurring every thousand years, by substituting one model by another using the rules described in Section 2.3.3.

2.3.1 The ecosystem models

All ecosystem models applied are briefly outlined below. A more detailed description can be found in /Avila 2006a/. The models are the same which were used in the assessments performed for SR-Can Interim /SKB 2004/, with the exception of the forest model /Avila 2006b/, which was not available at that time and was especially developed for SR-Can.

Aquatic ecosystems

For Lake and Sea Objects, compartment models as described in /Avila 2006a/ were used (see Figures 2-5 and 2-6). These are the same models used in previous safety assessments /SKB 1999, 2004/ with the following modifications:

i) In both models, the sediment compartments were further sub-divided in order to handle direct releases to sediments.

ii) The parameter specifying the residence time in the lake model was replaced by an equation that uses the average run-off at the site, the area of the lake and the catchment area as parameters.

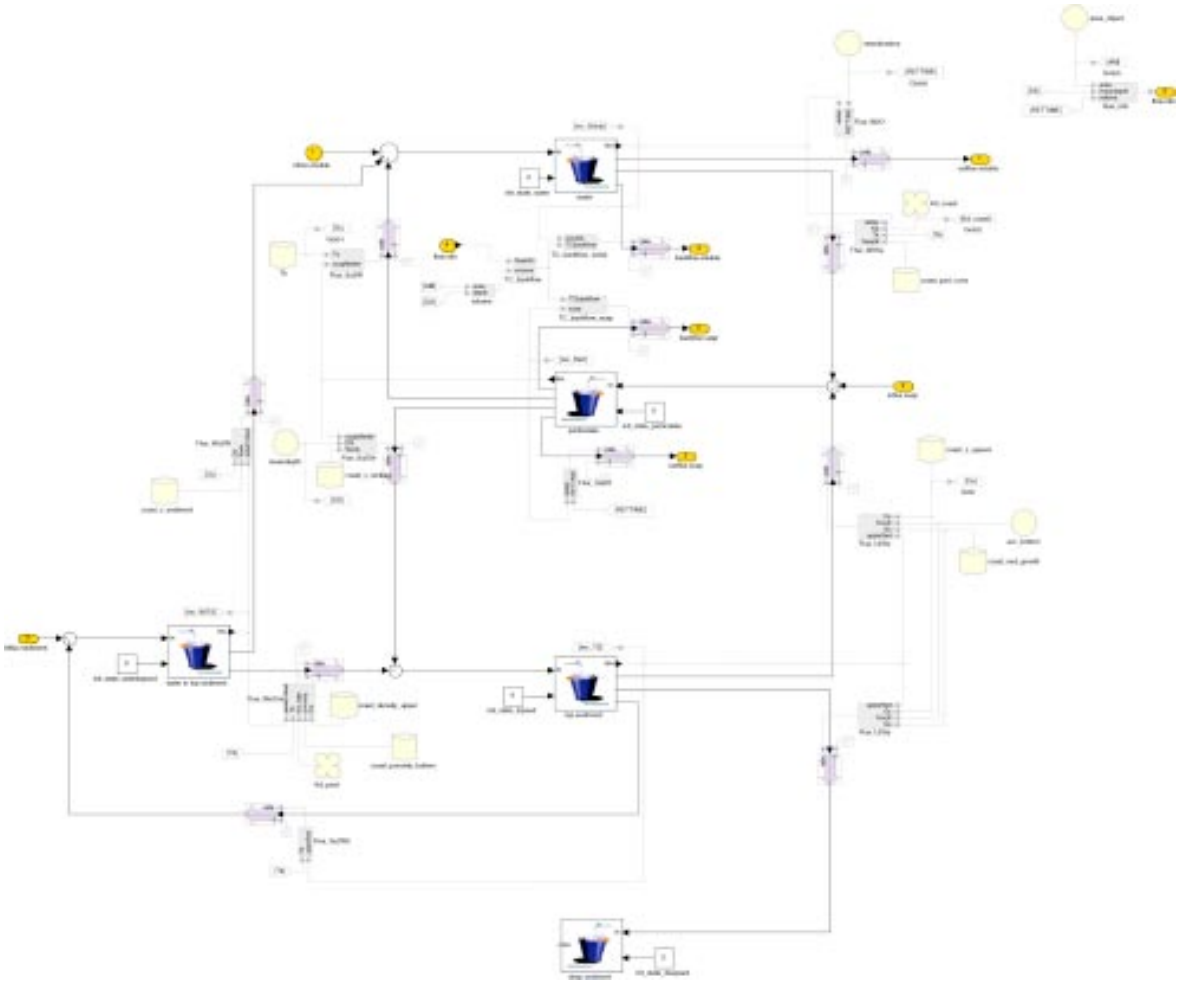

Figure 2-5. *Schematic representation of the Sea model. The squares represent model compartments, the big arrows correspond to fluxes between compartments. The boxes connected to the big arrows represent transfer rate coefficients used for the flux calculations. The model parameters are represented using different symbols depending on their type: the radionuclide-dependent parameters with a cross, the site-specific parameters with a cylinder and generic parameters with a circle /Avila 2006a/.*

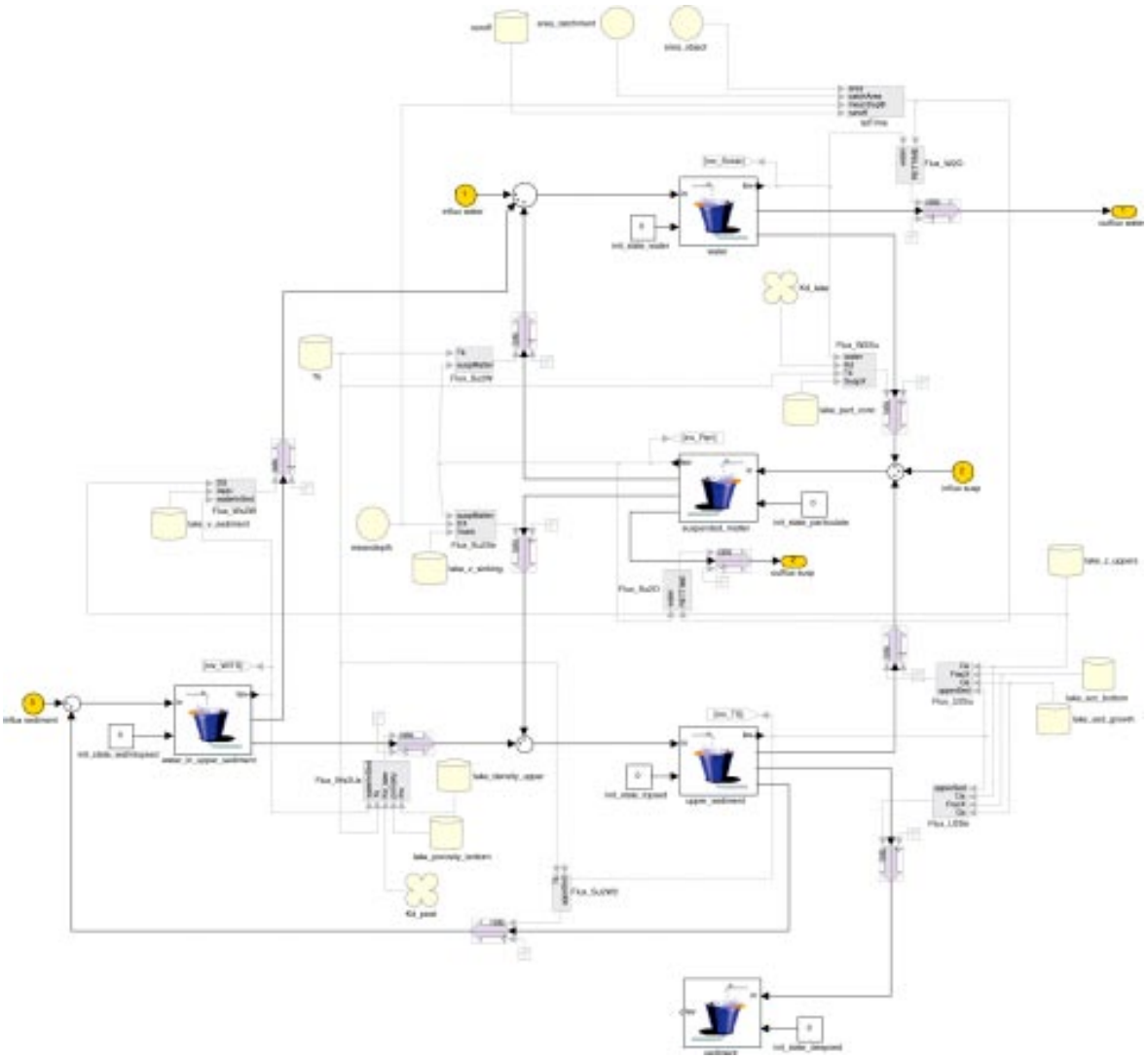

Figure 2-6. *Schematic representation of the Lake model. The squares represent model compartments, the big arrows correspond to fluxes between compartments. The boxes connected to the big arrows represent transfer rate coefficients used for the flux calculations. The model parameters are represented using different symbols depending on their type: the radionuclide-dependent parameters with a cross, the site-specific parameters with a cylinder and generic parameters with a circle /Avila 2006a/.*

For Running Waters, a compartment model was not used. Instead, instantaneous and complete mixing of the released radionuclides with the running water was assumed.

Terrestrial ecosystems

For agricultural lands, forests and mires, compartment models as described in /Avila 2006a/ were used (see Figures 2-7, 2-8 and 2-9). For agricultural lands and mires the applied models are the same as those used in previous assessments /SKB 1999, 2004/), whereas the forest model /Avila 2006b/ was especially developed for SR-Can. The original models assumed that the water fluxes through the objects were determined by the amount of rain falling directly on the object, but not by the water flowing through upstream objects. In order to take into account the contribution of fluxes from upstream objects, the equation used for calculation of the water fluxes was modified by a factor equal to the ratio between the catchment and object areas see /Avila 2006a/.

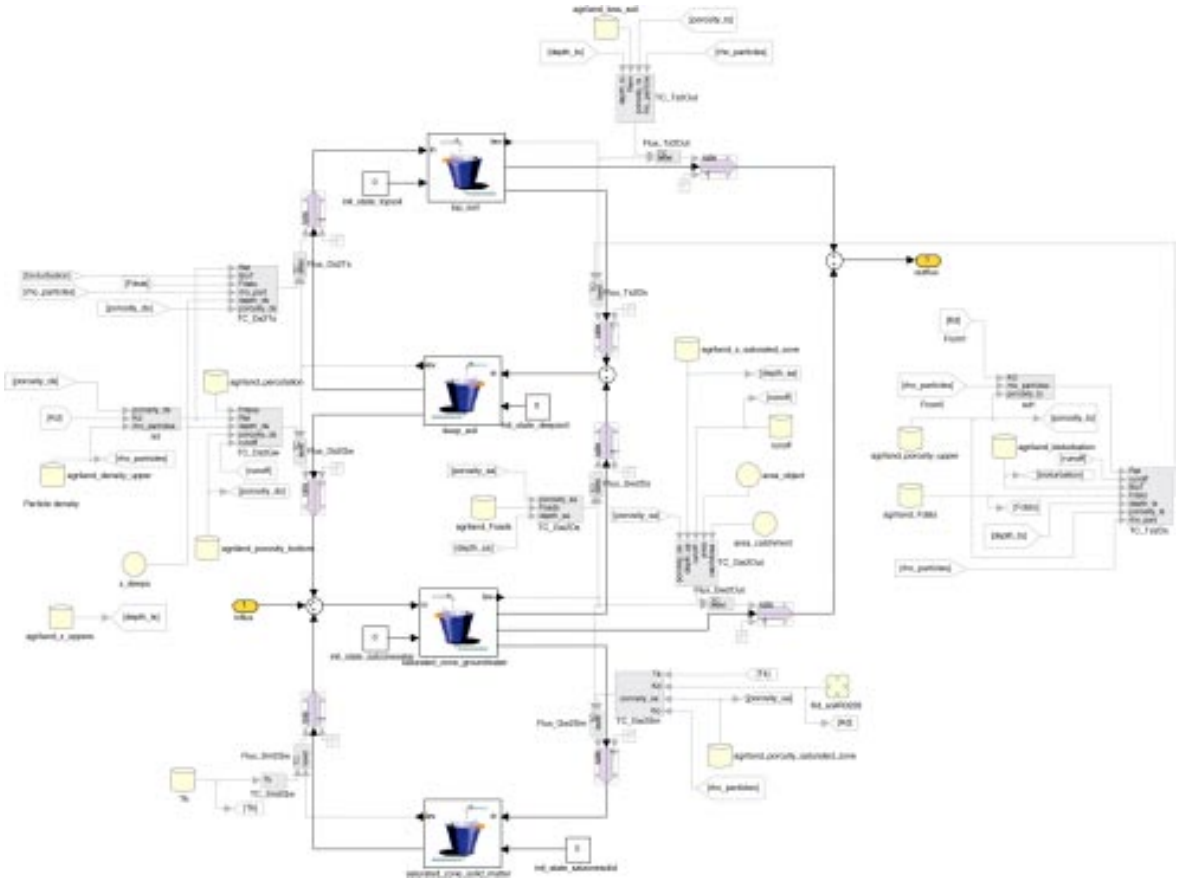

Figure 2-7. *Schematic representation of the Agricultural Land model. The squares represent model compartments, the big arrows correspond to fluxes between compartments. The boxes connected to the big arrows represent transfer rate coefficients used for the flux calculations. The model parameters are represented using different symbols depending on their type: the radionuclide-dependent parameters with a cross, the site-specific parameters with a cylinder and generic parameters with a circle /Avila 2006a/.*

Irrigation of agricultural lands was not considered in the mass balance of the landscape model. Instead, at each time step, a contribution from irrigation was added to the estimates of radionuclide concentrations in the food products. The contribution from irrigation was estimated by multiplying the radionuclide concentrations in freshwater (from lakes, running waters and lakes) by a pre-calculated factor. This factor relates radionuclide concentrations in vegetables and irrigation water and was estimated from simulations with the irrigation model described in /Bergström and Barkefors 2004/. More details about how irrigation was handled can be found in /Avila 2006a/. It should be noted, that if irrigation occurs within a single object, it does not change the water mass balance and is, in any event, a small perturbation in the considered climatic conditions.

Treatment of the well

For evaluation of the impact of releases to wells, it was assumed that the contaminated groundwater on its path to the discharge point always passes a well. The concentration of the radionuclide in the well water was calculated by dividing the release rate by the well capacity, estimated from data obtained from existing wells in Forsmark and Laxemar. This means that for calculation of the concentrations complete capture of the plume was assumed.

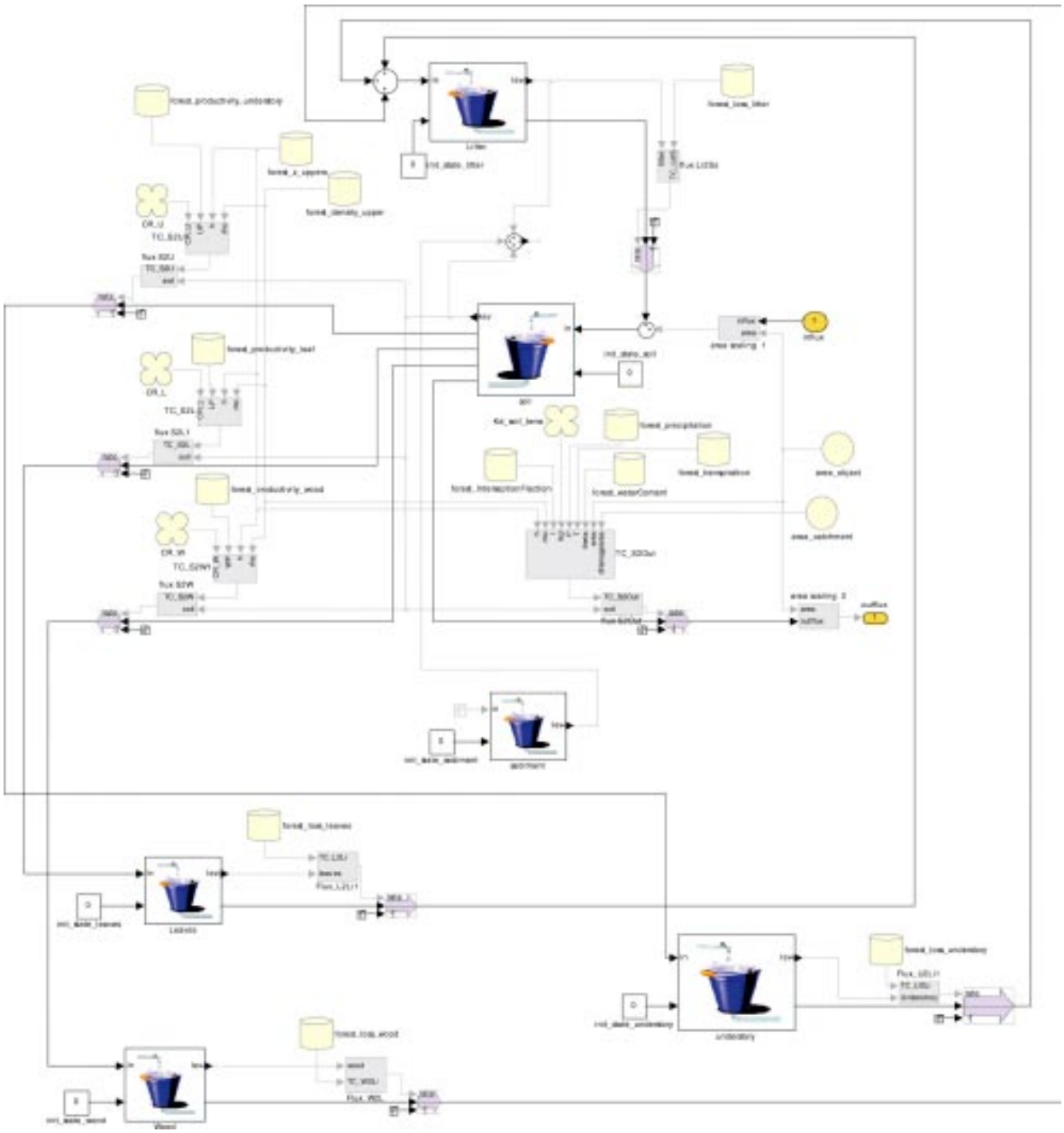

Figure 2-8. *Schematic representation of the Forest model. The squares represent model compartments, the big arrows correspond to fluxes between compartments. The boxes connected to the big arrows represent transfer rate coefficients used for the flux calculations. The model parameters are represented using different symbols depending on their type: the radionuclide-dependent parameters with a cross, the site-specific parameters with a cylinder and generic parameters with a circle /Avila 2006a/.*

It was assumed that abstraction of radionuclides from the well does not affect substantially the radionuclide releases rate to the receptor object in the landscape. If the well is used by a limited number of individuals, for example 2 families or about 10 individuals, the volume of abstracted water will be only about 10 of the well capacity is abstracted. If a larger number of individuals were to use the well, then a larger fraction of radionuclides would be abstracted and would not reach the receptor object in the landscape. The doses to the individuals using the well would be the same, but the size of the group would be larger. At the same time, the doses to individuals exposed to radionuclides discharged into the landscape would be lower, although the same number of individuals would be exposed by this pathway.

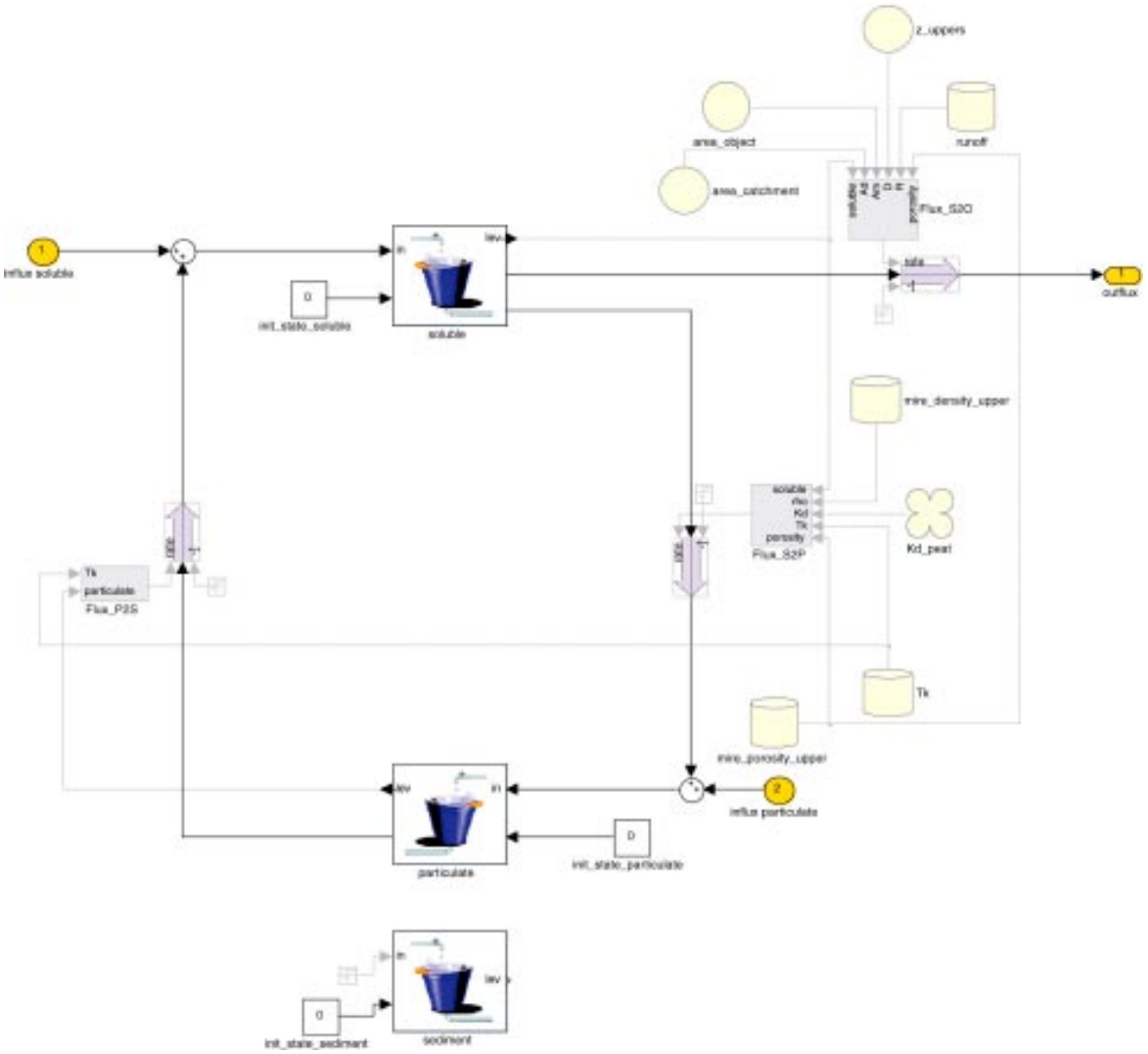

Figure 2-9. *Schematic representation of the Mire model. The squares represent model compartments, the big arrows correspond to fluxes between compartments. The boxes connected to the big arrows represent transfer rate coefficients used for the flux calculations. The model parameters are represented using different symbols depending on their type: the radionuclide-dependent parameters with a cross, the site-specific parameters with a cylinder and generic parameters with a circle /Avila 2006a/.*

2.3.2 Model parameters

The model parameters are, for convenience, distinguished in the presentation below into two broad categories: radionuclide-independent and radionuclide-dependent parameters. An overview of the parameters used and their values is provided below.

Radionuclide-independent parameters

Most of the parameters used in the model correspond to hydrological and ecological properties of the landscape and the ecosystems and are radionuclide-independent. This category of parameters is described in more detail in /SKB 2006a/ and /SKB 2006b/, where the origin of the data is also provided. For most of these parameters, the values were derived from information provided from the site investigation programmes. Tables with the parameter values used for Forsmark and Laxemar are provided in Appendix A. As the parameter values vary among the various objects, an interval of variation is provided for each parameter, which was used in the sensitivity studies presented in Section 6.1.These tables also include a generic interval of variation for most of the

parameters, which was taken from reports describing each particular ecosystem model /Avila 2006a/. It should be noted, that, as far as possible, site-specific and object-specific parameter values were used in the simulations. The parameter values used for each specific object can be found in /SKB 2006a/ and /SKB 2006b/.

As mentioned above, different parameter values were used for different objects. Moreover, time-dependent values were used for parameters associated with features and processes that are affected by the land rise (the depth of the water bodies, the areas of the objects); and by transformations in the sea bottoms (the fraction of accumulation bottoms, i.e. the fraction of the bottoms with positive sedimentation rates). Examples of time dependencies assumed are presented for Laxemar in Figures 2-10 and 2-11. Similar dependencies were assumed for Forsmark. For Laxemar, there is a generally increasing trend in the fraction of accumulation bottoms, which will result in an increase with time of radionuclide retention in these objects. However, the time dynamics of the fraction of accumulation bottoms is non-monotonic, which should result in a complex dynamics of radionuclide accumulation. A decreasing trend of the area of the objects is observed, which should lead to an increase of radionuclide concentrations with time.

Radionuclide-dependent parameters

Radionuclide-dependent parameters in the model are the distribution coefficients (K_d) and the transfer factors from soils and waters to biota. The values of these parameters are given in /Avila 2006a/ for each ecosystem type. In the landscape models, the same values of these parameters were used in all instances of the ecosystem models. For example, the K_d values and transfer factors were used for all forest ecosystems in the landscape models. Also, the same values of the radionuclide-dependent parameters were used in the Forsmark and Laxemar models.

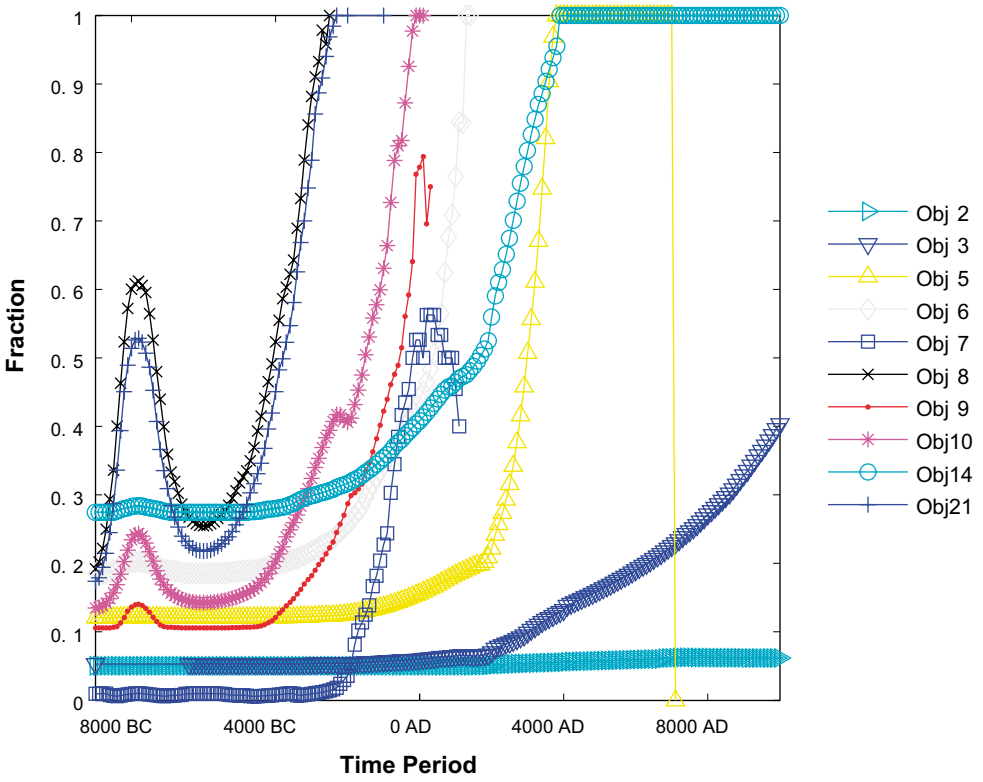

Figure 2-10. *Time variation of the fraction of accumulation bottoms in Sea Objects at Laxemar.*

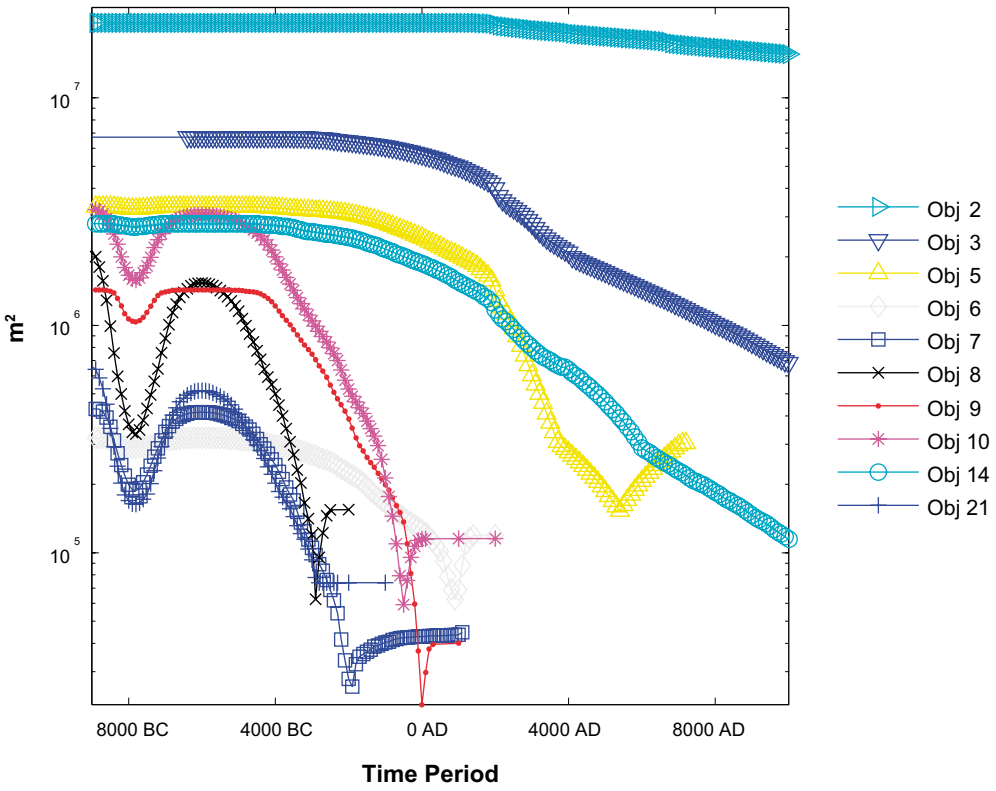

Figure 2-11. *Time dynamics of the area of some of the objects in the Laxemar landscape model.*

It should be noted that for these parameters the selection of values was done separately for each ecosystem model. Hence, there can be inconsistencies in how the parameter values vary from one ecosystem to the other. This is illustrated in Figure 2-12 for the K_d values. For example, the K_d values for Se-79 show a very different variation between ecosystems, as compared with other radionuclides. Note that this is not necessarily wrong. For example, one should expect different variation of redox-sensitive and redox-insensitive elements.

2.3.3 Handling of changes in the landscape

The transformation between ecosystems (every thousand years) was modelled as discrete events, by substituting one model by another. The activity in different compartments of the "mother" ecosystem was transferred instantaneously to the appropriate compartments of the "daughter" ecosystem following the rules in Table 2-3. These rules were set so as not to underestimate the potential doses. For example, if an ecosystem was transformed into a forest from e.g. a seabed or mire, then the total activity in the ecosystem, including the fraction in the deep sediment, was transferred to the root zone of the forest soil. As the inventory is transferred instantaneously, this is equivalent to setting the initial conditions of the compartments in the daughter ecosystem to a value equal to the transferred inventory.

In the Laxemar model, all future objects are present in the landscape model from the start of the simulation period (see Figure 2-4), and for this reason the application of the above rules is straightforward. However, in the Forsmark model, there are only three objects at the start of the simulation period (see Figure 2-2), i.e. objects 1, 3 and 17. All other future objects in the model develop from object 3; although these objects do not cover all land emerging from object 3. To be on the conservative side, no activity was transferred to emerging lands that are not included in the model. This means that, over the whole simulation period, all activity accumulated in the sea is either transferred to Terrestrial Objects in the model or remains in object 3. Note that the reason for not including some of the emerging lands in the model is that these lands are upstream from potential release points.

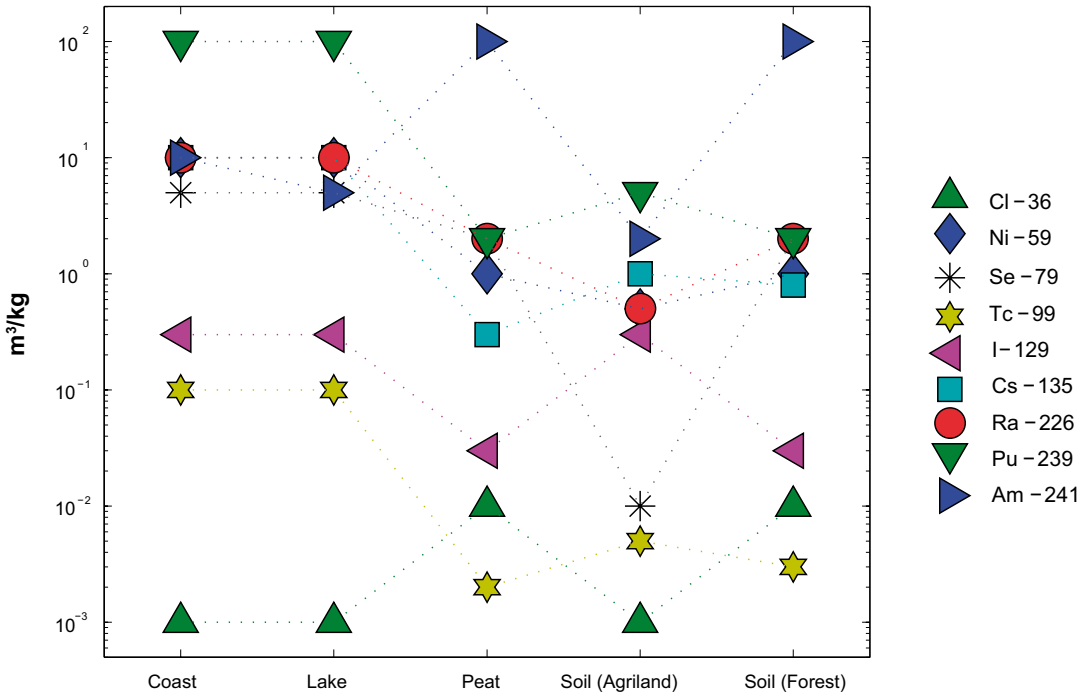

Figure 2-12. *Distribution coefficients (K_d) used in the particular realisations illustrated in this report. The K_d-coast and K_d-lake were used to describe the distribution between suspended solids and water, the K_d-peat was used for the distribution between solids and water in the mire model and in the sediments of the lake and sea model. Different K_d values were also used for the agricultural land and forest models.*

Table 2-3. Rules applied for the transfer of activity to the compartments of the emerging ecosystem when an ecosystem shift occurs.

Ecosystem shift	Rules for the activity transfer
Sea to Mire	Total activity in water compartments (Water and Particulate) is transferred to the Soluble compartment. Total activity in sediment compartments (Water Top Sediment, Top Sediment and Deep Sediment) is transferred to the Sediment compartment.
Sea to Lake	Since both models have the same compartments, the activity in each compartment of the coastal model is transferred to the corresponding compartment of the Lake Model.
Sea to Agricultural Land	The activity in the Water compartment is transferred to the compartment Saturated Zone Groundwater. The total activity in the rest of the compartments is transferred to the compartments Top Soil and Deep Soil in proportion to their relative depths.
Sea to Forest Mire to Forest Agricultural Land to Forest	The total activity in the ecosystem is transferred to the soil compartment.
Lake to Mire	The activity in the compartment Soluble is transferred to the compartment Soluble. Total activity in sediment compartments (Water Top Sediment, Top Sediment and Deep Sediment) is transferred to the Sediment compartment.
Mire to Agricultural Land	The activity in the compartment Soluble is transferred to the compartment Saturated Zone Groundwater. The total activity in the rest of the compartments is transferred to the compartments Top Soil and Deep Soil in proportion to their relative depths.

2.3.4 Model implementation

The landscape models were implemented using the software package Pandora /Åstrand et al. 2005/. Pandora is an extension of the well-known software Matlab© and Simulink© from Mathworks (www.mathworks.com). Pandora simplifies the development of models described by large systems of differential equations and the handling of radionuclide decay chains. The Pandora tool comprises a library of Simulink© blocks that facilitates the creation of compartment models and a standalone toolbox for management of parameter values and probabilistic simulations.

Pandora has been benchmarked, tested and compared with other similar tools /Åstrand et al. 2005/. The solutions obtained with the predecessor of Pandora (Tensit) were compared with analytical results, as well as with numerical results obtained with other simulation tools /Jones et al. 2004/. These comparisons have shown that Pandora provides reliable solutions.

A library of ecosystem models was created in Pandora, which facilitates handling several instances of the ecosystem models in the landscape model. For each landscape object a Simulink© subsystem was created, which includes models of all ecosystem types that may exist within this object during the whole simulation period. The discrete transition between ecosystem models was implemented using switches available in Simulink©. The decay and ingrowth of radionuclides in a chain was handled with the help of the Pandora radionuclide block. For integrating the model, the solver ode15s was used, which is an appropriate solver for stiff systems of equations with discrete events. The activity concentrations and doses were calculated from the amounts of activity in different compartments predicted with the Pandora model by using a post-processing routine created in Matlab©.

3 Predictions of the long-term distribution of radionuclides in the landscape

This section presents predictions of the long-term distribution of the studied radionuclides in the landscape resulting from unit continuous release rates. It is assumed that the radionuclides enter the landscape objects from below with groundwater discharges.

3.1 Radionuclides included in the study

The radionuclides included in the simulations are presented in Table 3-1. For radionuclides with decay chains, the distribution of the daughter radionuclides in the landscape, resulting from unit release rates of the parent, was also studied. The results in this and the following sections are presented in more detail for a reduced set of radionuclides, including those which based on the previous assessments /SKB 1999, 2004/, are expected to give the highest dose contributions, Ni-59, Se-79, I-129 and Ra-226. Some further radionuclides (Cl-36, Tc-99, Cs-135, Pu-239 and Am-241) with contrasting properties and environmental behaviour are also considered. It should be noted that C-14, which is also a potentially important radionuclide, was not included in the study. The reason for excluding C-14 was that the applied models are not directly applicable to this radionuclide. The required upgrading of the models is currently ongoing by utilising the information gained in the site investigation program about carbon cycling, which will allow the inclusion of C-14 in future assessments. It should be noted that, as it was shown in /Kumblad et al. 2003/, by explicitly modelling the carbon cycling, it is possible to model the turnover of C-14 and in general improve the radionuclide transport models.

3.2 Calculation variants and endpoints

The objective of the simulations was to obtain estimates of the radionuclide distribution in the landscape resulting from unit radionuclide release rates. The results of the simulations depend on the start time of the releases and on the release location in the landscape.

The start time of the releases depends on the point in time at which waste packages fail. In this study, the conservative assumption is made that the start of releases coincides with the start of an interglacial period since this would lead, through the accumulation of radionuclides in the various landscape objects, to the highest doses as compared to a start of releases within an interglacial period or in a glacial period. The validity of this assumption is investigated in variant calculations assuming the start of releases to take place at different times within an interglacial period.

As discussed already in Chapter 2, the current interglacial period which started 8,000 BC is chosen as model for future interglacial periods. On this basis, the main calculation variant described below is based on the current interglacial period with hypothetical releases from a repository starting at its beginning, i.e. at 8,000 BC.

Table 3-1. Radionuclides included in the study. For radionuclides with decay chains the daughter radionuclides included in the simulations are also included.

Radionuclide	Decay half life (years)	Daughter radionuclides						
Cl-36	3.010E+05							
Ca-41	1.030E+05							
Ni-59	7.600E+04							
Ni-63	1.001E+02							
Se-79	1.130E+06							
Sr-90	2.878E+01							
Zr-93	1.530E+06							
Nb-94	2.030E+04							
Tc-99	2.111E+05							
Pd-107	6.500E+06							
Ag-108m	4.180E+02							
Sn-126	1.000E+05							
I-129	1.570E+07							
Cs-135	2.300E+06							
Cs-137	3.007E+01							
Sm-151	9.000E+01							
Ho-166m	1.200E+03							
Pb-210	2.230E+01	Po-210						
Ra-226	1.600E+03	Pb-210	Po-210					
Th-229	7.340E+03	Th-229						
Th-230	7.584E+04	Ra-226	Pb-210	Po-210				
Th-232	1.405E+10							
Pa-231	3.276E+04							
U-233	1.592E+05	Th-229						
U-234	2.455E+08	Th-230	Ra-226	Pb-210	Po-210			
U-235	7.038E+08	Pa-231						
U-236	2.342E+07	Th-232						
U-238	4.468E+09	U-234	Th-230	Ra-226	Pb-210	Po-210		
Np-237	2.144E+06	U-233	Th-229					
Pu-239	2.411E+04	U-235	Pa-231					
Pu-240	6.563E+03	U-236	Th-232					
Pu-242	3.733E+08	U-238	U-234	Th-230	Ra-226	Pb-210	Po-210	
Am-241	4.322E+02	Np-237	U-233	Th-229				
Am-243	7.370E+03	Pu-239	U-235	Pa-231				
Cm-244	1.810E+01	Pu-240	U-236	Th-232				
Cm-245	8.500E+03	Am-241	Np-237	U-233	Th-229			
Cm-246	4.730E+03	Pu-242	U-238	U-234	Th-230	Ra-226	Pb-210	Po-210

3.2.1 Main calculation variant

For the assessments presented in this study, a main calculation variant was adopted for both sites. Releases were assumed to occur continuosly during the interglacial period; i.e. from 8,000 BC to 10,000 AD; and to be distributed between the landscape objects according to the release fractions provided in Tables 3-2 and 3-3. This variant is called in the following sections, 8,000 BC-All, indicating that the releases start at 8,000 BC and are directed to the sub-set of landscape objects that could potentially receive a discharge of radionuclides.

The releases fractions were obtained from analyses of results of the hydrological modelling as described in /SKB 2006ab/. As mentioned above, the time evolution of the landscape was modelled differently for Forsmark and Laxemar. In the case of Forsmark, only three objects were considered during the Sea Period, whereas in the case of Laxemar, all objects were included in the model from the start of the simulations. This choice reflects the availability of site-specific information at the moment when the landscape models were developed. In future assessments, all landscape objects will be included from the start in the models for both sites.

In the case of Forsmark, the hydrological models show that the releases during the Sea Period are directed exclusivly to object 17 (see Figure 3-1). At the present day object 17 is located at the cooling water inlet to the nuclear power plant, where a deep blasted channel in the rock has been constructed. Over the whole of the interglacial period, a few objects (7 in Forsmark and 10 in Laxemar) receive nearly 100% of the releases (Figures 3-1 and 3-2).

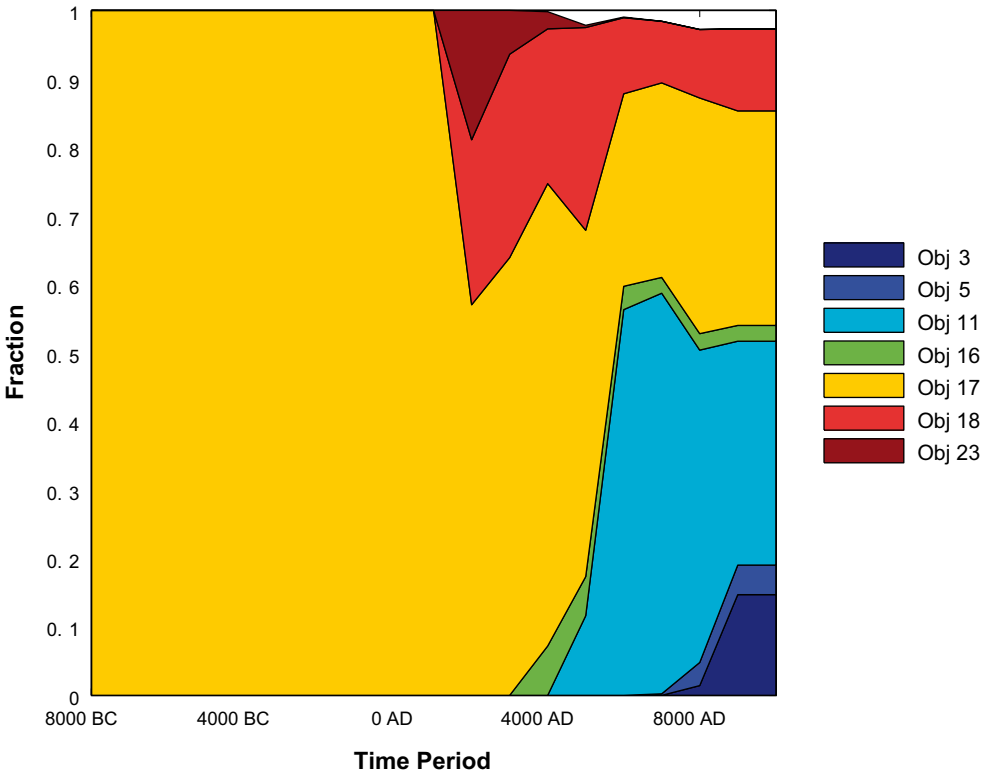

Figure 3-1. *Distribution of the release fractions between landscape objects in the Forsmark model for different times in the interglacial period.*

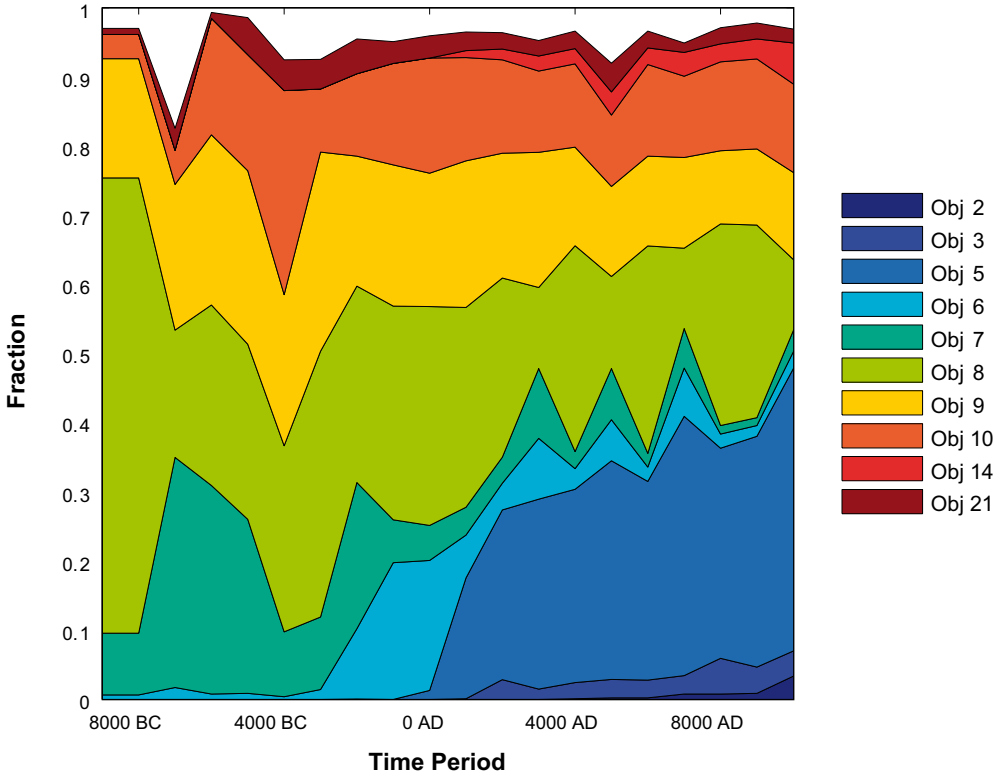

Figure 3-2. *Distribution of the release fractions between landscape objects in the Laxemar model for different times in the interglacial period.*

Simulation periods for other climatic conditions

For the glacial conditions the simulations were carried over 120,000 years, i.e. covering the whole period of the Weichselian glacial cycle. Ice-marginal conditions are worse than ice-covered condtions in radiological impact terms. Thus, even though ice-marginal conditions are likely to be transitory, they have be taken to persist throughout the whole of glacial periods. The simulations for permafrost conditions were carried out for the period from 8,000 BC to 60,000 AD. For greenhouse conditions it was assumed that the interglacial period is prolonged until 60,000 AD, i.e. the same simulation period as for permafrost conditions was used. Note that in the greenhouse variant a protracted interglacial period is expected to occur.

3.2.2 Complementary calculation variants

To study the effect of the start time and location of the releases, a series of complementary simulation variants were carry out for Forsmark. Similar simulations were not carried out for Laxemar, but are planned for future studies.

In one group of complementary variants the start time of the releases was changed to the beginning of each thousand year interval (this resulted in 18 variants from 8,000 BC to 9,000 AD). The purpose of these variant calculations is to investigate the validity of the assumption that starting releases at the beginning of an interglacial period (i.e. at 8,000 BC) is conservative compared to cases in which releases start at some point in time during an interglacial period.

The assumed input of 1 Bq/y is distributed between existing landscape objects according to the release fractions given in Table 3-2 (i.e. 1Bq/y multiplied by the corresponding fraction was released to each object every year from the starting time to 10,000 AD). These variants are hereafter called 8,000 BC-All, 7,000 BC-All, etc depending on the start time of the releases.

Table 3-2. Fraction of discharge points in different objects of the landscape at the Forsmark site for different times in an interglacial period.

Object	8,000 BC	7,000 BC	6,000 BC	5,000 BC	4,000 BC	3,000 BC	2,000 BC	1,000 BC	0 AD	1,000 AD	2,000 AD	3,000 AD	4,000 AD	5,000 AD	6,000 AD	7,000 AD	8,000 AD	9,000 AD
1	0	0	0	0	0	0	0	0	0	0	0	0	0	0	0	0	0	0
2	0	0	0	0	0	0	0	0	0	0	0	0	0	0	0	0	0	0
3	0	0	0	0	0	0	0	0	0	0	0	0	0	0	0	0	0.014	0.147
4	0	0	0	0	0	0	0	0	0	0	0	0	0	0	0	0	0	0
5	0	0	0	0	0	0	0	0	0	0	0	0	0	0	0	0.002	0.034	0.043
6	0	0	0	0	0	0	0	0	0	0	0	0	0	0	0	0	0	0.001
7	0	0	0	0	0	0	0	0	0	0	0	0	0	0	0	0.002	0.004	0.002
8	0	0	0	0	0	0	0	0	0	0	0	0	0	0	0	0	0	0.001
9	0	0	0	0	0	0	0	0	0	0	0	0	0	0	0	0	0	0
10	0	0	0	0	0	0	0	0	0	0	0	0	0	0	0	0.005	0.011	0.015
11	0	0	0	0	0	0	0	0	0	0	0	0	0	0.116	0.563	0.585	0.456	0.327
12	0	0	0	0	0	0	0	0	0	0	0	0	0	0	0	0	0	0
13	0	0	0	0	0	0	0	0	0	0	0	0	0	0	0	0	0	0
14	0	0	0	0	0	0	0	0	0	0	0	0	0.001	0.021	0.008	0.005	0.006	0.002
15	0	0	0	0	0	0	0	0	0	0	0	0	0	0	0	0	0	0
16	0	0	0	0	0	0	0	0	0	0	0	0	0.072	0.057	0.034	0.023	0.024	0.023
17	1	1	1	1	1	1	1	1	1	1	0.57	0.639	0.675	0.506	0.281	0.284	0.344	0.313
18	0	0	0	0	0	0	0	0	0	0	0.241	0.297	0.226	0.296	0.111	0.09	0.1	0.12
19	0	0	0	0	0	0	0	0	0	0	0	0	0	0	0	0	0	0
20	0	0	0	0	0	0	0	0	0	0	0	0	0	0	0	0	0	0
21	0	0	0	0	0	0	0	0	0	0	0	0	0	0.001	0.002	0.005	0.006	0.006
22	0	0	0	0	0	0	0	0	0	0	0	0	0	0	0	0	0	0
23	0	0	0	0	0	0	0	0	0	0	0.189	0.064	0.025	0.003	0.001	0	0	0
24	0	0	0	0	0	0	0	0	0	0	0	0	0	0	0	0	0	0
25	0	0	0	0	0	0	0	0	0	0	0	0	0	0	0	0	0	0

Table 3-3. Fraction of discharge points in different objects of the landscape at the Laxemar site for different times in an interglacial period.

Object	9,000 BC	8,000 BC	7,000 BC	6,000 BC	5,000 BC	4,000 BC	3,000 BC	2,000 BC	1,000 BC	0 AD	1,000 AD	2,000 AD	3,000 AD	4,000 AD	5,000 AD	6,000 AD	7,000 AD	8,000 AD	9,000 AD	10,000 AD
1	0	0	0	0	0	0	0	0	0	0	0	0	0	0	0	0	0	0	0	0
2	0	0	0	0	0	0	0	0	0	0	0	0	0	0.001	0.002	0.002	0.008	0.007	0.009	0.034
3	0	0	0	0	0	0	0	0	0	0	0.001	0.028	0.015	0.023	0.026	0.026	0.027	0.052	0.038	0.036
4	0	0	0	0	0	0	0	0	0	0	0	0	0	0	0	0	0	0	0	0
5	0	0	0	0	0	0	0	0	0	0.013	0.175	0.245	0.275	0.279	0.316	0.287	0.375	0.304	0.334	0.409
6	0.006	0.006	0.017	0.008	0.009	0.004	0.014	0.102	0.197	0.188	0.062	0.039	0.088	0.03	0.059	0.021	0.07	0.02	0.016	0.024
7	0.089	0.089	0.333	0.301	0.252	0.094	0.105	0.211	0.062	0.051	0.04	0.038	0.101	0.025	0.074	0.02	0.057	0.012	0.011	0.031
8	0.658	0.658	0.184	0.261	0.253	0.269	0.384	0.284	0.309	0.316	0.289	0.259	0.117	0.298	0.133	0.3	0.116	0.291	0.278	0.102
9	0.172	0.172	0.211	0.246	0.251	0.218	0.288	0.188	0.204	0.193	0.212	0.18	0.195	0.143	0.13	0.13	0.131	0.106	0.11	0.126
10	0.035	0.035	0.049	0.169	0.168	0.295	0.091	0.119	0.147	0.166	0.149	0.135	0.118	0.12	0.103	0.132	0.118	0.129	0.13	0.128
11	0	0	0	0	0	0	0	0	0	0.001	0.006	0.01	0.015	0.015	0.016	0.015	0.017	0.013	0.008	0.013
12	0	0	0.003	0.001	0.004	0.071	0.045	0.006	0.002	0.002	0.002	0.001	0	0	0.001	0	0	0	0	0
13	0	0	0	0	0	0	0	0	0	0	0	0	0	0	0	0	0	0	0	0
14	0	0	0	0	0	0	0	0	0	0	0.01	0.015	0.021	0.022	0.033	0.024	0.034	0.026	0.029	0.06
15	0	0	0	0	0	0	0	0	0	0.017	0.013	0.005	0.01	0.004	0.009	0.002	0.01	0.001	0.002	0.004
16	0	0	0	0	0	0	0	0	0	0	0	0.002	0	0	0	0	0.002	0.001	0	0
17	0	0	0	0	0	0	0	0	0	0	0	0	0	0	0.001	0	0.001	0	0.001	0.002
18	0.018	0.018	0.082	0.004	0.004	0	0.024	0.008	0.008	0.004	0.005	0.003	0.007	0.002	0.038	0.004	0.006	0.002	0.001	0.003
19	0	0	0	0	0	0	0	0.01	0.031	0.011	0.006	0.008	0.006	0.008	0.013	0.009	0.012	0.009	0.008	0.008
20	0.012	0.012	0.089	0.002	0.007	0.005	0.005	0.02	0.008	0.006	0.003	0.007	0.008	0.003	0.004	0.004	0.003	0.002	0.002	0.002
21	0.009	0.009	0.032	0.008	0.054	0.045	0.043	0.05	0.031	0.032	0.027	0.024	0.023	0.025	0.042	0.024	0.013	0.024	0.023	0.02

The simulations for all such variants were carried out until 10,000 AD, i.e. as a maximum the accumulation time was 18,000 years (for the variant starting at 8,000 BC) and as a minimum 1,000 years (for the variant starting at 9,000 AD).

In the other group of calculation variants the start time of the releases was also changes to the beginning of each thousand year interval from 8,000 BC to 9,000 AD, but the release rate of 1 Bq/y was kept constant in only one object during the whole simulation period. Only objects that had a non-zero probability of receiving a release, according to Table 3-2, were considered. These variants are hereafter called 8,000 BC object 17, 7,000 BC object 17, etc. The simulations in all variants of this type were also carried out until 10,000 AD.

3.2.3 Simulation endpoints

The endpoints of the simulations were time series of the radionuclide inventory, expressed in units of Bq per Bq/y, in different compartments and the activity concentrations, expressed in Bq/m^3 or Bq/kg per Bq/y, in different environmental media, comprising of soils, waters and sediments.

3.3 Predictions for Forsmark

This section presents the results obtained for Forsmark for the interglacial period. For other scenarios (permafrost conditions, glacial period and greenhouse conditions) the LDF values were calculated directly (see Chapter 5), using the same methodology as that adopted for the interglacial scenario. The results are presented only for a representative set of radionuclides (see Section 3.1) for the calculation variant 8,000 BC-All, i.e. for unit releases starting from year 8,000 BC and distributed among the landscape objects according to the fractions given in Table 3-2. All results are given only for the landscape objects within the Grepen, i.e. excluding the Baltic Sea, where radionuclides will be strongly diluted, resulting in very low concentrations and dose rates. The results for the complementary variants are discussed in Chapter 4.

3.3.1 Radionuclide inventories in the landscape

Time dynamics of the inventories

The prediction of the time dynamics of the total inventory in the Grepen is shown in Figure 3-3. The total inventory in Grepen of radionuclides with very long half-life (Cl-36, Ni-59, Se-79, Tc-99, I-129, Cs-135 and Pu-239) increases monotonically and reaches a maximum or a value close to the maximum at the end of the simulation period (10,000 AD). The non-monotonic time variation observed for Am-241 and Ra-226 can be explained by their shorter half-lives. During the first 4,000 years of the Sea Period these radionuclides also show a monotonic increase. During this period, the fractions of accumulation bottoms in object 17, which receives all radionuclide releases (see Table 3-2 and Figure 3-1), is one, and therefore, the radionuclides are highly retained in the sediments.

The impact of the assumptions for the fraction of accumulation bottoms can be clearly seen from Figure 3-4 showing the time dynamics of the inventory in objects 17 and 3, which are the only two objects that exist in the Grepen during the Sea Period. The inventory in object 17 during the first 4,000 years of the Sea Period is high, whereas much lower values are observed in object 3, which does not receive direct releases from the geosphere, i.e. the radionuclide inputs to this object come solely from object 17. After year 4,000 BC and up to year 0 AD the fraction of accumulation bottoms is near zero and, therefore, there is no further retention in object 17 and a sharp increase of the inventory in object 3 takes place. Overall, most of the radionuclide retention during the Sea Period takes place in object 17, which has a much higher inventory than object 3. Since all future Terrestrial Objects emerge from object 3 due to land

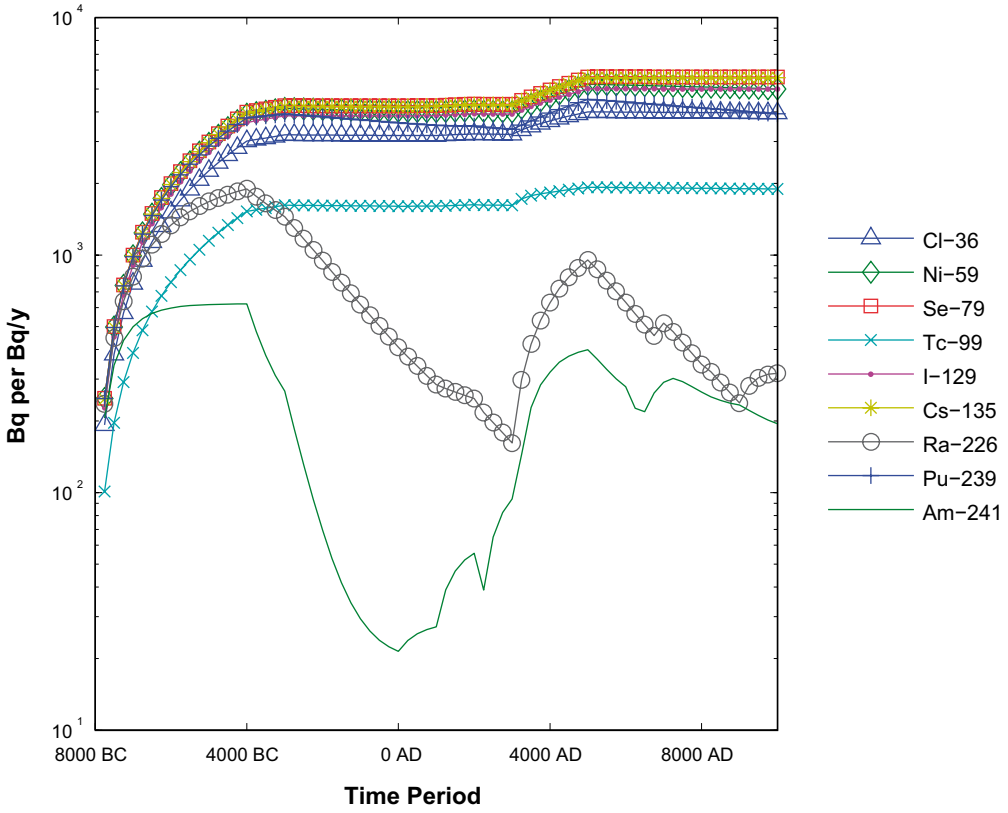

Figure 3-3. *Total inventory in the Grepen (sum of all objects excluding the Baltic Sea – object 1) for the variant 8,000 BC-All.*

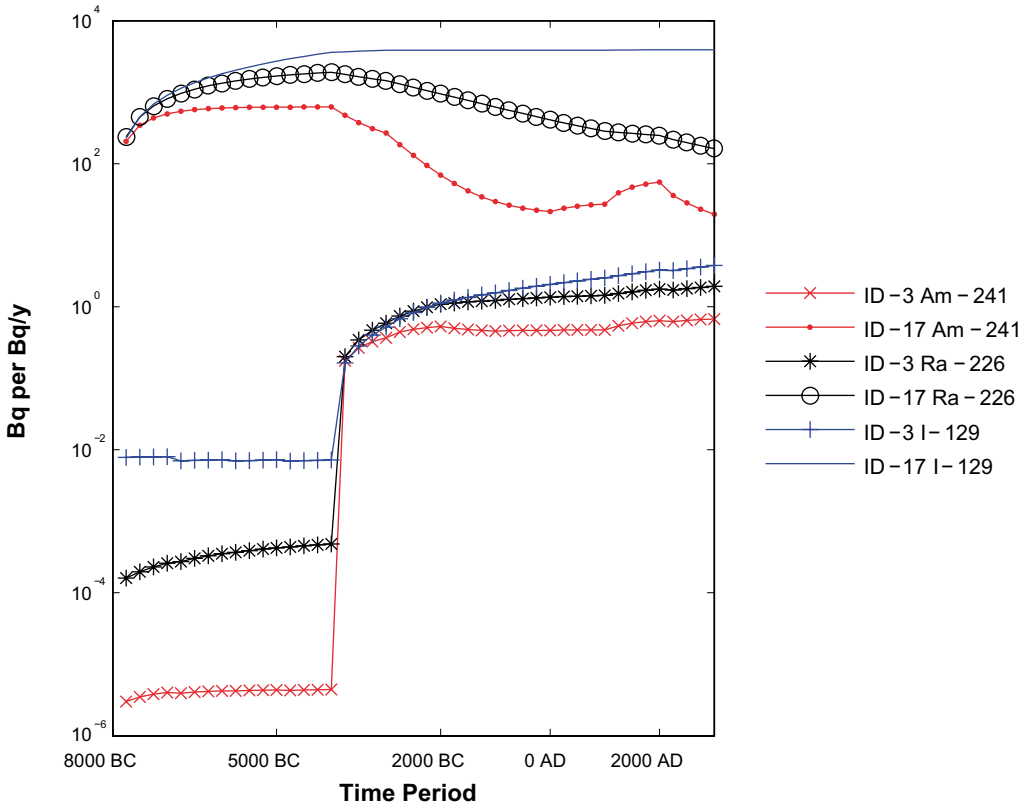

Figure 3-4. *Time variation of the total inventory in objects 17 and 3 during the Sea Period (from 8,000 BC to 2,000 AD) for the variant 8,000 BC-All.*

rise, we should expect a weak effect of accumulation during the Sea Period on the radionuclide concentrations and the dose rates for these future Terrestrial Objects. Note that there are other sea objects that receive releases after 3,000 AD.

Retention of the radionuclides

The retention in the Grepen of the released long-lived radionuclides is between 10 and 40% at the end of the simulation period (Figure 3-5). The remaining fraction of the releases ends up in the Baltic Sea. Hence, the inventories of these radionuclides in the Grepen cannot be underestimated by more than a factor of 10. Lower values of inventories are observed for Am-241 and Ra-226 because of their shorter half-lives. The differences across radionuclides in the retained inventory can be fully explained by differences in their distribution coefficients (K_d) and/or the half-lives. For example, Tc-99 and Cl-36, which have low K_d values, showed the lowest retention; whereas radionuclides with high K_d values showed much higher retention. It should, however, be noted that the variation in the inventories is in general lower than the variation in the K_d values.

Spatial distribution of the retained radionuclides

All landscape objects have some radionuclide inventory at the end of the simulation period, independently of whether or not they receive a release fraction. This is illustrated in Figure 3-6, which shows the inventory of I-129 and Ra-226 in the different objects at year 10,000 AD. There is, however, a large variation across objects. The differences are more pronounced for I-129, which shows a difference of a factor of 10 between the two objects with the highest inventory. For both radionuclides, the highest inventory is observed in objects 11 and 17, which have the largest fraction of release points (see Table 3-2). Note that object 17 receives direct releases for the entire simulation period.

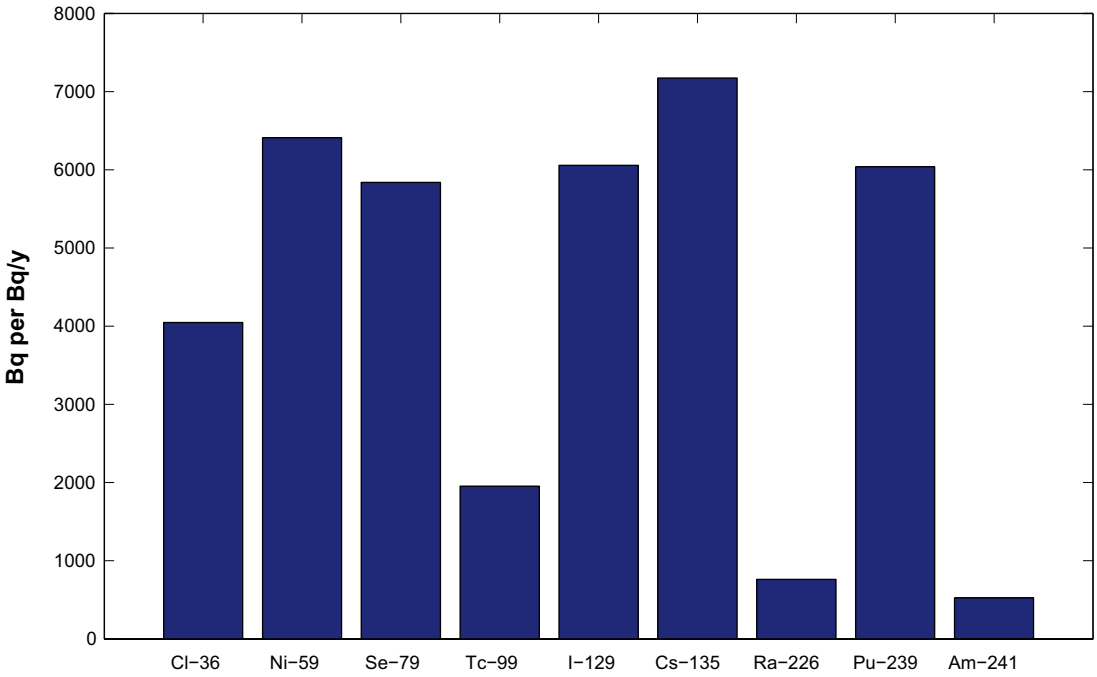

Figure 3-5. *Total radionuclide inventory retained in the Grepen at the end of the simulation period (10,000 AD) for the variant 8,000 BC-All.*

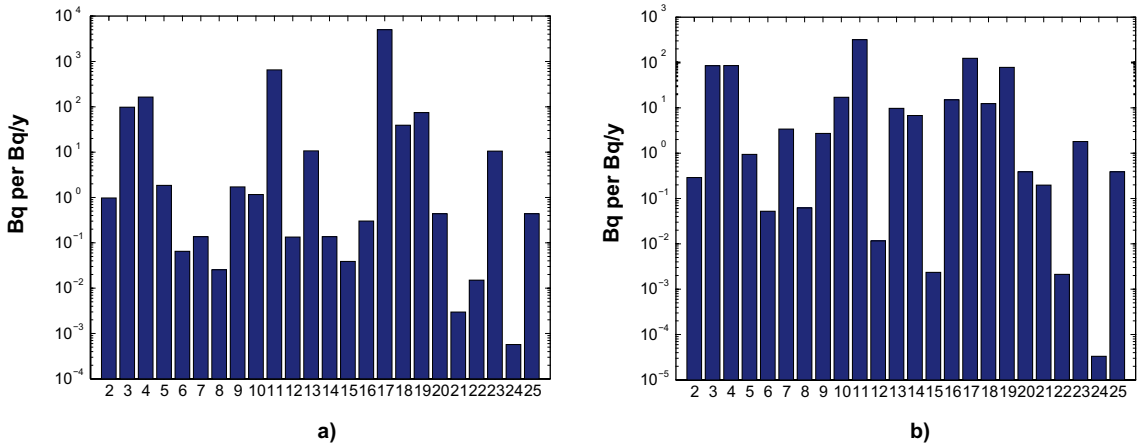

Figure 3-6. *Total inventory of I-129 (a) and Ra-226 (b) in different objects at the end of the simulation period (10,000 AD) for the variant 8,000 BC-All.*

Accessibility of the retained radionuclides

For exposure assessments, it is important to know the fraction of the retained radionuclides that can result in direct human exposure, which we call here "the accessible fraction". Radionuclides present in topsoil and water compartments at a given moment of time can give direct exposure and are considered to be accessible. In contrast, radionuclides present in the deep soil and sediment compartments can only give rise to exposures at future times and are, therefore, considered unaccessible.

Figure 3-7 shows estimations of the available fraction at the end of the whole simulation period in all objects in the Grepen excluding object 17. For most radionuclides, except Cl-36 and Tc-99, more than 40% of the inventory (note that for most radionuclides this fraction is nearly

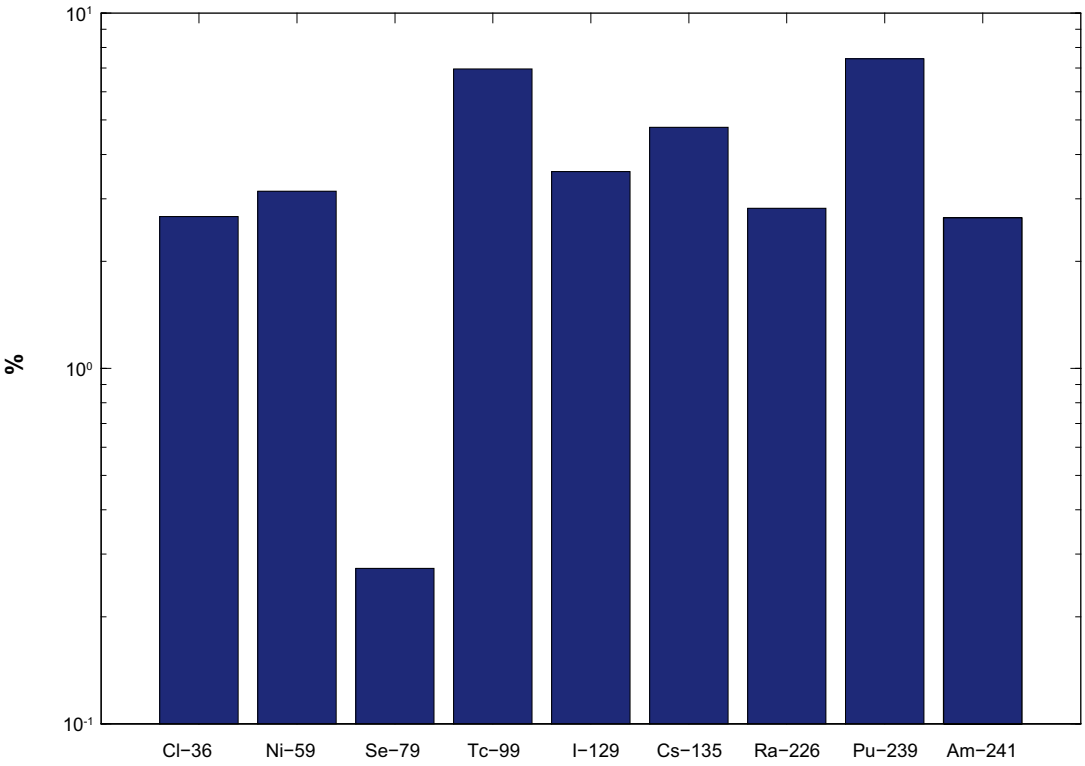

Figure 3-7. *Fraction of total inventory in percent, excluding object 17, in ecosystem compartments that can give dose at a given time (fraction of available inventory). The values are given for the end of the simulation period (10,000 AD) for the variant 8,000 BC-All.*

100%) is accessible. The lower values observed for Cl-36 and Tc-99 are explained by their higher mobility, which leads to fast release to object 3 with downstream fluxes, where these radionuclides accumulate in sediments.

Hence, for the objects in the Grepen, excluding object 17, calculated dose rates at a given time will capture most of the potential contribution to those dose rates from past releases, including the effect of accumulation. This is not the case for object 17, for which the inventory is mostly in "unaccessible" form. Hence, this object gives low dose rates at any given time, but may give higher dose rates at future times, for example if future human actions result in transfer of the inventory into an accessible form. As mentioned in Chapter 3, discharge points tend to cluster in this object. However, because of its properties, it is unlikely that object 17 would ever be used for agricultural purposes.

3.3.2 Activity concentrations in soils

Time dynamics of the activity concentrations in soils

Predictions of the maximum activity concentration in soils over all objects that have a soil compartment (forests mires and agricultural lands) are presented in Figure 3-8. Values are shown starting from year 3,000 AD, when the first object with a soil compartment appears in the landscape model. The activity concentrations start with a nonzero value corresponding to the inventory inherited from the predecessor object, mainly from marine or lake sediments. The observed differences across radionuclides can be explained by differences in the K_d values, with radionuclides with higher K_d values showing higher soil concentrations.

The activity concentrations in soil of forests, mires and agricultural lands show a slight decrease with time. Different time kinetics, as compared to other radionuclides, is observed for I-129 in the period between 5,000 AD and 6,000 AD when object 23 is transformed from mire to

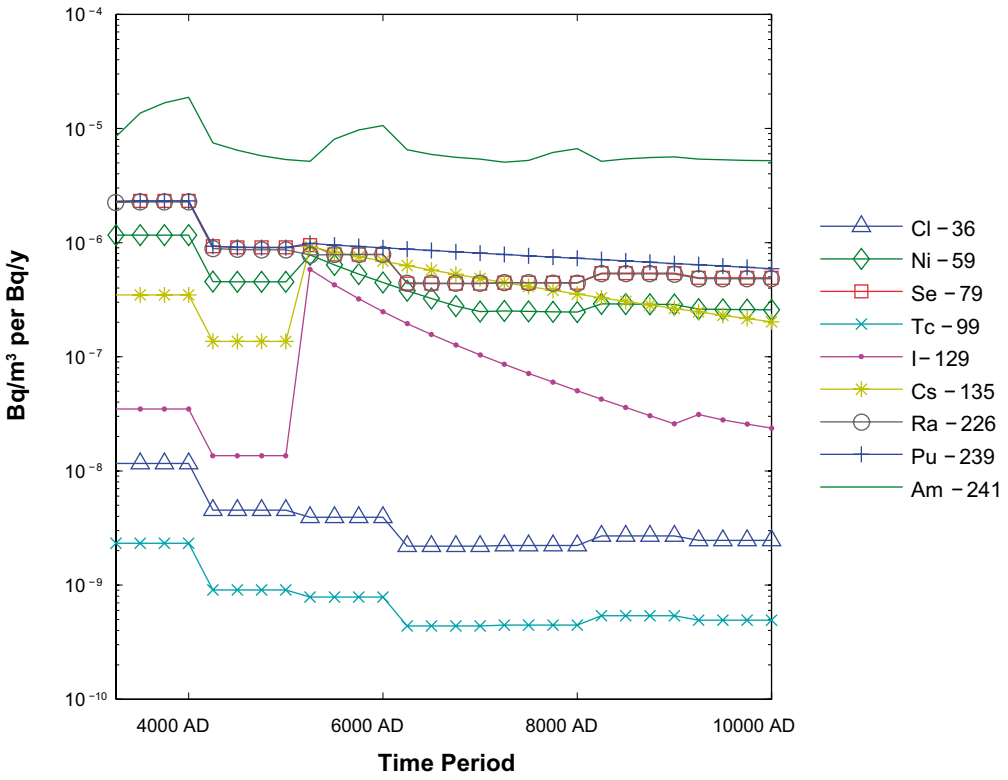

Figure 3-8. *Time variation from 3,000AD of the maximum radionuclide concentrations in soils of forests, mires and agricultural lands at Forsmark for the variant 8,000 BC-All.*

agricultural land. This seems to be an artefact of how K_d were varied in the transition from mire to agricultural land (see Figure 2-8). For I-129 a higher K_d is used for agricultural lands than for mires, while for all other radionuclides the opposite is true (with the exception of Cl-36 and Tc-99 for which very low K_d values are used in both ecosystem types). Overall, there is no substantial accumulation of radionuclides in topsoils during the Terrestrial Period. It should be notes that, as mentioned in Chapter 2, mires are assumed to be transformed to agricultural lands unless factors such as small size and boulder content makes this unlikely. This is not necessarily always cautious for estimating radiological impacts on humans. A mire that persisted for a long period, even though it could have been transformed to agricultural land, and was then transformed, could release a large pulse of radionuclides than if had been transformed immediately this became possible. Furthermore, early transformation of mires to agricultural land may not be cautious for exposure of biota other than humans.

Spatial distribution of soil activity concentrations

Pronounced differences in the activity concentrations in soil are observed between the different objects (Figure 3-9), with a few objects having concentrations more than 10 times higher than the rest of the objects. A pronounced variation of the dose rates for these objects can, therefore, be expected. Objects with the highest release fractions often show the highest concentrations. However, there are also differences in the spatial patterns observed for I-129 and Ra-226, that can be explained by differences in K_d and half-life. For example, objects 6 and 8 receive a small fraction of direct releases and this occurs only at the end of the simulation period, when these objects are mires. For these objects, the I-129 concentrations in soil are very low compared with other objects, whereas the Ra-226 concentrations are similar to the concentrations in objects that receive higher release fractions over a longer period. This difference can be explained, firstly by the assumption of a lower K_d value for I-129 than for Ra-226. Secondly, the shorter decay half-life of Ra-226 reduces the effect of the accumulation period on soil concentrations.

3.3.3 Activity concentrations in freshwaters

Time dynamics of the activity concentrations in freshwaters

The time dynamics of the maximum activity concentrations in the water compartment of freshwater objects appearing after the Sea Period is shown in Figure 3-10. The same time dynamics are observed for the mean concentrations across freshwater objects. The maximum radionuclide concentrations in fresh water (in lakes and running waters) for all radionuclides, except for Am-241 because of its shorter half-life, stabilise at the same value starting from

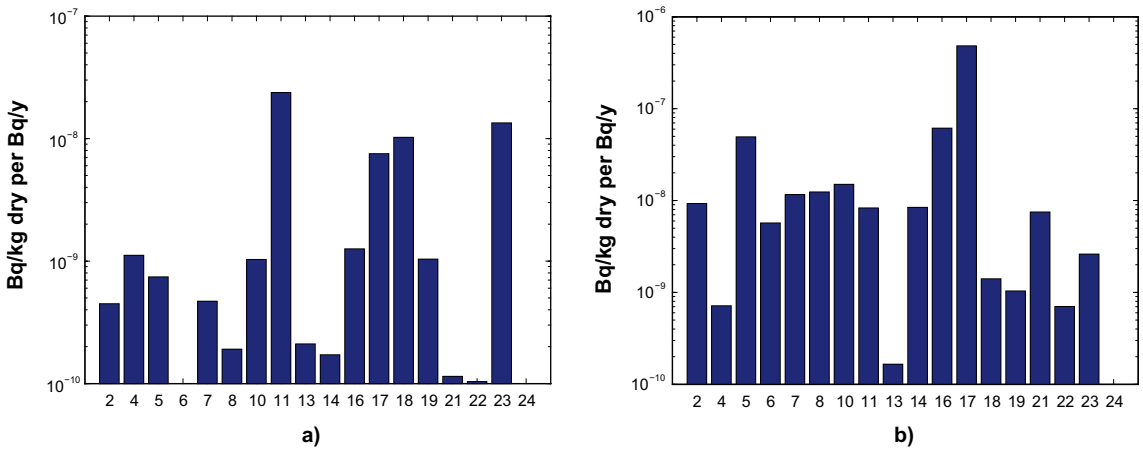

Figure 3-9. *Activity concentrations of I-129 (a) and Ra-226 (b) in soils of Terrestrial objects existing in Forsmark at 10,000 AD.*

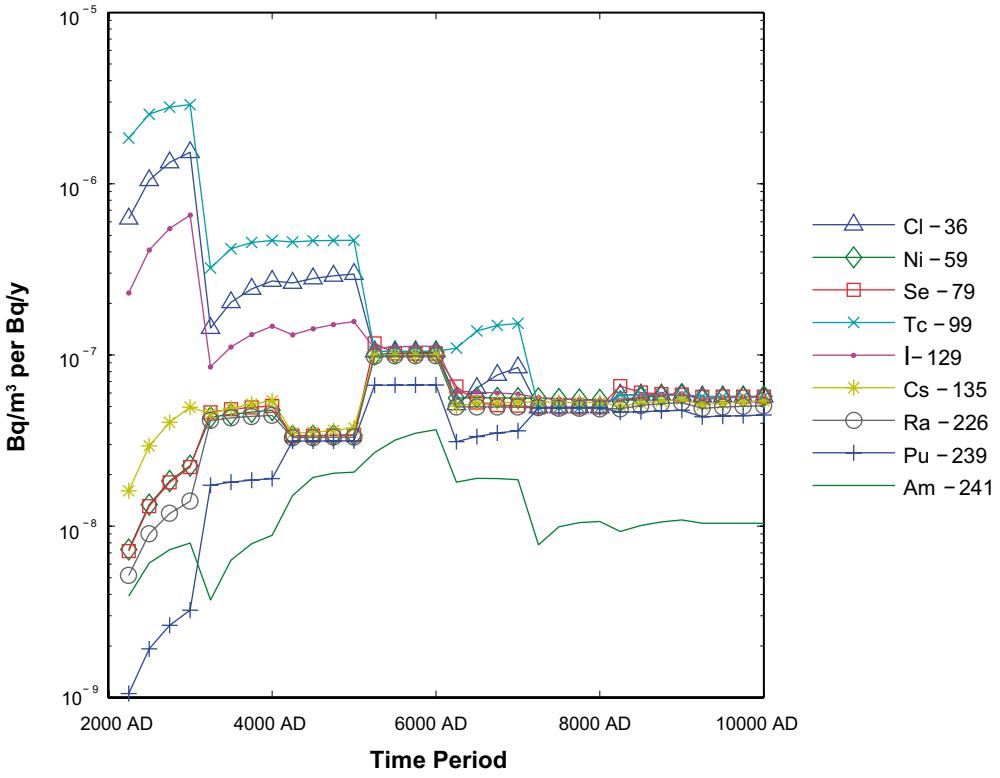

Figure 3-10. *Time variation of the maximum activity concentrations in waters of lakes and running water at Forsmark for the variant 8,000 BC-All.*

around 5,000 AD. The maximum concentration of the most mobile radionuclides (Tc-99, Cl-36 and I-129) starts from a higher value and decreases to the same level. Less mobile radionuclides, on the contrary, start from a lower value and increase to the common level. After 5,000 AD, the highest concentrations in fresh water are observed in the running water flowing through the mire objects. In the case of a continuous constant input rate, the concentrations in the water phase of the mire, as well as in soil pore water, tend to reach the same value for all elements, independent of their K_d value. The same behaviour was predicted in /Avila 2006b/ for forest ecosystems from model simulations and has been observed by /Sheppard et al. 1999/ in studies of heavy metals emissions from the mining industry. This stable concentrations in the water phase of mires explains the observed stabilisation of the radionuclide concentrations in running waters after 5,000 AD, as running waters receive radionuclides inputs with the pore water leaching from mires.

The reason for the difference in the kinetics of the mobile and less mobile radionuclides in the period from 2,000 AD to 5,000 AD needs to be further investigated. It seems that it could be explained by differences across radionuclides in sea water concentrations in objects 3 and 17 (see Section 3.3.4). The lakes that appear in this period originate from these objects.

Spatial distribution of activity concentrations in freshwaters

The highest between-object difference in freshwater activity concentrations is observed at the end of the simulation period. At this time, there are three freshwater objects left in the Grepen: two lakes and one running water. The two lakes showed similar activity concentrations (Figure 3-11), but the values are more than ten times higher for the running water. It should be noted that the running water cannot supply even a single person with food (see Table 4-1).

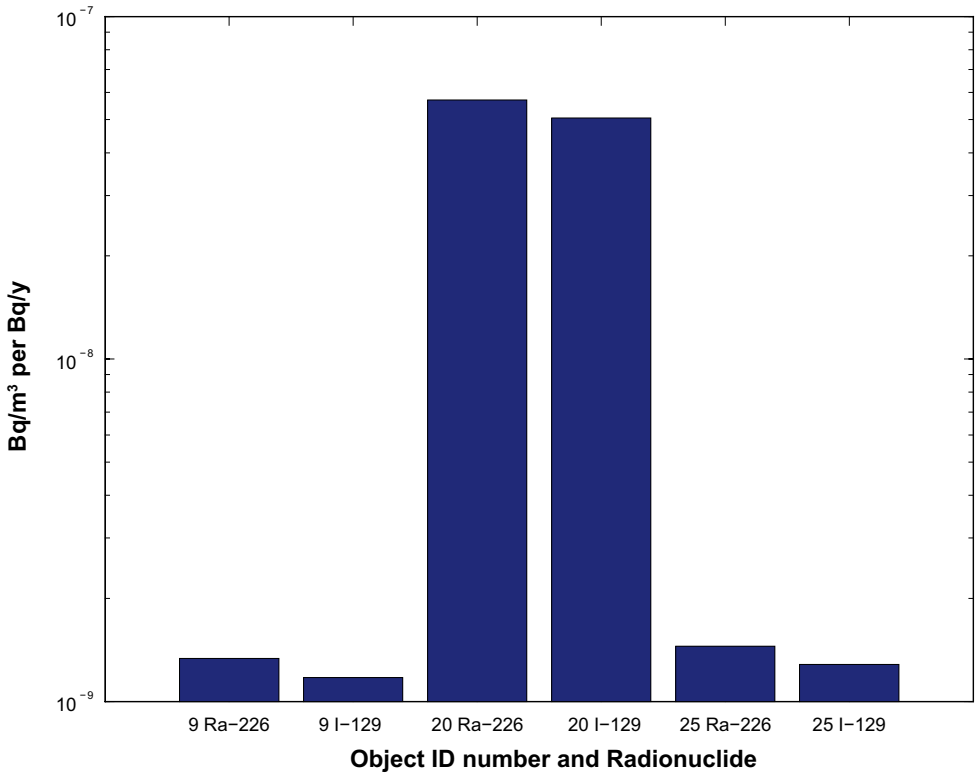

Figure 3-11. *Activity concentrations of I-129 and Ra-226 in water of lakes and running waters existing at Forsmark at 10,000 AD for the variant 8,000 BC-All.*

3.3.4 Activity concentrations in sea water

Time dynamics of the activity concentrations in sea water

The predicted time dynamics of the maximum activity concentrations in sea water for constant unit release rates are shown in Figure 3-12. An increasing trend is observed, except for the period from 2,000 AD to 5,000 AD when a decrease is observed, due to transformation of object 3 from sea to several terrestrial objects, which leads to a "loss" of inventory from the sea.

In the period from 8,000 BC to 4,000 BC pronounced differences are observed between the radionuclides, with the most mobile radionuclides showing the highest activity concentrations in water. During this period, there is a large fraction of accumulation bottoms in object 17, which receives all releases. This means that fractions of the released radionuclides are retained in sediments, which leads to lower activity concentrations in water. The effect is greatest for radionuclides that exhibit a high degree of sorption. In the period from 4,000 BC to 2,000 AD there is no further accumulation of the radionuclides in sediments, i.e. the radionuclides are directly released to water. Since there is a constant and equal input and output of all radionuclides, their concentrations in water approach the same value. After 2,000 AD, retention of radionuclides in bottom sediments begins again to occur, due to the increase in the fraction of accumulation bottoms. For this reason, between-radionuclide differences in activity concentrations in water begin again to appear. This explains why freshwater objects that emerge during this period start from different concentration levels (see Section 3.4.3). At the end of the simulation period, the activity concentrations in sea water are similar for all radionuclides (Figure 3-13). The largest difference is observed for Am-241, because of its shorter decay half-life. This confirms the observation that concentrations in water tend to stabilise with time and become less dependent on K_d values.

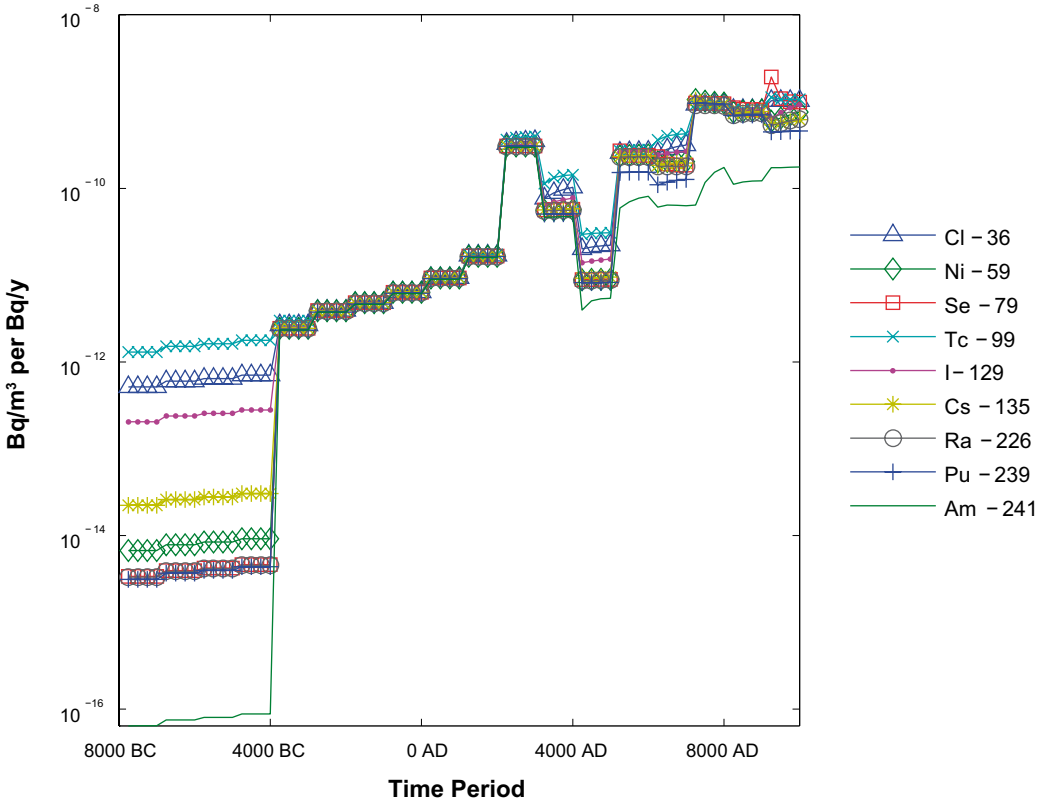

Figure 3-12. *Time variation of the maximum radionuclide concentrations in sea water at Forsmark for the variant 8,000 BC-All.*

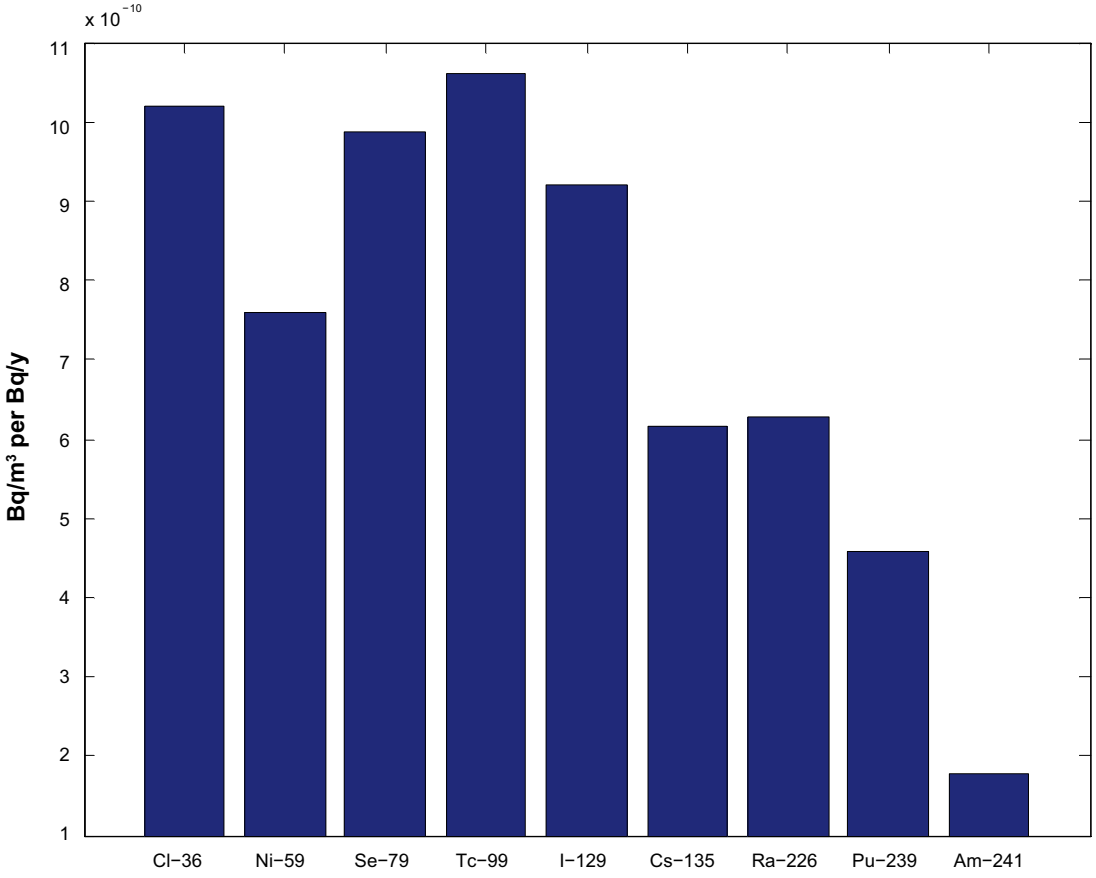

Figure 3-13. *Maximum activity concentrations of radionuclides in sea water of sea Objects existing at Forsmark at 10,000 AD for the variant 8,000 BC-All.*

Spatial distribution of activity concentrations in sea water

During most of the simulation period, the between-object differences in sea water concentrations were small and they approached nearly the same value for the various radionuclides at the end of the period.

3.4 Predictions for Laxemar

This section presents the results obtained for Laxemar for the interglacial period. For other climate conditions (permafrost, glacial period and greenhouse) the LDF values were calculated directly (see Chapter 5), using the same methodology as for the interglacial period. The results are presented only for a representative set of radionuclides (see Section 3.1) for unit release rates starting from year 8,000 BC and distributed among the landscape objects according to the fractions given in Table 3-3. All results are given only for the landscape objects in the area with release points, i.e. excluding the Baltic Sea, where radionuclides will be strongly diluted, resulting in very low concentrations and dose rates.

3.4.1 Radionuclide inventories in the landscape

Time dynamics of the inventories

The prediction of time dynamics of the inventory in all landscape objects (total inventory per unit release rate) excluding the Baltic Sea (object 1) is shown in Figure 3-14. For all radionuclides the total inventory increases monotonically during the Sea Period (8,000 BC to 3,000 BC). This is true even for Am-241 which has a shorter half-life. This behavior is consistent with the persistence of accumulation conditions in the sediments during the whole period, as determined by the presence of accumulation bottoms. For Pu-239 and Am-241, which have the highest K_d values, a continuous monotonic increase is observed during the whole simulation period with a tendency for stabilisation at the end of the period. Different time dynamics are observed for the most mobile radionuclides, Cl-36 and Tc-99, with decreases

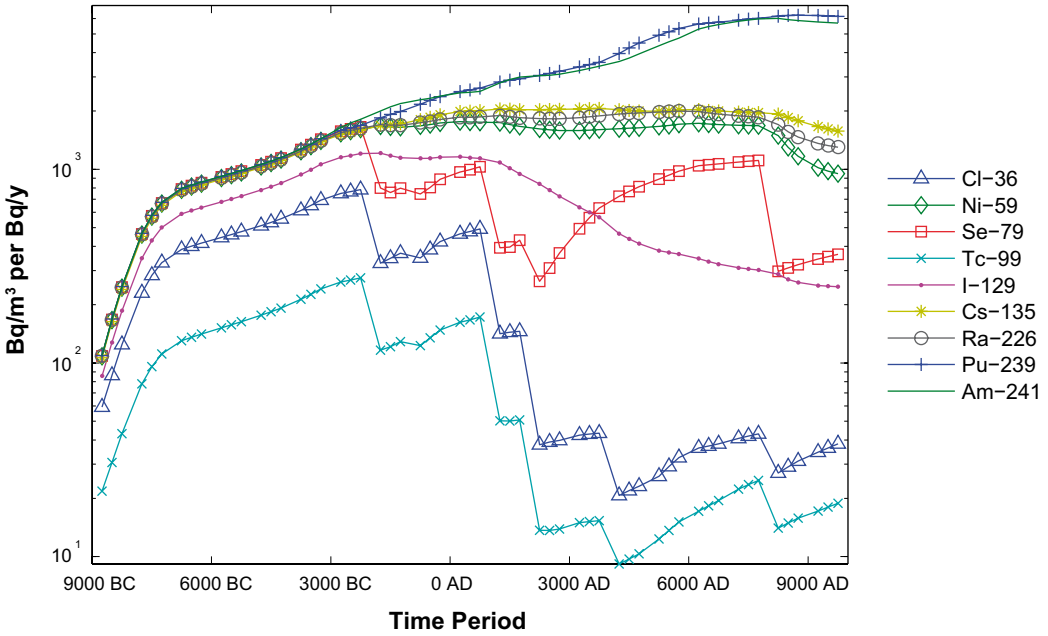

Figure 3-14. *Total inventory in all objects in the Laxemar model (sum of all objects excluding the Baltic Sea – object 1) for continuous release rates of 1 Bq/y to all objects of the landscape, with release fractions as given in Table 3-3.*

during the Coastal Period (3,000 BC to 4,000AD) and stabilisation during the Terrestrial Period. The behaviour of other radionuclides lies between these two extremes. The observed between-radionuclide differences in the time dynamics are consistent with the assumed between-radionuclide differences in K_d values (see Figure 2-8). For instance, the non-monotonic pattern of the time dynamics of the Se-79 inventories is explained by the large differences in the K_d values between different ecosystems.

Retention of radionuclides

Retention in the landscape varies strongly between radionuclides (Figure 3-15), ranging at the end of the simulation period from less than 1% for the most mobile radionuclides (Tc-99 and Cl-36) to around 30% for the radionuclides with the highest K_d values (Pu-239 and Am-241). The remaining fraction of the releases ends up in the Baltic Sea. As for Forsmark, the between-radionuclide variation in the retained inventories is lower than the assumed variability of K_d values. At the end of the simulation period, the retained fractions of all radionuclides, except for Pu-239 and Am-241, are close to the values for Forsmark, when object 17 is not included.

Spatial distribution of the retained radionuclides

All landscape objects retain some radionuclide inventory at the end of the simulation period, independent of whether or not they receive a release fraction. This is illustrated in Figure 3-16, which shows the inventory of I-129 and Ra-226 in the different objects at year 10,000 AD, excluding the Baltic Sea (object 1) and running waters (objects 22, 23, 24 and 25), which were not considered in the mass balance. There is variation across objects, which is less pronounced than the variations at Forsmark. The differences are slightly more pronounced for I-129 than for Ra-226. There is no notable relationship between the inventory in an object and the fraction of release points directed to that object (see Table 3-3).

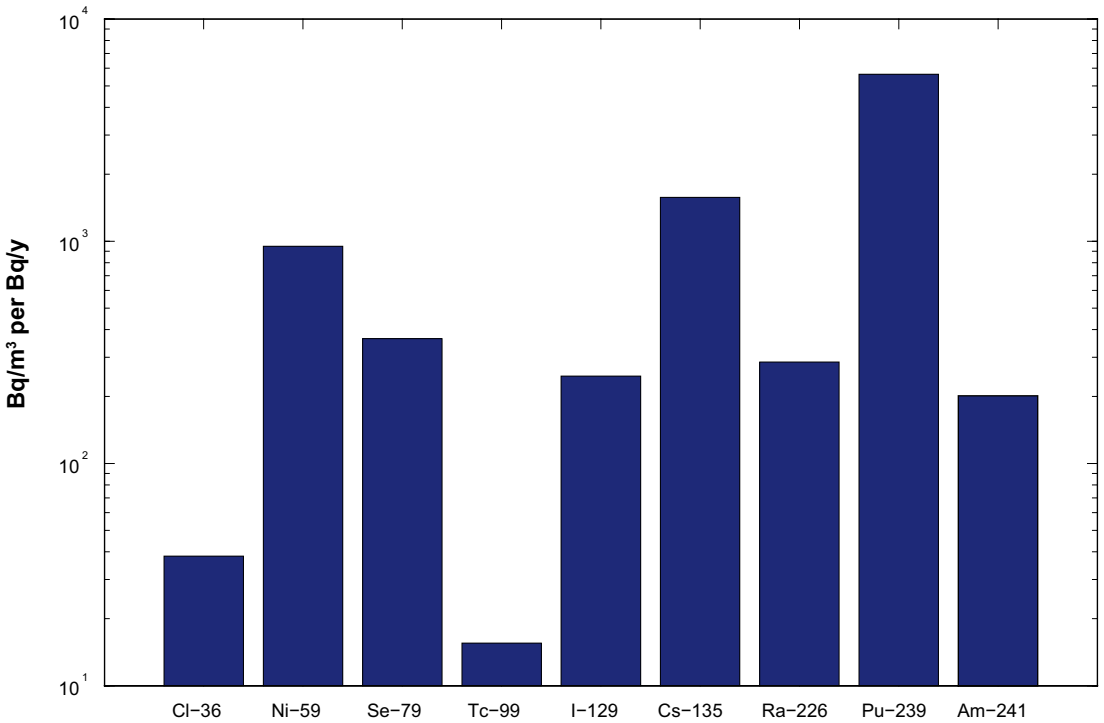

Figure 3-15. *Total radionuclide inventory retained in all objects, excluding the Baltic Sea (object 1), of Laxemar at the end of the simulation period (10,000 AD).*

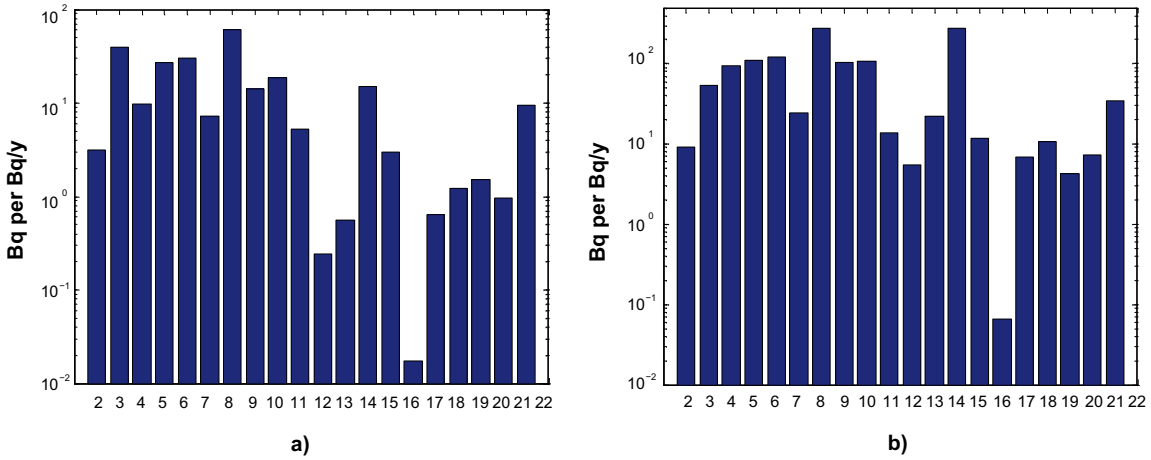

Figure 3-16. *Inventory of I-129 (a) and Ra-226 (b) in different landscape objects at Laxemar, excluding the Baltic Sea (object 1) and running waters (objects 22, 23, 24 and 25) at the end of the simulation period (10,000 AD).*

Accessibility of the retained radionuclides

At the end of the simulation period only a small percentage of the retained radionuclides, less than 10%, is available (Figure 3-17). It should noted that the accessible fraction at early periods can be higher. However, the radionuclides in running waters, which are accessible for immediate exposure, are not included in the accesible fraction. Also it is important to estimate the potential dose rates from unaccessible radionuclides for example by calculating latent dose rates.

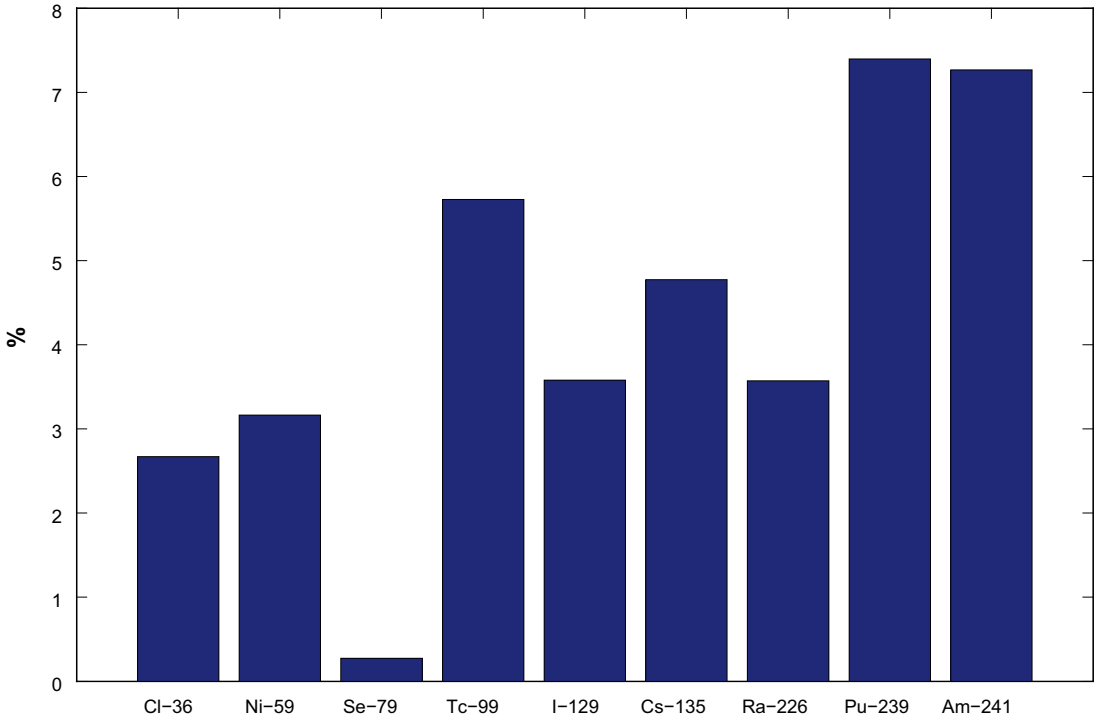

Figure 3-17. *Percentage of the total inventory in ecosystem compartments that can give dose at a given time (available fraction). The values are given for the end of the simulation period (10,000 AD).*

3.4.2 Activity concentrations in soils

Time dynamics of activity concentrations in soils

Predictions of the maximum activity concentrations in soil over all Laxemar objects with a soil compartment (forests, mires and agricultural lands) are presented in Figure 3-18. Values are shown starting from year 3,000 BC, when the first object with a soil compartment appears in the landscape model. The activity concentrations start with at a nonzero value corresponding to the inventory inherited from the predecessor object. The observed differences across radionuclides can be explained by differences in K_d values, with radionuclides with higher K_d values having higher soil concentrations.

The soil activity concentrations at the end of the simulation period are nearly the same or in some cases lower than at the beginning of the Coastal Period (3,000 BC). For Pu-239 there is a slight increase. Hence, as for Forsmark, there is no sunstantial accumulation of radionuclides in topsoils during the Terrestrial Period.

Spatial distribution of soil activity concentrations

Pronounced differences in the activity concentrations in soil are observed between the different objects (Figure 3-19), with a few objects having concentrations more than 10 times higher than the rest of the objects. A pronounced variation of the dose ratess for these objects can therefore be expected. Objects with the highest release fractions often show higher concentrations. As for Forsmark, there are differences between I-129 and Ra-226, in the spatial patterns, which can be explained by their differences in K_d and half-life. For example, object 6 receives a relatively small fraction of direct releases, but shows one of the highest concentration values of I-129, but not of Ra-226. This is because this object receives relatively higher inputs of I-129 than of Ra-226 from other landscape objects, due to the higher mobility of I-129. Also, this object receives direct inputs mainly at the beginning of the Coastal Period and therefore substantial decay of Ra-226 has taken place by the end of the simulation period.

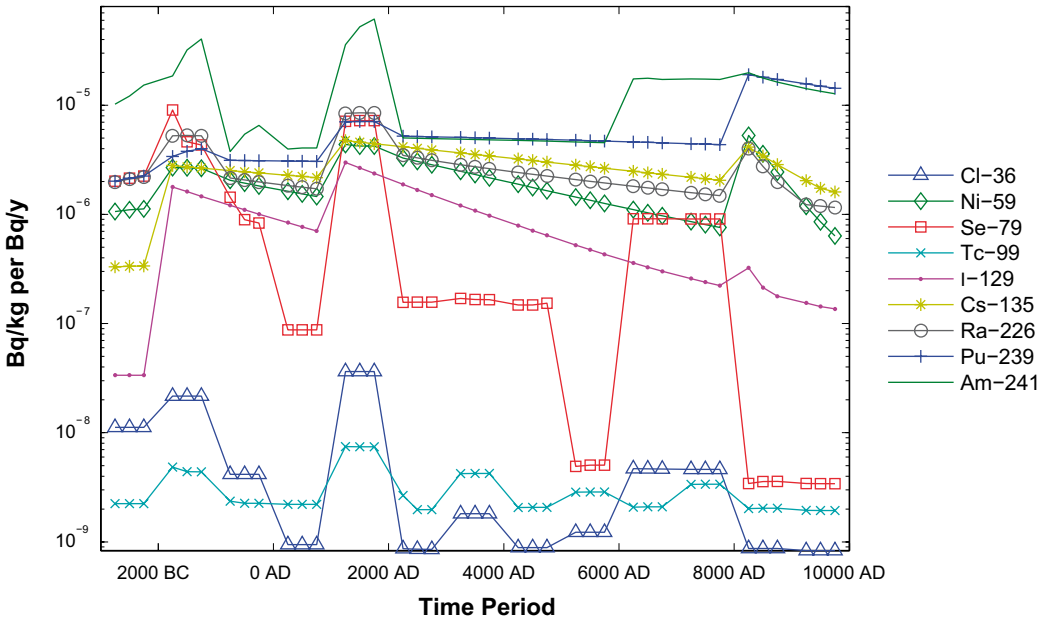

Figure 3-18. *Time dynamics at Laxemar of the maximum activity concentrations in soil during the Coastal and Terrestrial Periods.*

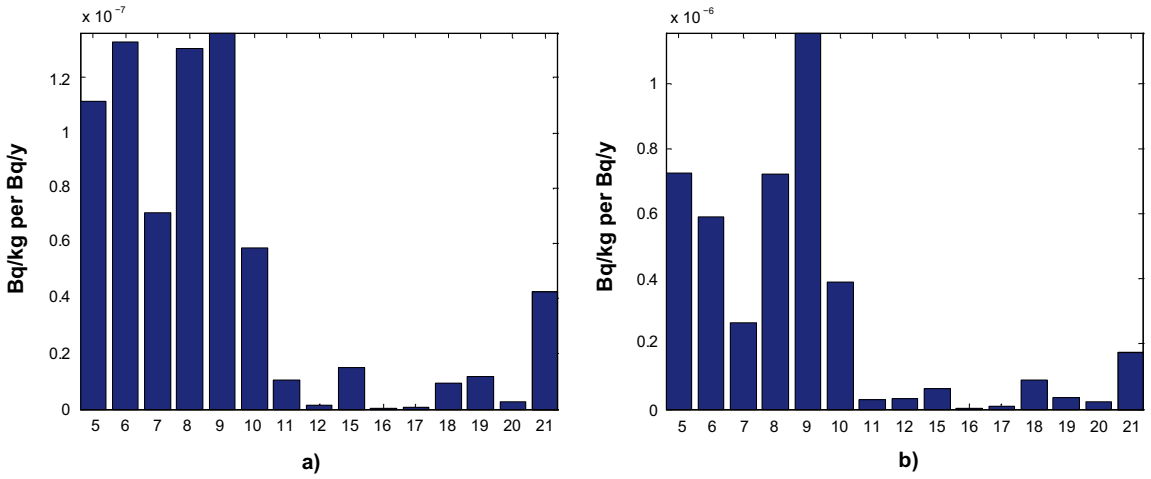

Figure 3-19. *Activity concentrations of I-129 (a) and Ra-226 (b) in soils of terrestrial Objects existing in Laxemar at 10,000 AD.*

3.4.3 Activity concentrations in freshwaters

Time dynamics of the activity concentrations in freshwaters

The time dynamics of the maximum activity concentrations in the water compartments of freshwater objects appearing after the Sea Period is shown in Figure 3-20. The same time dynamics is observed for the mean concentrations across freshwater objects. As for Forsmark, the maximum radionuclide concentrations in waters of lakes and running waters of all radionuclides, except for Am-241, stabilise at the same value from around 2,000 AD. After 2,000 AD the highest concentrations in fresh water are observed in the running water flowing through the mire objects and receiving inputs also from agricultural lands. As explained above for Forsmark, this is due to stabilisation of the activity concentrations in pore waters, which is characteristic for situations with continuous uniform input rates.

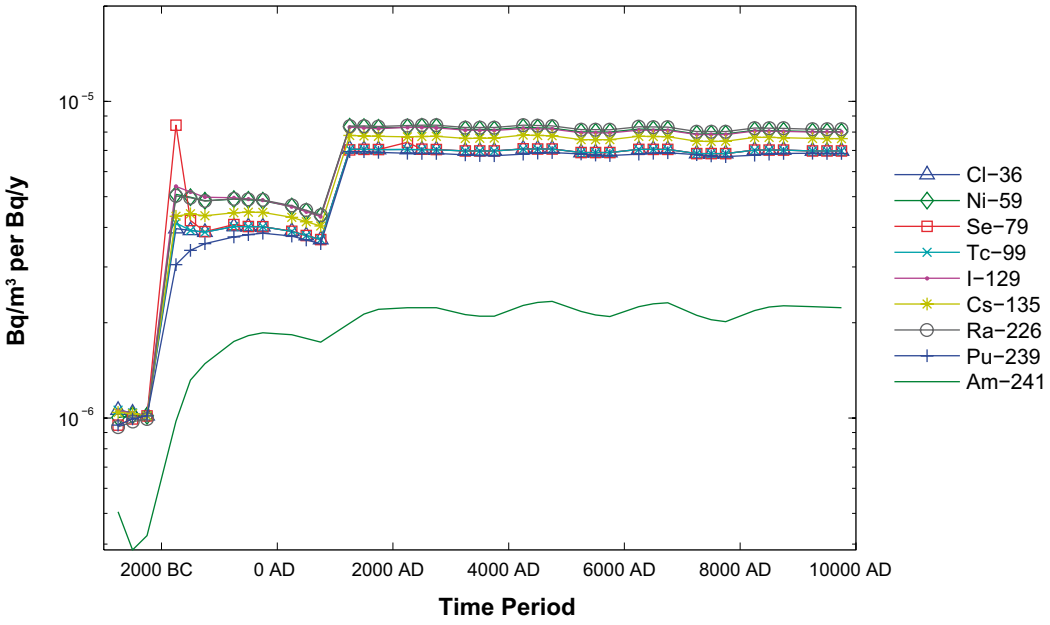

Figure 3-20. *Time dynamics of the maximum activity concentrations in waters of freshwater objects at Laxemar during the Coastal and Terrestrial Periods.*

Spatial distribution of activity concentrations in freshwaters

A high between-objects difference in freshwater activity concentrations is observed at the end of the simulation period (Figure 3-21). Object 25, which is a running water, shows much higher concentrations than all other freshwater objects. This running water is the largest represented in the simulation and receives inputs from several Terrestrial Objects, which in combination with the assumption of complete instantaneous mixing of the releases in the Running Water water, leads to high activity concentrations. It should be noted that this running water can supply less than one person with food (see Table 4-2).

From examination of Figure 3-21 it can be seen, that the activity concentrations of I-129 and Ra-226 are nearly the same in each of the freshwater objects. Hence each object receives nearly the same input of each of these two radionuclides.

3.4.4 Activity concentrations in sea water

Time dynamics of the activity concentrations in sea water

The predicted time dynamics of the maximum activity concentrations in sea water objects for the case of a constant unit release rates distributed in the landscape is shown in Figure 3-22. An increasing non-monotonic trend is observed for all radionuclides with some periods of decrease due to transformations in the objects from sea to Terrestrial Objects, leading to "losses" of inventory from the sea. The form of the time dynamics resembles the time variation of the fraction of accumulation bottoms and the area of the sea objects that receive the largest fraction of the direct releases (see Figures 2-6 and 2-7).

The activity concentrations of different radionuclides are very similar during the whole simulation period. The largest difference is observed for Am-241, which shows lower values during most part of the simulation period. Lower values for all radionuclides are observed at the end of simulation period, due to greater retention in sediments (Figure 3-23).

Spatial distribution of activity concentrations in sea water

The between-object differences in sea water concentrations were small through most part of the simulation period and approached nearly the same value for different radionuclides at the end of the period.

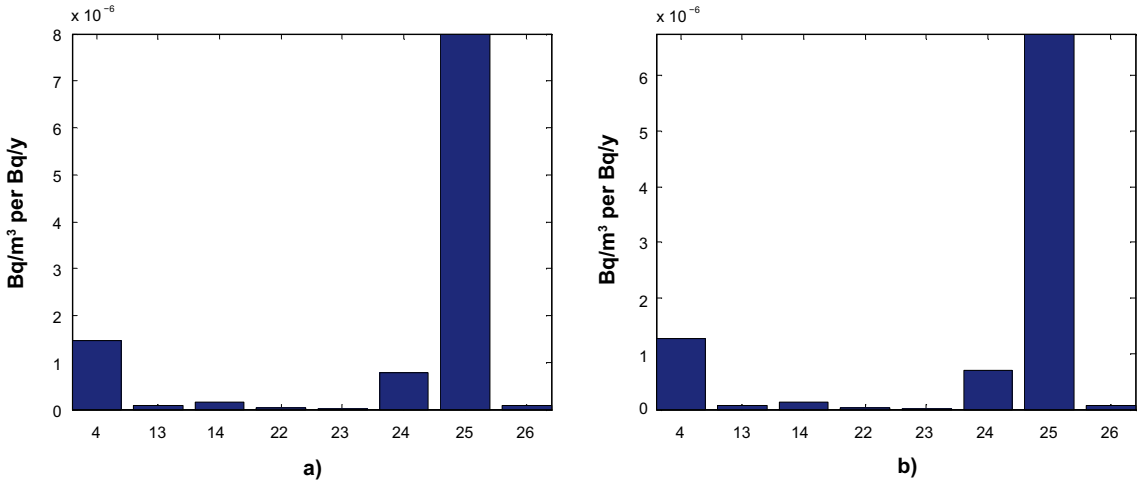

Figure 3-21. *Activity concentrations of I-129 (a) and Ra-226 (b) in Freshwater Objects existing at Laxemar at 10,000 AD.*

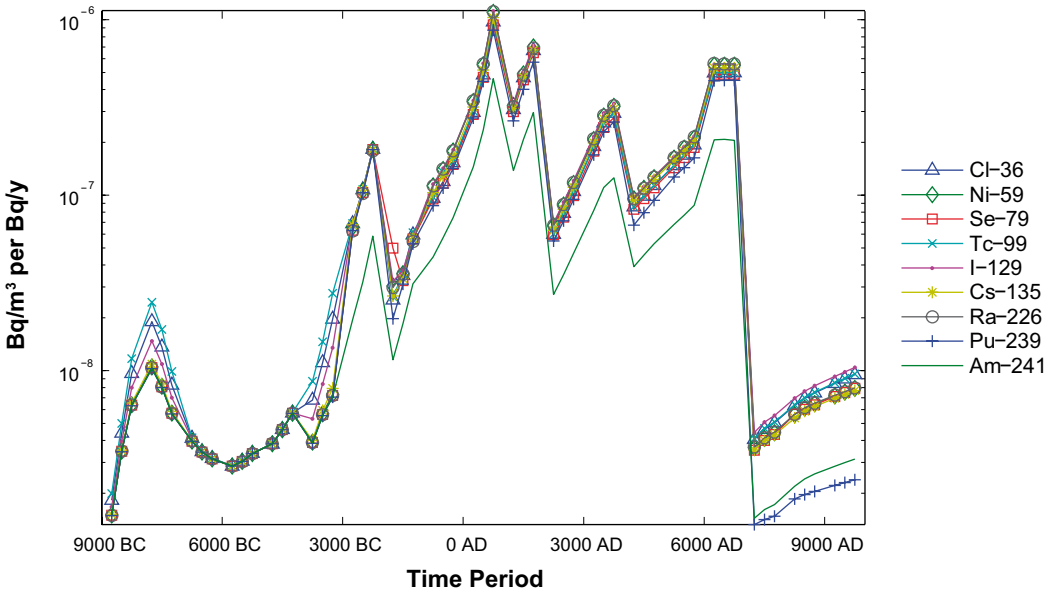

Figure 3-22. *Time dynamics of the maximum activity concentrations in water of Sea Objects at Laxemar.*

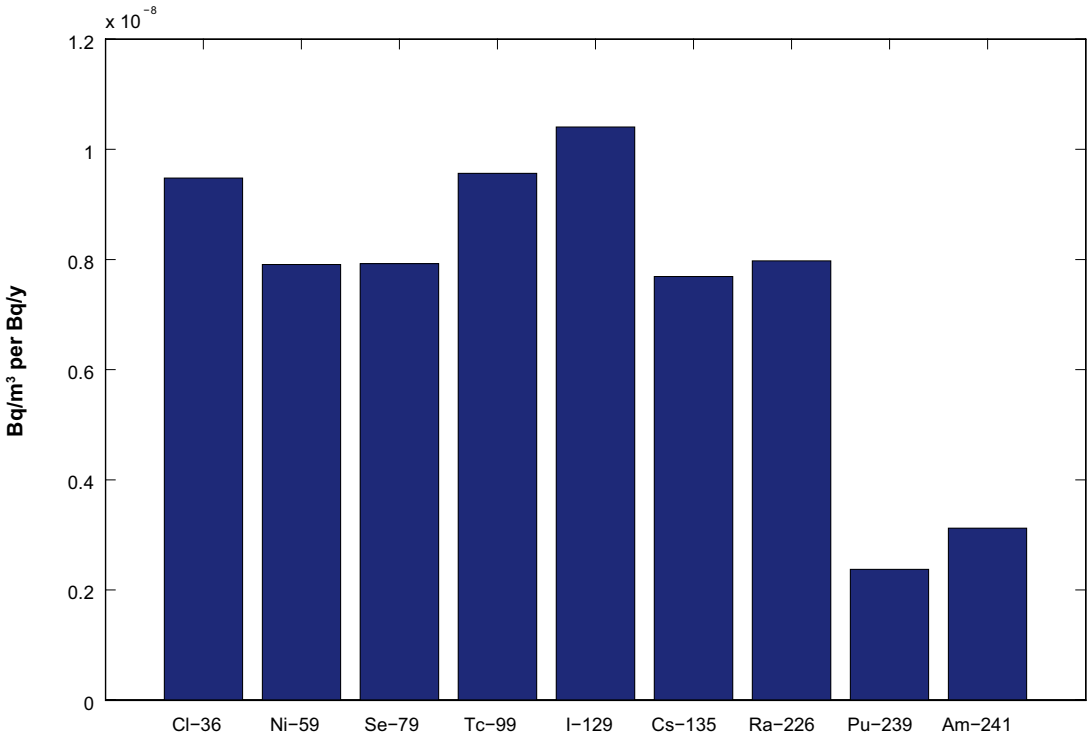

Figure 3-23. *Maximum activity concentrations of radionuclides in sea water of Sea Objects existing at Laxemar at 10,000 AD.*

4 Dose Conversion Factors

The predictions of the distribution of radionuclides in the landscape for unit release rates, obtained as described in Chapter 3, were used to derive time-dependent Dose Conversion Factors for each landscape object and for the whole landscape. Although the Dose Conversion Factors were derived for all radionuclides included in the study (Table 3-1), the discussion of the results in this section is focussed on the selected set of radionuclides (see Chapter 3).

4.1 Dose Conversion Factors for each landscape object

In order to ensure that the dose to a representative member of the most exposed subgroup in the population was identified, calculations of the dose rate were performed for population groups taken to occupy a single landscape object and obtain all their resources from that object. This ensures that individuals make maximum reasonable use of local resources and that the dose rate arising from utilising the most potentially contaminated part of the landscape is not diluted by utilisation of less contaminated parts of the landscape.

Having adopted this approach, it is possible to estimate not only the dose rate to individuals utilising a particular landscape object, but also the number of individuals that the object can fully support. For the object giving the highest dose rate, this is the maximum number of people that could be associated with that dose rate. In practice, individuals may utilise resources from more than one landscape object, so the dose rate that they receive would be lower. The number of individuals that can be sustained by a landscape object (Tables 4-1 and 4-2) was calculated for each time period by dividing the potential food production, in the particular ecosystem present at the time, by the yearly food demand of a reference adult person, assumed to be 110 kg C/year /Avila and Bergström 2006/. The potential food production was estimated by multiplying the area of the object by the overall productivity of the relevant ecosystem, expressed in units of kg C/m^2/year (the values used for each ecosystem type are given in /Avila 2006a/).

4.1.1 Calculation of doses for each landscape object

The dose rates from food and water ingestion, inhalation and external exposure were calculated using the methodology described in /Avila and Bergström 2006/ and the parameter values recommended therein. For freshwater objects (lakes and running waters) only doses due to ingestion of water and food (fish) were calculated, as previous assessments /SKB 1999, 2004/ have shown that other exposure pathways are unimportant. For the same reason, only doses from food ingestion were calculated for sea objects. In the case of terrestrial objects (forests, mires and agricultural lands), all exposure pathways were considered in the dose calculations. The total individual dose rate for each object was obtained by adding the dose rates from all considered pathways.

The method used for calculation of food ingestion dose rates /Avila and Bergström 2006/ uses the radionuclide concentrations in food expressed in units of Bq/kg C as input. These were obtained by multiplying the concentrations in water (for sea, lakes and running waters) or soil (for forests, mires and agricultural land) by an aggregated transfer factor that relates the radionuclide concentration in the food produced, expressed in units of Bq/kg C, to the concentration in the corresponding environmental media, water (in Bq/m^3) or soil (Bq/kg DW). The values of the aggregated transfer factors and the method used for their derivation are given in /Avila 2006a/.

Table 4-1. Maximum population sustainable on the yield of food from each landscape object at Forsmark for different time periods.

Object	0–1,000 AD	1,000–2,000 AD	2,000–3,000 AD	3,000–4,000 AD	4,000–5,000 AD	5,000–6,000 AD	6,000–7,000 AD	7,000–8,000 AD	8,000–9,000 AD	9,000–10,000 AD
2						405	202	54	0.6	0.6
3	17,098	14,598	11,101	8,907	5,889	514	408	243	205	168
4						62	49	1	2	1,462
5							21	16	1	1
6								13	10	0.3
7						1	1	1	1	1
8						8	0.2	0.4	0.4	0.4
9						662	339	199	134	89
10						4	4	4	4	4
11			654	510	283	78	63	2	2	2,752
12								27	21	1
13				73	57	2	3	3	2,376	2,376
14					3	3	3	3	3	3
15							11	0.3	0.5	1
16				14	10	0.4	1	1	1	1
17	1,066	753	37	10	7	0.4	0.4	0.5	1	1
18			178	88	0.4	0.4	303	303	303	303
19					50	23	17	1	1,104	1,271
20				0.1	0.4	1	1	1	1	1
21			0.1	0.1	0.1	53	53	0.1	0.1	0.1
22			3	0.0	0.1	0.1	0.1	0.1	0.1	0.1
23			3	0.0	0.1	105	105	105	105	105
24			22	18	0.4	0.6	778	778	778	778
25						0.0	0.2	0.4	0.4	0.4
Sum	18,164	15,351	11,998	9,621	6,299	1,922	2,363	1,757	5,054	9,319

Table 4-2. Maximum population sustainable on the yield of food from each landscape object at Laxemar for different time periods.

Object	9,000–8,000 BC	8,000–7,000 BC	7,000–6,000 BC	6,000–5,000 BC	5,000–4,000 BC	4,000–3,000 BC	3,000–2,000 BC	2,000–1,000 BC	1,000 BC–0 AD	0–1,000 AD
2	1,274	1,274	1,274	1,274	1,274	1,274	1,274	1,274	1,274	1,274
3	401	401	401	401	401	400	396	379	358	327
4	65	65	65	65	65	65	64	56	48	39
5	198	194	198	198	198	195	190	181	162	138
6	19	17	19	19	19	17	16	13	9	7
7	25	11	23	25	21	12	5	0.0	88	88
8	101	20	71	90	57	22	0.1	304	304	304
9	85	62	85	85	84	64	38	18	10	0.0
10	187	95	171	182	163	101	55	27	8	0.1
11	67	60	67	67	66	61	48	34	19	10
12	42	22	40	41	37	24	9	0.0	170	170
13	118	118	118	118	118	118	117	111	96	78
14	167	162	167	167	167	162	152	142	124	107
15	34	33	34	34	34	33	29	21	15	11

Object	9,000–8,000 BC	8,000–7,000 BC	7,000–6,000 BC	6,000–5,000 BC	5,000–4,000 BC	4,000–3,000 BC	3,000–2,000 BC	2,000–1,000 BC	1,000 BC–0 AD	0–1,000 AD
16	123	90	110	118	106	92	74	52	30	56
17	151	116	146	150	143	119	88	65	36	9
18	45	17	38	43	34	18	7	0.0	109	109
19	55	49	55	55	54	50	31	10	0.0	88
20	79	47	67	75	63	48	30	15	0.1	264
21	33	10	25	30	20	10	2	0.0	145	145
22								0.0	0.0	0.0
23										0.2
24							0.0	0.0	0.0	0.1
25							0.1	0.1	0.1	0.1
26										0.1
Sum	3,269	2,864	3,172	3,237	3,124	2,884	2,623	2,702	3,005	3,224

Table 4-2 (cont). Maximum population sustainable on the yield of food from each landscape object at Laxemar for different time periods.

Object	1,000–2,000 AD	2,000–3,000 AD	3,000–4,000 AD	4,000–5,000 AD	5,000–6,000 AD	6,000–7,000 AD	7,000–8,000 AD	8,000–9,000 AD	9,000–10,000 AD
2	1,273	1,230	1,181	1,136	1,102	1,070	1,016	984	952
3	285	208	151	115	98	83	69	58	47
4	31	19	13	10	6	4	1	0.2	0.1
5	115	69	29	6	4	0.1	0.2	597	597
6	0.1	235	235	235	235	235	235	235	235
7	88	88	88	88	88	88	88	88	88
8	304	304	304	304	304	304	304	304	304
9	79	79	79	79	79	79	79	79	79
10	227	227	227	227	227	227	227	227	227
11	3	2	0.0	0.1	258	258	258	258	258
12	170	170	170	170	170	170	170	170	170
13	57	28	16	12	11	3	2	1	1
14	88	63	44	13	9	6	5	4	3
15	4	0.0	0.0	142	142	142	142	142	142
16	56	56	56	56	56	56	56	56	56
17	9	0.2	764	764	764	764	764	764	764
18	109	109	109	109	109	109	109	109	109
19	88	88	88	88	88	88	88	88	88
20	279	279	279	279	279	279	279	279	279
21	145	145	145	145	145	145	145	145	145
22	0.0	0.0	0.0	0.0	0.0	0.0	0.0	0.0	0.0
23	0.2	0.2	0.2	0.2	0.3	0.3	0.3	0.3	0.3
24	0.1	0.1	0.1	0.1	0.1	0.1	0.1	0.1	0.1
25	0.1	0.1	0.1	0.1	0.1	0.1	0.1	0.1	0.1
26	0.2	0.2	0.3	0.4	0.4	0.4	0.4	0.5	0.5
Sum	3,411	3,399	3,978	3,978	4,174	4,110	4,037	4,588	4,545

For aquatic ecosystems only consumption of fish was considered. Hence the applied aggregated transfer factors are the same as the bioaccumulation factors for fish commonly reported in the literature, but corrected by the carbon content in fish. In the case of agricultural lands, it was assumed that there is equal probability of using the land for cultivation of different crop types (vegetables, roots, and cereals) and for cow grazing. The concentration ratios relating the activity concentration in the agricultural food products (crops, meat and milk) and the soil, were corrected by the carbon content of the different food products. The mean values, across different agricultural products, of the corrected concentration ratios was used as aggregated transfer factors. The same procedure was applied for the forest and mire ecosystems, considering ingestion of game meat.

Latent doses

It can be the case that at a given time only part of the radionuclide inventory in the objects is present in a form that can give direct doses. For example, radionuclides in lake and sea sediments at a given time will not give exposure at that time. In some cases, a partion of this "unavailable" inventory will give rise to doses at a later stage, when an ecosystem shift has taken place; but this will not always be the case. In order to obtain an estimate of the maximum possible dose rates at any time from all radionuclides retained in an object, latent doses were calculated. The latent dose is calculated using the whole radionuclide inventory in an object, independent of the compartment where the radionuclide is present, i.e. even "unaccessible" compartments are included. For example, for a lake, even the inventory present in the sediment is included in the dose calculation. Further, for calculating the dose, it is assumed that the whole inventory is distributed in a 1 m deep soil layer, which is used for agricultural purposes. This recognises that objects such as lakes and mires can become transformed to agricultural land at a subsequent stage of evolution.

4.1.2 Calculation of doses from the use of wells

Dose rates from use of a well were calculated using the same methods as for other landscape objects see /Avila and Bergström 2006/. The dose rates were estimated for a subsistence farmer who drinks water from the well and uses the well water for irrigation of a garden plot and as a drinking water supply for cattle. All exposure pathways were considered.

4.2 Landscape Dose Factors

The number of individuals that can be supported from each landscape object varies from less than one for some Terrestrial Objects to many thousands in the case of Marine Objects (see Tables 4-1 and 4-2 objects that give the highest dose rate often can support less than one person). If the number of persons which can be supported by and object is substantially lower than one, the calculated dose rate would be too high to be applicable to the most exposed individual, since an individual utilising that object would also have to utilise resources from other objects. In contrast, for larger numbers the dose rates could be higher than the model estimates, because of potential heterogeneities in the contamination not accounted for by the model. To reduce the impact of these problems, which essentially arise from the representation of the landscape as a finite number of objects, results of the dose rate calculation for each object are plotted as a complementary cumulative distribution function (CCDF) in which the number of people exceeding a particular dose rate is plotted against the dose rate. Because these plots are based on calculations for finite-size landscape objects they exhibit a stepwise pattern. Examination of the CCDF shows that they are typically well fitted by lognormal distributions, so such distributions were adopted as a continuous representation of the spatial distribution of the Dose Conversion Factors. Once these curves had been obtained, average Dose Conversion Factors for different groups in the landscape, including the most exposed group could be derived (see Chapter 5). These Dose Conversion Factors take into account the distribution of radionuclides in the whole landscape and are here termed Landscape Dose Factors (LDFs).

The average dose rate from food ingestion to the whole group utilising the affected landscape at a given time was estimated by taking a weighted average over all landscape objects. The weighting factor used for each landscape object was the number of people that can be sustained by that landscape object divided by the total number of people that can be sustained by the landscape. The same weighting factors were used to obtain a weighted variance over all landscape objects. For other exposure pathways (water ingestion, inhalation and external exposure) simple arithmetic means and variances were taken over all relevant objects. The mean and variance of the total dose rates were obtained by summing up the values for all exposure pathways. These were then used as parameter values for the fitting of lognormal distributions.

4.3 Dose Conversion Factors for Forsmark

4.3.1 Time dynamics of the Dose Conversion Factors

The results for Forsmark are presented for the main calculation variant and for the complementary variants, i.e. assuming continuous releases of 1 Bq/y to all landscape objects according to the release fractions given in Table 3-2 and varying the starting time of the release at 1,000 years intervals starting from 8,000 BC, as well as assuming continuous releases of 1 Bq/y to each landscape object and varying the starting time of the release at 1,000 years intervals.

The predictions of the time dynamics of the maximum dose rates (maximum dose rates over all objects) per unit release rate for the variant 8,000 BC-All, are shown in Figure 4-1. All radionuclides show the same trend with increasing dose rates during the Sea and Coastal Periods and stabilisation with slight decrease after 5,000 AD for the Terrestrial Period. For most radionuclides, the values at 10,000 AD are near the maximum values for the whole period. However, for Tc-99 and Cl-36 a decrease is observed during the Terrestrial Period, since these radionuclides are poorly absorbed and end up being released to the Baltic Sea, resulting in a lower inventory in the rest of the model domain.

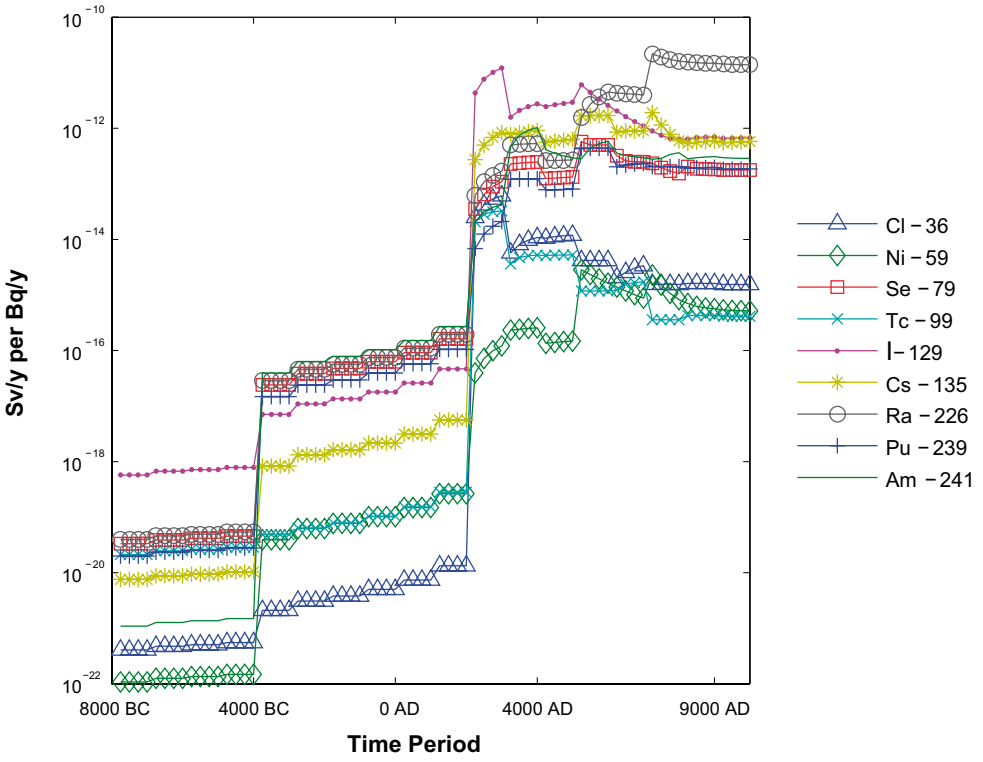

Figure 4-1. *Time variation of the maximum Dose Conversion Factors for the landscape objects (maximum over all objects) at Forsmark for the variant 8,000 BC-All.*

The large time variation observed means that the risk to an individual will vary strongly depending on when in an interglacial period the individual lives. For releases starting at 8,000 BC the dose rates are substantially lower during the Sea Period and follow the same dynamics as the activity concentrations in sea water. The individual living in the Coastal and Terrestrial Periods will have the highest potential risk.

Influence of the starting time of the releases on the peak dose rates

It can be expected that for an individual the exposure risk will also depend on the starting time of the releases, since this will determine the duration of the accumulation period of radionuclides in the landscape before the exposure. The effect of the starting time of the releases is illustrated in Table 4-1, which shows the maximum dose rates over all objects for realisations with releases to all objects in the landscape, when varying the starting time of the release at 1,000 year intervals starting from 8,000 BC. It is shown at which time point and in which object the maximum is observed for each radionuclide. The type of ecosystem, just up to the moment of the maximum, i.e. representing the period before an ecosystem shift at 1,000 years intervals, is also indicated. The values obtained for the first set of realisations, corresponding to releases starting from 8,000 BC to 1,000 AC, are equal to the peak dose rates in Figure 4-1.

For Cl-36, Ni-59, Se-79, Tc-99 and I-129 all realisations starting in the period 8,000 BC to 2,000 AD gave the same peak dose rate. For other radionuclides, releases starting at even later times gave the same peak dose rate. For example, for Pu-239 the same peak dose rate was observed for realisations with releases starting from 8,000 BC to 5,000 AD. Hence, the maximum peak dose rates are associated with releases occurring during the Coastal Period. It appears that accumulation during the Sea Period is not important for dose rates occurring at later times. However, it should be taken into account that during the Sea Period the accumulation occurs only in the sediments of object 17, which afterwards becomes a lake where deep sediments do not give immediate exposure of humans.

These results confirm the basic assumption that hypothetical releases starting at the beginning of an interglacial period represent the conservative calculational case as compared to starting points of releases within such period.

Time to peak dose rates

Different radionuclides peak dose rates at different times during the simulation period (Table 4-1). As mentioned above, for Cl-36, Ni-59, Se-79, Tc-99 and I-129, the realisations starting at 2,000 AD or before give the same peak maximum dose rates, which are observed 1,000 years after for Cl-36, Tc-99 and I-129, and 3,250 years after for for Ni-59 and Se-79. All realisations with releases starting at a later time give lower maximum dose rates. The behaviour for other radionuclides is similar with times from the start of the release to the peak dose rate ranging from 1,000 years (for Pu-239 and Am-241) to 3,250 years (for Cs-135 and Ra-226).

Objects and ecosystem types with peak dose rates

The objects and ecosystem types in which peak dose rates are observed vary between radionuclides (see Table 4-1). For Cl-36, Tc-99 and I-129, the peak dose rates are observed for object 23, when this object is a lake. This object also has the peak dose rates for Am-241, when the ecosystem has shifted into mire and for Ni-59, when the mire has shifted to agricultural land. For Se-79 and Pu-239, the peak dose rates are observed in a lake (object 19), whereas for Cs-135 and Ra-226, the peak dose rates are observed in a forest ecosystem (object 16). Note that none of the objects where peak dose rates are observed is among objects with the highest release fractions, i.e. objects 11 and 17 (see Table 3-2). From these results, it follows that it is not possible to choose any single object or ecosystem type that would provide a conservative estimate for all radionuclides. This is true for all considered starting times of the releases.

Table 4-3. Peak values of the maximum total dose rates (Sv/y per Bq/y) over the whole period for different starting times of the releases (from 8,000 BC to 9,000 AD). The maximum is over landscaoe objects at each time. It is also shown at which time point and in which object the peak is observed. The type of ecosystem just up to the moment of the maximum is also indicated.

Start time		Cl-36	Ni-59	Se-79	Tc-99	I-129	Cs-135	Ra-226	Pu-239	Am-241
8,000 BC to 1,000 AD	Time of peak dose	3,000 AD	5,250 AD	5,250 AD	3,000 AD	3,000 AD	7,250 AD	7,250 AD	6,000 AD	4,000 AD
	Object	23	23	19	23	23	16	16	19	23
	Dose	6.09E–14	2.84E–15	5.73E–13	3.25E–14	1.22E–11	1.91E–12	2.18E–11	4.34E–13	1.03E–12
	Ecosystem Type	Lake	Agricultural Land	Lake	Lake	Lake	Forest	Forest	Lake	Mire
2,000 AD	Time of peak dose	3,000 AD	5,250 AD	5,250 AD	3,000 AD	3,000 AD	7,250 AD	7,250 AD	6,000 AD	4,000 AD
	Object	23	23	19	23	23	16	16	19	23
	Value	6.09E–14	2.84E–15	5.73E–13	3.25E–14	1.22E–11	1.91E–12	2.18E–11	4.34E–13	1.03E–12
	Ecosystem Type	Lake	Agricultural Land	Lake	Lake	Lake	Forest	Forest	Lake	Mire
3,000 AD	Time of peak dose	5,000 AD	7,250 AD	5,250 AD	5,000 AD	5,000 AD	7,250 AD	7,250 AD	6,000 AD	4,000 AD
	Object	17	16	19	17	17	16	16	19	23
	Value	1.19E–14	2.28E–15	5.01E–13	5.25E–15	2.92E–12	1.91E–12	2.18E–11	4.33E–13	1.03E–12
	Ecosystem Type	Lake	Forest	Lake	Lake	Lake	Forest	Forest	Lake	Mire
4,000 AD	Time of peak dose	5,000 AD	7,250 AD	5,250 AD	5,000 AD	5,000 AD	7,250 AD	7,250 AD	6,000 AD	6,000 AD
	Object	17	16	19	17	17	16	16	19	17
	Value	1.00E–14	2.28E–15	5.01E–13	5.16E–15	2.28E–12	1.91E–12	2.18E–11	4.33E–13	5.81E–13
	Ecosystem Type	Lake	Forest	Lake	Lake	Lake	Forest	Forest	Lake	Mire
5,000 AD	Time of peak dose	6,000 AD	6,000 AD	6,000 AD	7,000 AD	6,000 AD	6,000 AD	10,000 AD	6,000 AD	6,000 AD
	Object	19	19	19	11	19	19	16	19	17
	Value	4.19E–15	5.31E–16	5.00E–13	1.71E–15	1.95E–12	1.67E–12	1.37E–11	4.33E–13	5.81E–13
	Ecosystem Type	Lake	Lake	Lake	Lake	Lake	Lake	Forest	Lake	Mire

Start time		Cl-36	Ni-59	Se-79	Tc-99	I-129	Cs-135	Ra-226	Pu-239	Am-241
6,000 AD	Time of peak dose	7,000 AD	9,000 AD	7,000 AD	7,000 AD	7,000 AD	7,000 AD	10,000 AD	7,000 AD	8,000 AD
	Object	11	16	19	11	19	19	16	19	11
	Value	3.24E–15	5.26E–16	2.48E–13	1.71E–15	9.56E–13	8.38E–13	1.37E–11	2.32E–13	3.64E–13
	Ecosystem Type	Lake	Forest	Lake	Lake	Lake	Lake	Forest	Lake	Mire
7,000 AD	Time of peak dose	9,000 AD	9,000 AD	8,250 AD	9,000 AD	9,000 AD	9,000 AD	10,000 AD	9,000 AD	8,000 AD
	Object	16	16	20	20	20	20	16	20	11
	Value	1.61E–15	5.26E–16	1.82E–13	4.23E–16	6.66E–13	5.53E–13	1.37E–11	1.95E–13	3.64E–13
	Ecosystem Type	Forest	Forest	Run.water	Run.water	Run.water	Run.water	Forest	Run.water	Mire
8,000 AD	Time of peak dose	9,000 AD	10,000 AD	9,000 AD	9,000 AD	9,000 AD	9,000 AD	10,000 AD	9,000 AD	10,000 AD
	Object	16	16	20	20	20	20	16	20	17
	Value	1.61E–15	5.08E–16	1.82E–13	4.23E–16	6.65E–13	5.47E–13	1.32E–11	1.93E–13	2.82E–13
	Ecosystem Type	Forest	Forest	Run.water	Run.water	Run.water	Run.water	Forest	Run.water	Mire
9,000 AD	Time of peak dose	10,000 AD	10,000 AD	10,000 AD	10,000 AD	10,000 AD	10,000 AD	10,000 AD	10,000 AD	10,000 AD
	Object	16	16	20	20	20	20	16	20	17
	Value	1.55E–15	4.60E–16	1.77E–13	4.13E–16	6.36E–13	5.09E–13	1.08E–11	1.76E–13	2.46E–13
	Ecosystem Type	Forest	Forest	Run.water	Run.water	Run.water	Run.water	Forest	Run.water	Mire

Latent dose rates

As mentioned above, an important part of the inventory accumulated during the Sea Period in sediments of object 17 remains in unaccessible form during the Coastal and Terrestrial Periods. But the question arises how large the dose rates could be (latent dose rates) if this part of the inventory were to become accessible at different points in time, for example if the mires were transformed by man into agricultural lands. A comparison of the latent dose rates against the calculated maximum dose rates (Figure 4-2) indicates that during the Terrestrial Period the peak of maximum dose rates over all objects is higher than the latent dose rates for object 17. Note that for the calculation of the latent dose rates, it is assumed that the whole inventory becomes available for use as agricultural land, whereas the peak dose rates may occur for other types of ecosystems where dose rates per unit of inventory could be higher. For example, for I-129, the peak of the maximum dose rate occurs at year 3,000 AD in object 23, which at this time is a lake.

Influence of the spatial distribution of releases on the peak dose rates

The estimates of release fractions to the different objects are uncertain. Hence, it is important to evaluate the impact of the spatial distribution of the releases on the estimates of the maximum dose rates. For this purpose, a series of realisations was carried out with releases directed to a single object during the whole simulation period. Note that the release was directed only to objects that existed at a given time and that at least once during the simulation period, had a non-zero release fraction (see Table 3-2). The results are presented in Table 4-2, which shows the peak maximum dose rates over all objects for each release start time.

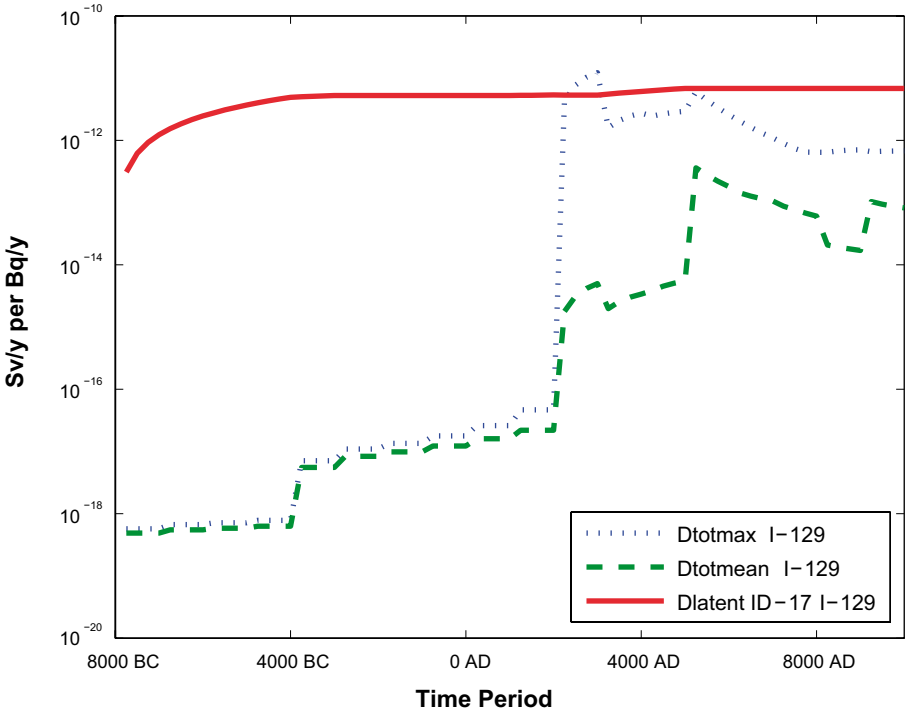

Figure 4-2. *Time variation at Forsmark of the maximum dose rate (Dtotmax), the mean dose rate (Dtomean) and the latent dose rate (Dlatent) for I-129 for the variant 8,000 BC-All.*

As for the realisations with releases to all objects, the time and object in which the peak dose rate is observed varied for different radionuclides. For Cl-36, Tc-99, I-129, Pu-239 and Am-241, the peak dose rates are observed when releases start in object 23, whereas for Ni-59, Se-79, Cs-135 and Ra-226 the peak dose rates were obtained for the case with releases starting in object 7. The peak dose rates are, with a few exceptions, observed for the same object in which the release starts.

The peak dose rates in the cases in which the releases are directed to objects 23 and 7 during the whole period (Table 4-2) are between 5 and 50 times higher than the peak dose rates when releases are directed to all objects (Table 4-1). Objects 23 and 7 are located upstream and, therefore, the water fluxes through these objects are low, which leads to greater retention of the radionuclides and higher concentrations. However, the probability of releases occurring to upstream objects is low, since radionuclides are expected to be released in groundwater discharge areas which are normally located downstream. Moreover, the number of people that can be sustained by objects 23 and 7 at the time of the peak dose rates is low, less than 1 and 20 persons, respectively. These numbers are overestimated, since it is assumed that these persons get all their food from a very small lake, a mire or a forest.

4.3.2 Spatial variation of the Dose Conversion Factors

The discussion in the previous section focused on the peak of the maximum dose rates over all objects of the landscape. In many cases, the objects in which peak dose rates are observed can only sustain a few individuals. In a real situation, people most likely will be exposed to environemental media from several objects in the affected region, which has a relatively small size. In order to make more realistic estimations of the individual dose rates, it necessary to know how dose rates can be distributed among the individuals that make use of the affected region.

Figure 4-3 shows the estimated total dose rates for each object in the landscape at the end of the simulation period for the realisation 8,000 BC-All. There is a difference of several orders of magnitude between the minimum and maximum values, with a few objects being associated with much higher dose rates than the others.There is also a large variation in the number of individuals that can be sustained by the different objects. The objects with highest dose rates usually can sustain a small number of individuals.

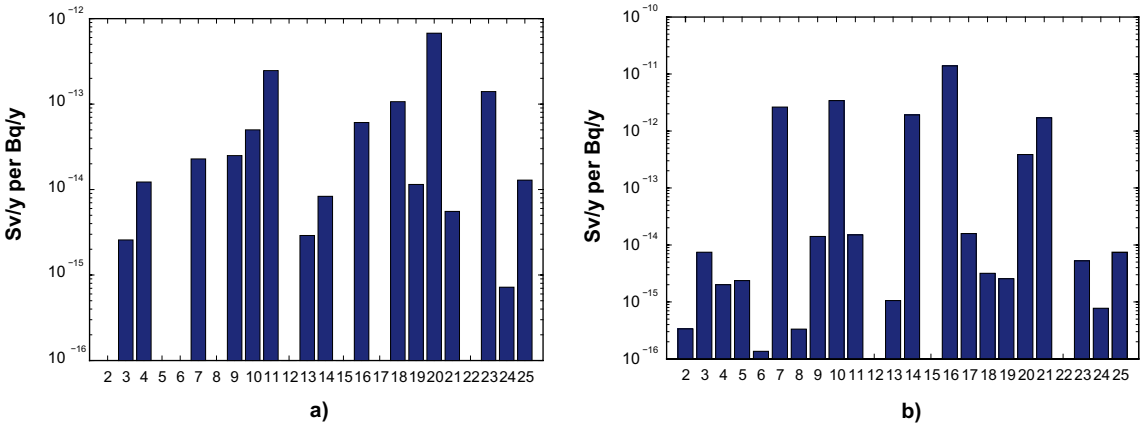

Figure 4-3. *Total dose rates from I-129 (a) and Ra-226 (b) for objects existing in Forsmark at 10,000 AD for the variant 8,000 BC-All.*

Table 4-4. Maximum dose rates (Sv/y per Bq/y) for releases starting at different times (from 8,000 BC to 9,000 AD) and objects. It is also shown for which starting object, at which time and in which object the maximum is observed. The type of ecosystem inmediately before the time of the maximum is also indicated.

Start time		Cl-36	Ni-59	Se-79	Tc-99	I-129	Cs-135	Ra-226	Pu-239	Am-241
8,000 BC	Start Object	17	17	17	17	17	17	17	17	17
to	Time of peak dose	5,000 AD	6,250 AD	6,250 AD	5,000 AD	5,000 AD	7,000 AD	6,500 AD	7,000 AD	6,000 AD
1,000 AD	Object	17	19	19	17	17	19	19	19	17
	Value	1.66E-14	6.76E-16	6.33E-13	7.46E-15	3.86E-12	2.13E-12	1.49E-12	6.34E-13	1.15E-12
	Ecosystem Type	Lake	Lake	Lake	Lake	Lake	Lake	Lake	Lake	Mire
2,000 AD	Start Object	23	23	23	23	23	23	23	23	23
	Time of peak dose	3,000 AD	5,250 AD	5,000 AD	3,000 AD	3,000 AD	5,000 AD	5,000 AD	5,000 AD	4,000 AD
	Object	23	23	17	23	23	17	17	17	23
	Value	3.22E-13	1.58E-14	3.54E-12	1.72E-13	6.48E-11	1.15E-11	7.75E-12	2.16E-12	1.60E-11
	Ecosystem Type	Lake	Agricultural Land	Lake	Lake	Lake	Lake	Lake	Lake	Mire
3,000 AD	Start Object	23	23	23	23	23	23	23	23	23
	Time of peak dose	4,250 AD	10,000 AD	5,000 AD	4,250 AD	5,000 AD	5,000 AD	5,000 AD	5,000 AD	4,000 AD
	Object	17	23	17	17	17	17	17	17	23
	Value	3.07E-14	4.98E-15	3.54E-12	8.64E-15	1.43E-11	1.15E-11	7.75E-12	2.16E-12	1.60E-11
	Ecosystem Type	Lake	Agricultural Land	Lake	Lake	Lake	Lake	Lake	Lake	Mire
4,000 AD	Start Object	14	16	16	16	23	16	16	23	23
	Time of peak dose	7,250 AD	7,250 AD	7,250 AD	5,000 AD	5,000 AD	7,250 AD	10,000 AD	5,000 AD	5,000 AD
	Object	14	16	16	16	17	16	16	17	23
	Value	1.06E-13	3.90E-14	3.97E-12	2.10E-14	1.43E-11	3.27E-11	5.93E-10	2.15E-12	8.35E-12
	Ecosystem Type	Forest	Forest	Lake	Lake	Lake	Lake	Lake	Lake	Mire
5,000 AD	Start Object	14	14	14	23	23	14	16	17	16
	Time of peak dose	8,250 AD	10,000 AD	10,000 AD	6,250 AD	10,000 AD	10,000 AD	10,000 AD	7,000 AD	6,000 AD
	Object	14	14	14	23	23	14	16	19	16
	Value	1.06E-13	3.08E-14	3.55E-12	5.34E-15	9.37E-12	2.54E-11	5.91E-10	6.34E-13	2.54E-12
	Ecosystem Type	Forest	Forest	Forest	Agricultural Land	Agricultural Land	Forest	Forest	Agricultural Land	Forest

Start time		Cl-36	Ni-59	Se-79	Tc-99	I-129	Cs-135	Ra-226	Pu-239	Am-241
6,000 AD	Start Object	14	14	16	23	23	14	16	17	16
	Time of peak dose	9,250 AD	10,000 AD	10,000 AD	7,000 AD	10,000 AD	10,000 AD	10,000 AD	7,000 AD	7,000 AD
	Object	14	14	16	23	23	14	16	19	16
	Value	1.06E-13	2.87E-14	3.45E-12	5.34E-15	8.80E-12	2.41E-11	5.91E-10	6.33E-13	1.19E-12
	Ecosystem Type	Forest	Forest	Mire	Agricultural Land	Agricultural Land	Forest	Forest	Agricultural Land	Forest
7,000 AD	Start Object	7	7	7	7	7	7	7	17	5
	Time of peak dose	10,000 AD	10,000 AD	10,000 AD	10,000 AD	9,250 AD	10,000 AD	10,000 AD	9,000 AD	9,000 AD
	Object	7	7	7	7	7	7	7	20	5
	Value	2.90E-13	6.98E-14	6.93E-12	1.12E-14	1.14E-11	5.96E-11	1.02E-09	5.41E-13	2.28E-12
	Ecosystem Type	Forest	Forest	Forest	Forest	Forest	Forest	Forest	Run.water	Mire
8,000 AD	Start Object	7	7	7	7	7	7	7	17	5
	Time of peak dose	10,000 AD	10,000 AD	10,000 AD	10,000 AD	10,000 AD	10,000 AD	10,000 AD	9,000 AD	9,000 AD
	Object	7	7	7	7	7	7	7	20	5
	Value	2.90E-13	5.60E-14	5.07E-12	1.12E-14	1.14E-11	4.90E-11	8.65E-10	5.41E-13	2.28E-12
	Ecosystem Type	Forest	Forest	Forest	Forest	Forest	Forest	Forest	Run.water	Mire
9,000 AD	Start Object	7	7	7	7	7	7	7	8	8
	Time of peak dose	10,000 AD	10,000 AD	10,000 AD	10,000 AD	10,000 AD	10,000 AD	10,000 AD	10,000 AD	10,000 AD
	Object	7	7	7	7	7	7	7	8	8
	Value	2.89E-13	3.42E-14	2.82E-12	1.12E-14	1.14E-11	3.10E-11	5.69E-10	6.69E-13	4.96E-12
	Ecosystem Type	Forest	Forest	Forest	Forest	Forest	Forest	Forest	Mire	Mire

By combining the information on the dose rates associated with each object and the number of potentially affected individuals, the assessed distribution of the dose rates among individuals can be obtained (see Figures 4-4 and 4-5). These are complementary cumulative distributions which show how many individuals receive a dose rate above a given value. If normalised by the total number of potentially affected individuals, these become non-parametric probability distributions, with an accuracy that is defined by the resolution of the adopted discretisation of the landscape, and the assumption that the individuals receive their exposure from single objects. These distributions are used in Chapter 5 for derivation of LDF values for use in SR-Can for assessment of dose rates to the most exposed groups.

The large spatial variation in the Dose Factors that is observed implies that there are significant differences between the maximum and average dose rates over all objects. This is illustrated in Table 4-5, which show maximum and mean values of the dose rates at the end of the simulation period. The maximum dose rates were 12–230 times higher than the mean dose rates, depending on the radionuclide.

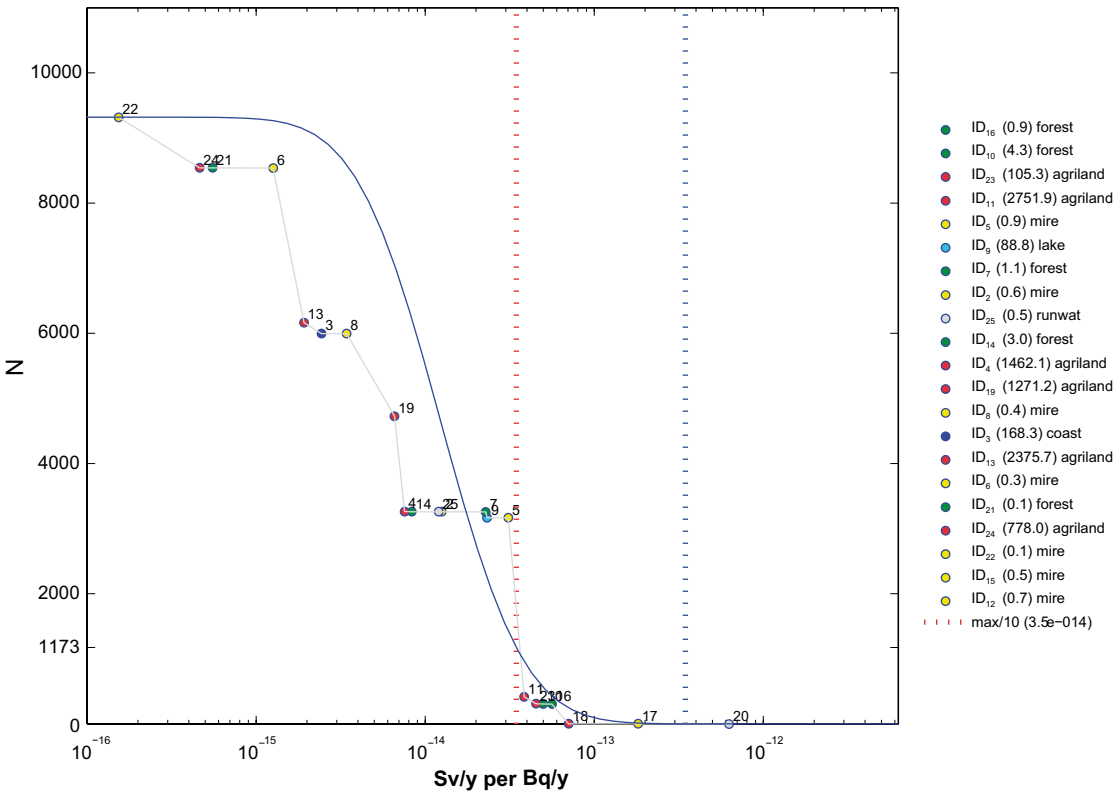

Figure 4-4. *Distribution of total dose rates from I-129 for objects existing at Forsmark at 10,000 AD for the variant 8,000 BC-All. The blue line is the fitted log-normal distribution. The legend gives the object number, ecosystem type and number of people (in brackets) that can be sustained by each landscape object. The vertical blue line indicates the maximum value of the Dose Conversion Factor; the vertical red line indicates 1/10 of the maximum value.*

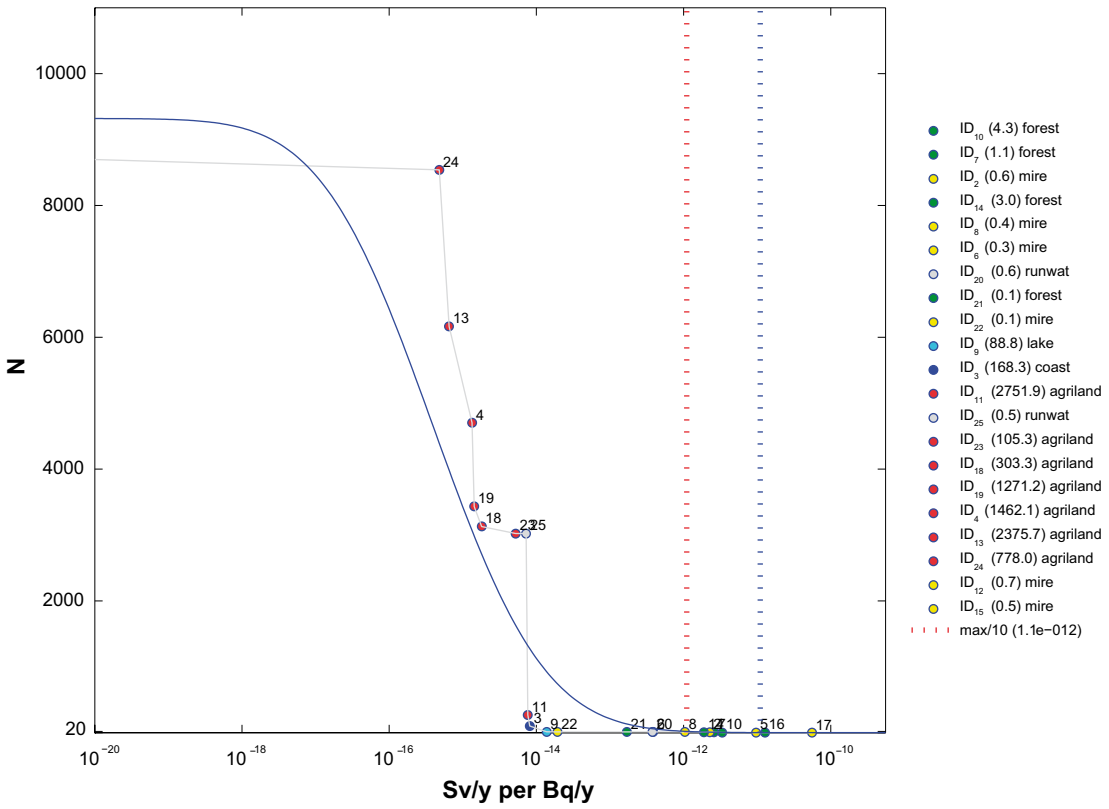

Figure 4-5. *Distribution of total dose rate from Ra-226 for objects existing at Forsmark at 10,000 AD for the variant 8,000 BC-All. The blue line is the fitted log-normal distribution. The legend gives the object number, ecosystem type and number of people (in brackets) that can be sustained by each landscape object. The vertical blue line indicates the maximum value of the Dose Conversion Factor; the vertical red line indicates 1/10 of the maximum value.*

Table 4-5. Maximum dose rates and mean dose rates over all objects existing at 10,000 AD for the variant 8,000 BC-All.

Radionuclide	Mean dose rate	Maximum dose rate	Max/ Mean
Cl-36	7.0E–17	2.0E–15	2.9E+01
Ni-59	4.8E–17	1.0E–15	2.1E+01
Se-79	1.0E–15	1.8E–13	1.8E+02
Tc-99	3.3E–17	4.1E–16	1.2E+01
I-129	8.2E–14	6.7E–13	8.2E+00
Cs-135	4.0E–15	5.8E–13	1.4E+02
Ra-226	6.0E–14	1.4E–11	2.3E+02
Pu-239	4.0E–15	1.9E–13	4.7E+01
Am-241	1.7E–14	2.9E–13	1.7E+01

4.4 Dose Conversion Factors for Laxemar

All simulations for Laxemar were carried out for a constant unit release rate starting at year 8,000 BC with release fractions as specified in Table 3-3.

4.4.1 Time dynamics of the Dose Conversion Factors

The predictions of the time dynamics of the maximum dose rates (maximum dose rates over all objects) per unit release rate are shown in Figure 4-6. All radionuclides show similar time dynamics. During the Sea Period, there is an increase during the first thousand years, which is followed by a slight decrease until the Coastal Period starts at 3,000 BC. When the Coastal Period starts, there is a fast increase that lasts about 2,000 years and after that the dose rates remain nearly constant for the rest of the simulation period. The Dose Conversion Factors are much lower during the Sea Period, which is about half the length of that in Forsmark.

The between-radionuclide differences are larger during the Sea Period. During the Coastal and Terrestrial Periods, two groups of radionuclides can be identified, with differences of two-three orders of magnitude between these groups (Figure 4-7). The Dose Conversion Factors within each group are of the same order of magnitude. The group with the lowest values includes the most mobile radionuclides (Cl-36 and Tc-99) and Ni-59. The lower values for Cl-36 and Tc-99 are due to their more limited retention in the landscape, whereas in the case of Ni-59, the lower values can be explained by lower transfer factors to biota and less radiotoxicity.

Latent dose rates

The maximum values of the latent dose rates over all objects were close to, or sometimes lower than the calculated maximum dose rates. This is illustrated for I-129 in Figure 4-8. During the Terrestrial Period the latent dose rates were lower than the maximum dose rates. This is because in this period the maximum dose rates are observed for object 25, which is a running water; whereas latent dose rates are calculated assuming the use of territory for agricultural purposes (see discussion for Forsmark in Section 4.4).

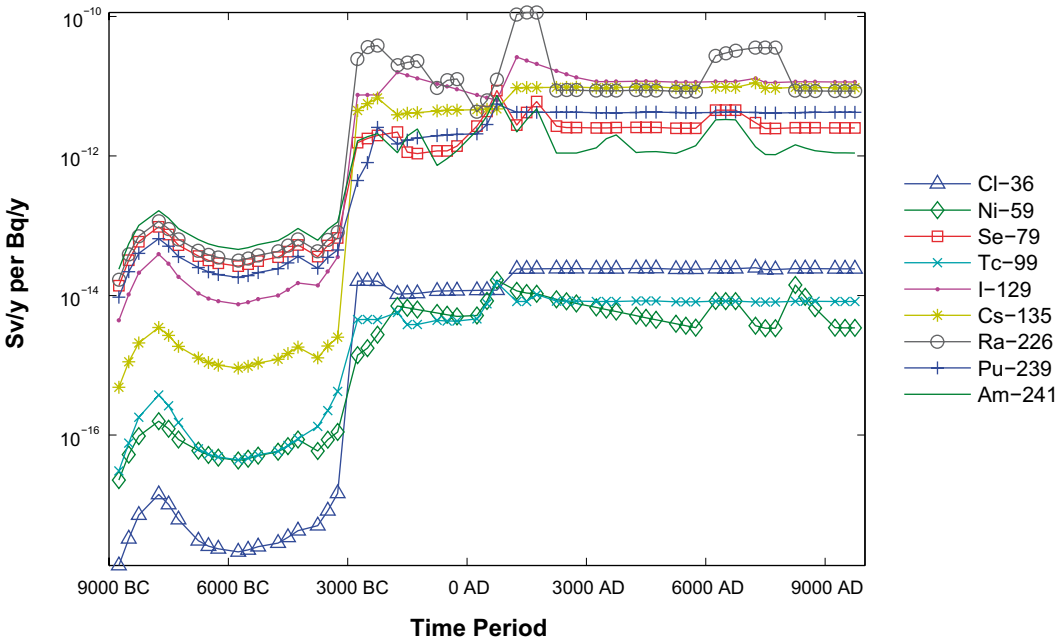

Figure 4-6. *Time variation of the maximum Dose Conversion Factors for the landscape objects (maximum over all objects) in Laxemar.*

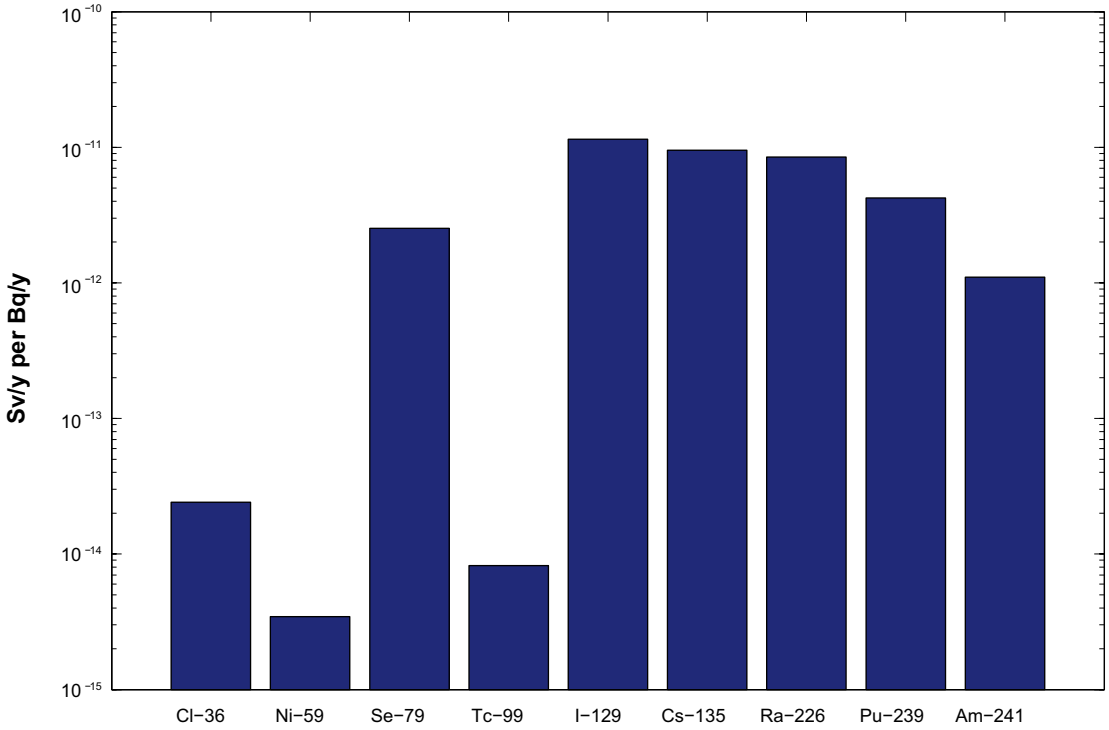

Figure 4-7. *Maximum values of the Dose Conversion Factors for the landscape objects at Laxemar (maximum over all landscape objects) at the end of the simulation period.*

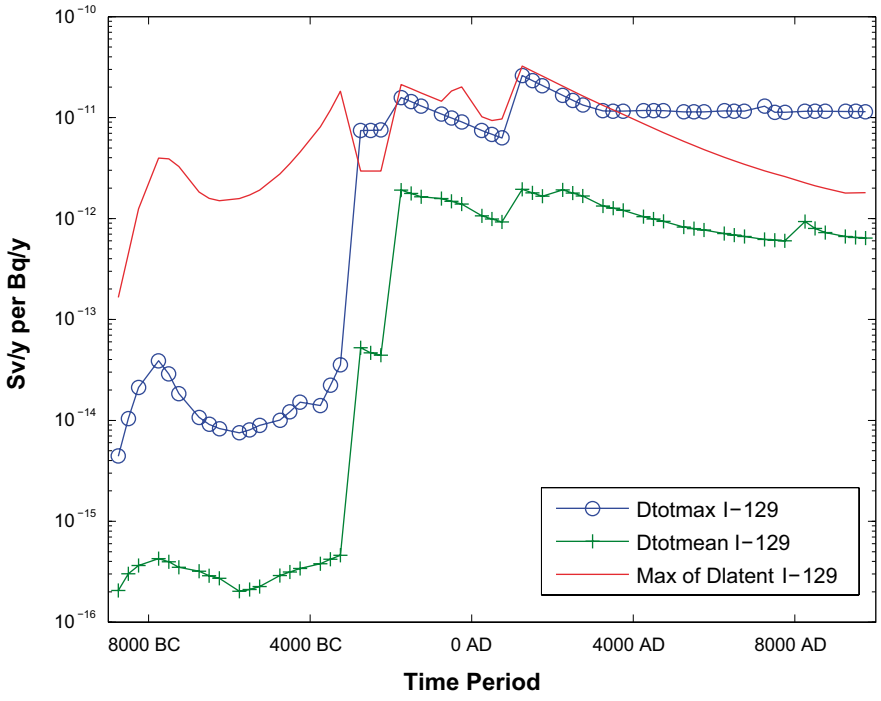

Figure 4-8. *Time variation at Laxemar of the maximum dose rate and the maximum latent dose rate from I-129.*

4.4.2 Spatial variation of the Dose Conversion Factors

Figure 4-9 shows values of the Dose Conversion Factors for each object in the landscape at the end of the simulation period. There is a difference of several orders of magnitude between the minimum and maximum values. Object 25, which is a running water, gives much higher dose rates than other objects. Also, there is a large variation in the number of individuals that can be sustained by different objects. The objects with highest dose rates usually can sustain a lower number of individuals. Note that object 25 cannot even supply a single individual with food. The lowest values are observed for the Sea Objects and running waters 22 and 23. All other objects, which are either lakes or agricultural lands, have similar Dose Conversion Factors.

The distribution of the Dose Conversion Factors for I-129 and Ra-226 is shown in Figures 4-10 and 4-11. There is a relatively good fit to the lognormal distribution for both radionuclides. The blue vertical line in these figures represents the maximum value of the Dose Conversion Factors, which in this case is obtained for object 25. The red vertical line corresponds to one tenth of the maximum value of the Dose Conversion Factors. The number of people between the maximum and one tenth of the maximum of the DCF is indicated by the vertical lines. This group can be considered as the maximally exposed group as defined in the Swedish regulations /SSI 2005/. Further details on the definition of the most exposed group and the derivation of LDF values for use in SR-Can are provided in Chapter 5.

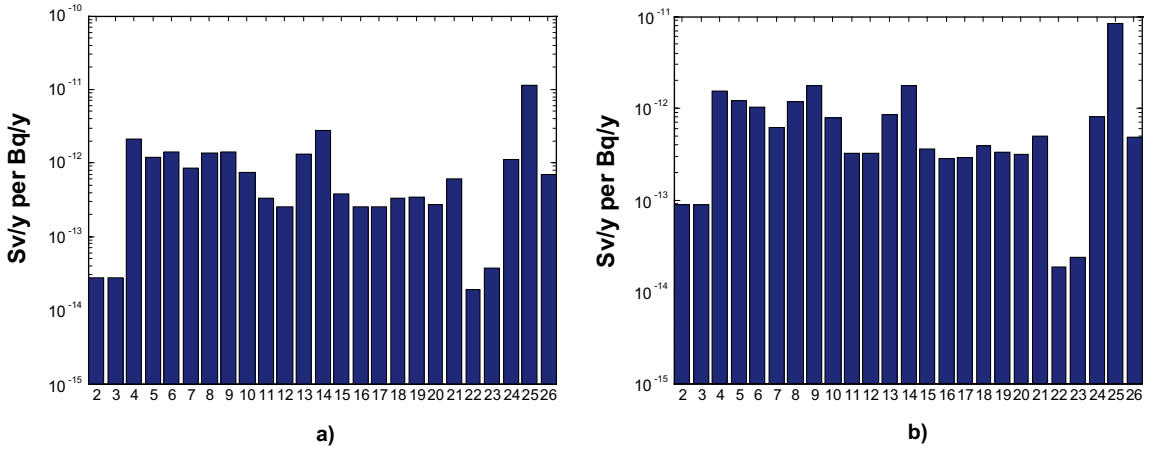

Figure 4-9. *Dose Conversion Factors for I-129 (a) and Ra-226 (b) for the objects at Laxemar at the end of the simulation period (10,000 AD).*

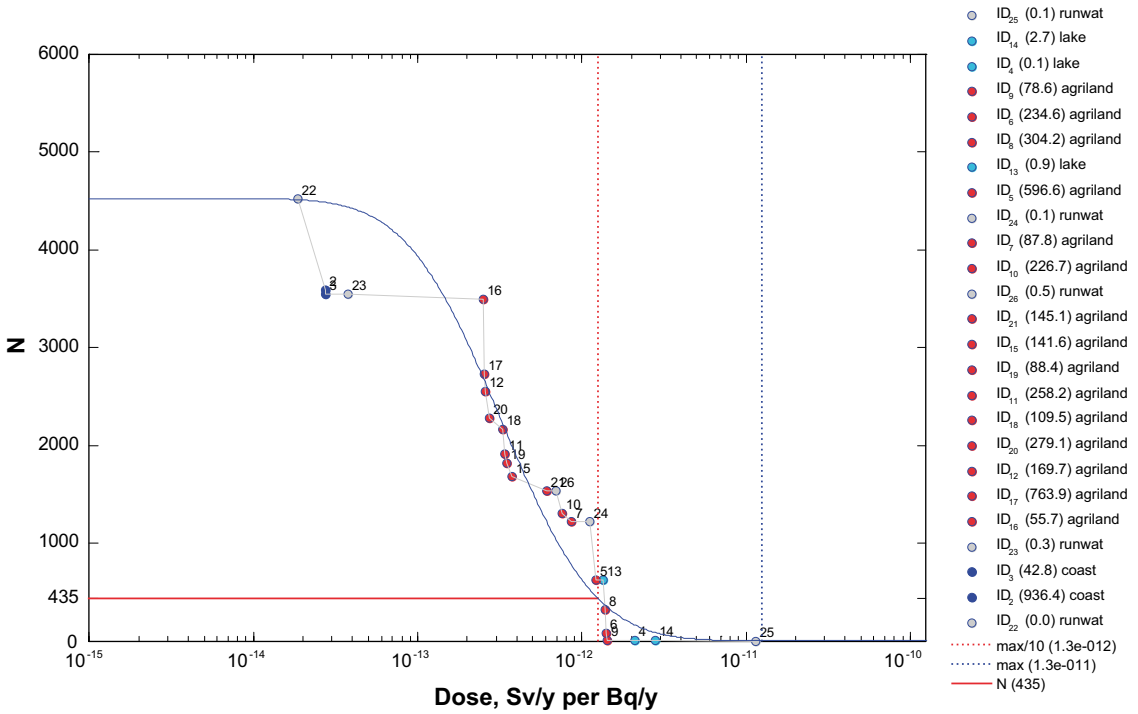

Figure 4-10. *Distribution of the Dose Conversion Factors for I-129 for different landscape objects at Laxemar. The blue line is the fitted log-normal distribution. The legend gives the object number, ecosystem type and number of people (in brackets) that can be sustained by each landscape object. The vertical blue line indicates the maximum value of the Dose Conversion Factor, the vertical red line indicates 1/10 of the maximum value.*

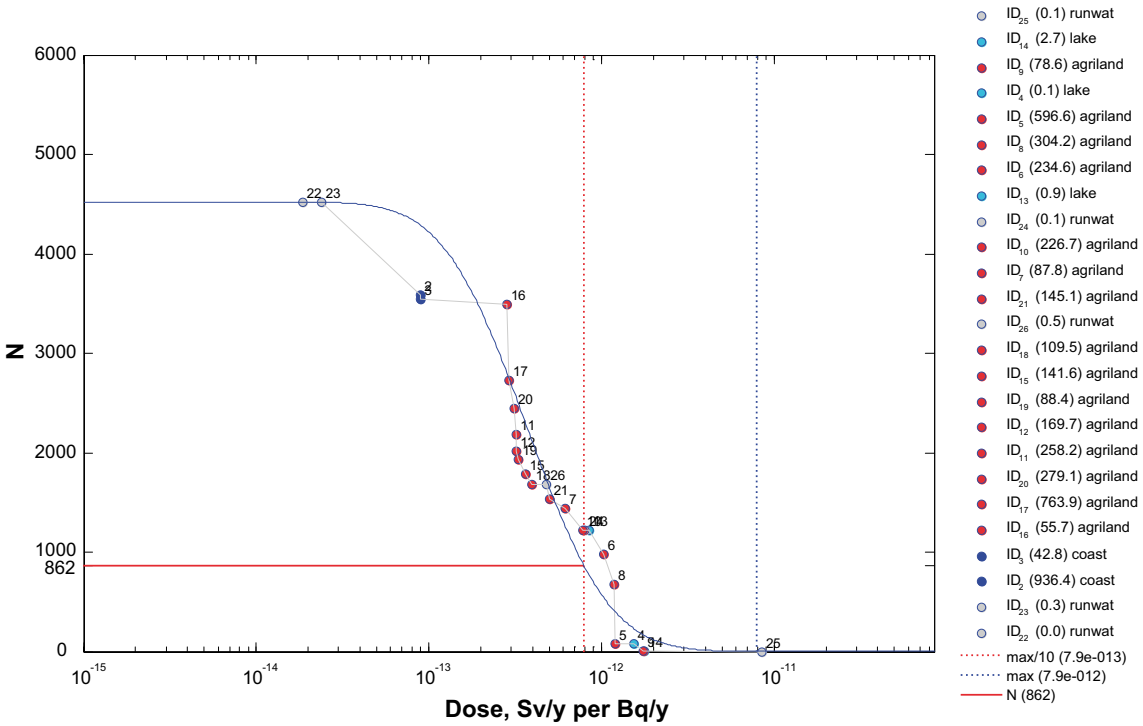

Figure 4-11. *Distribution of the Dose Conversion Factors for Ra-226 for different landscape objects at Laxemar. The blue line is the fitted log-normal distribution. The legend gives the object number, ecosystem type and number of people (in brackets) that can be sustained by each landscape object. The vertical blue line indicates the maximum value of the Dose Conversion Factor, the vertical red line indicates 1/10 of the maximum value.*

5 Derivation of Landscape Dose Factors for SR-Can

In principle, for the SR-Can dose assessments, it would be possible to apply the landscape model with time-dependent radionuclide fluxes derived from the near field model of the repository, and the geosphere transport model. Such an approach would yield time-dependent radionuclide concentrations in the environmental media of the various landscape objects and hence time-dependent dose rates to individuals utilising those landscape objects. However, radionuclide fluxes from the geosphere are likely to vary slowly with time. For practical purposes, it is convenient to decouple the calculation of those fluxes from calculations of their radiological impacts carried out with the landscape model. Therefore, in conformance with previous SKB practice, and with an approach that is widely adopted internationally, radiological impacts are calculated for constant unit release rates of radionuclides to the surface environment. By this approach, single values of Landscape Dose Factors (LDFs), i.e. dose rates for unit flux of each radionuclide, are derived using the method described below.

The rationale is that the single LDF values derived for each radionuclide can then be multiplied by radionuclide fluxes from the geosphere to obtain cautious estimates of dose rates to the most exposed group, as defined in the Swedish regulations /SSI 2005/:

One way of defining the most exposed group is to include the individuals that receive a risk in the interval from the highest risk down to a tenth of this risk. If a larger number of individuals are considered to be included in such a group, the arithmetic average of individual risks in the group should be used for demonstrating compliance with the criterion for individual risk in the regulations (i.e. 10^{-6} per year)…

If the group only consists of a few individuals, the criterion of the regulations of individual risks can be considered of being complied with if the highest calculated individual risk does not exceed 10^{-5} per year…

According to this definition, for demonstrating compliance with the regulations it is useful to estimate the size of the most exposed group, since the size will determine the risk criterion that should be used.

In the sections below, the method used for derivation of the LDF values for use in the SR-Can dose assessments is outlined. The LDF values obtained for the interglacial period and other climatic conditions are presented. Complementary, Dose Conversion Factors are given for the well, since, in the present work, the use of wells was considered separately. In future developments of the approach it should be possible to integrate exposures from the use of well water with other exposures in the landscape.

5.1 Method for derivation of the Landscape Dose Factors

The method applied for derivation of the LDF values for use in SR-Can consists of the following steps:

- **Step 1.** The radionuclide landscape models for Forsmark and Laxemar, described in Chapter 2, are used for estimating the time dynamics of the distribution and accumulation of radionuclides in the landscape (see Chapter 3) resulting from continuous unit release rates. The releases are directed to various landscape objects during the whole simulation period, in accordance with release fractions (Tables 3-2 and 3-3). The duration of the simulation period is different for different climatic scenarios (see Chapter 3).

- **Step 2.** The radionuclide concentrations in soils and waters obtained from the simulations in step 1 are used for estimating dose rates to individuals that expend all time and get the whole of their yearly demand of food from each landscape object (Chapter 4). For each radionuclide and time of evaluation, taken at every 1,000 years from the start of the simulation, a complementary cumulative distribution function (CCDF) was obtained by plotting the number of individuals against the dose rate for all landscape objects.
- **Step 3.** The CCDFs obtained in step 2 are fitted to lognormal distributions using the weighted means and standard deviations of the dose rates over all landscape objects (see Chapter 4) as parameters. The fitted distributions for each time and radionuclide are used to calculate the dose rate to the most exposed individual, i.e. the dose rate at which the fitted distribution gives one person exceeding that dose rate. As an example, the CCDF obtained for Ra-226 at Laxemar for the time period 6,000 AD is presented in Figure 5-1. The blue curve is the fitted log-normal distribution and the blue vertical line indicates the dose rate to the most exposed individual.
- **Step 4.** From the fitted distributions the dose rate to an individual representative of the most exposed group are determined. The most exposed group is defined, in accordance with the Swedish regulations /SSI 2005/, as the group including individuals receiving a dose rate between the maximum value (vertical red line in Figure 5-1) and one tenth of that value (vertical red line in Figure 5-1). The dose rate to a representative individual from this group was assumed to equal the arithmetic mean of the fitted lognormal distribution between the maximum dose rate and one tenth of the maximum. The size of the group (horizontal red line in Figure 5-1) is estimated by finding the fraction of the CCDF falling between the maximum and one tenth of the maximum.

A possible description of the most exposed group, identified from the CCDF in Figure 5-1, could be as follows: the most exposed group consists of around 100 people (horizontal red line in Figure 5-1) that spend all their time in the area delimited by objects 8 and 9 (terrestrial objects inside the two vertical lines and/or below the horizontal line) and get all their food (the whole yearly demand) from objects 4, 5, 8, 9 and 25. The group obtains most of the food from farming in objects 8 and 9 but a very small fraction of the yearly food demand is obtained from fishing at the coast (object 4) and in a running water (object 25). Additionally, the group receives a very small contribution to the dose rate from object 5 (a mire) by ingestion of food and external exposure.

- **Step 5.** The maximum of the dose rate to a representative individual over all time periods considered is determined for each radionuclide. These values were selected as LDF values for use in the SR-Can dose calculations.

Note that in a non-evolving landscape with a constant rate of input of a radionuclide, concentrations of that radionuclide in the various environmental media are expected to increase monotonically and, if the period of discharge is sufficiently long, would stabilise at constant values. Thus, in this context, the concept of equilibrium LDF values is potentially applicable. However, with an evolving landscape, as is represented in the landscape model used here, such a concept of equilibrium is not applicable. For example, radionuclides can accumulate in marine or lacustrine sediments, but give rise to an increased radiological impact when, as a consequence of land uplift, those sediments are converted to agricultural land. To allow for this, the LDF values used are the maximum values of dose rate that apply over the whole release period. This is a cautious assumption, as it implies that the geosphere release is sufficiently protracted for the maximum value to be realised. Furthermore, the maxima for different radionuclides occur at different times, so multiplying geosphere fluxes by these maximum values and summing the results, will over-estimate the overall dose rate, as when one radionuclide is exhibiting its maximum dose rate others will be exhibiting less than their maximum dose rates.

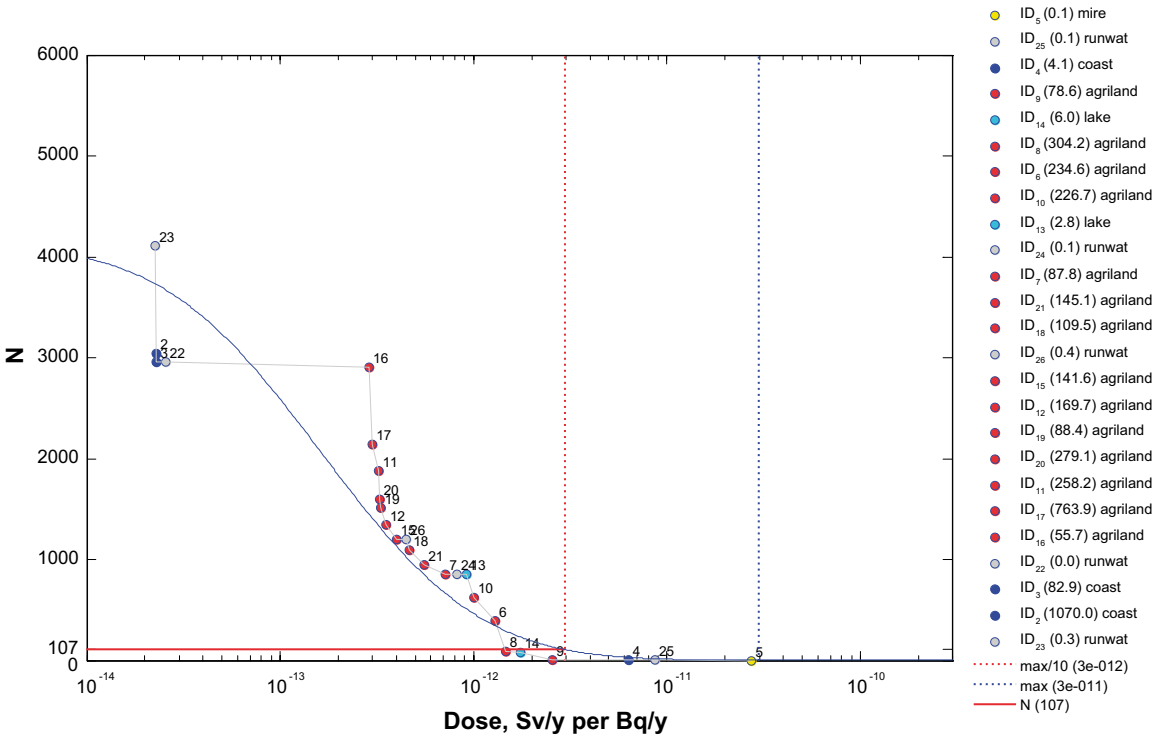

Figure 5-1. *Distribution of the Dose Conversion Factors for Ra-226 over landscape objects at Laxemar at year 6,000 AD of the interglacial period. The blue curve is the fitted log-normal distribution. The legend gives the object number, ecosystem type and number of people (in brackets) that can be sustained by each landscape object. The vertical blue line indicates the maximum value of the Dose Conversion Factor; the vertical red line indicates 1/10th of the maximum value. The horizontal line indicates the number of people in the most exposed group.*

5.2 Landscape Dose Factors for Forsmark

5.2.1 Landscape Dose Factors for the interglacial period

The values of the Landscape Dose Factors selected for the interglacial period are presented in Table 5-1, where Dose Conversion Factors for the well are also included. The values range from $6.6 \cdot 10^{-17}$ for Sm-151 to $6.9 \cdot 10^{-11}$ for Ag-108 m, i.e. six orders of magnitude. The maximum LDF values are observed at different times either during the Coastal or the Terrestrial Periods. The number of persons in the most exposed group also varies from radionuclide to radionuclide. The larger values of the number of people in the group are obtained for radionuclides with a predominant contribution of external exposure and/or inhalation to the dose rates, i.e. for Nb-94, Ag-108 m, Ho-166 m, etc. For some radionuclides, (uranium isotopes and actinides), the Dose Conversion Factors for the well are larger than the LDFs. In these cases the well DCFs are used in the risk estimations for SR-Can.

5.2.2 Landscape Dose Factors for other climatic conditions

The LDF values obtained for the glacial period and greenhouse conditions are presented in Table 5-2. The values for the glacial period are much lower than the values for the interglacial period, and the values for greenhouse conditions are up-to ten times lower (Figure 5-2). The LDF values for greenhouse conditions were higher than the values for the well for some radionuclides and lower for others. In the case of Forsmark, due to lack of time, calculations for the permafrost period were not carried out. These calculations will be carried out in future assessments.

Table 5-1. Landscape Dose Factor (LDF) values for an interglacial period at Forsmark expressed in units of Sv/y per Bq/y. N is the number of persons in the most exposed group, Year (AD) indicates the time when the maximum LDF is observed, DCF Well is the Dose Conversion Factor for the well and Maximum indicates which conversion factor has the highest value.

Radionuclide	LDF	N	Year (AD)	DCF Well	Maximum
Cl-36	1,3E–14	128	2,500	3.5E–15	LDF
Ca-41	1,7E–15	41	8,000	5.2E–16	LDF
Ni-59	4,2E–16	67	8,000	2.3E–16	LDF
Ni-63	4,2E–16	23	8,000	5.5E–16	Well
Se-79	6,7E–14	23	3,000	1.2E–14	LDF
Sr-90	1,7E–13	18	8,000	1.0E–13	LDF
Zr-93	6,3E–15	36	6,000	4.0E–15	LDF
Nb-94	1,3E–11	422	4,000	4.4E–14	LDF
Tc-99	4,4E–15	301	2,500	2.4E–15	LDF
Pd-107	2,0E–16	67	3,000	1.4E–16	LDF
Ag-108 m	6,9E–11	421	4,000	4.3E–13	LDF
Sn-126	4,2E–13	52	5,250	3.0E–14	LDF
I-129	5,5E–12	42	2,750	4.1E–13	LDF
Cs-135	6,3E–13	19	3,000	7.4E–15	LDF
Cs-137	1,2E–12	19	2,750	1.8E–13	LDF
Sm-151	6,6E–17	68	8,000	3.8E–16	Well
Ho-166 m	1,9E–11	422	4,000	1.3E–13	LDF
Pb-210	2,6E–12	22	8,000	2.5E–12	LDF
Ra-226	9,0E–12	22	8,000	1.0E–12	LDF
Th-229	6,9E–12	741	4,000	1.8E–12	LDF
Th-230	8,1E–12	64	10,000	7.8E–13	LDF
Th-232	1,3E–12	119	10,000	8.5E–13	LDF
Pa-231	4,0E–13	89	8,000	2.6E–12	Well
U-233	4,8E–14	414	3,000	1.9E–13	Well
U-234	6,8E–14	47	7,250	1.8E–13	Well
U-235	4,4E–14	414	3,000	2.0E–13	Well
U-236	4,4E–14	414	3,000	1.7E–13	Well
U-238	4,2E–14	414	3,000	1.6E–13	Well
Np-237	1,4E–13	129	3,000	4.2E–13	Well
Pu-239	1,4E–13	103	6,000	9.3E–13	Well
Pu-240	1,4E–13	98	5,500	9.3E–13	Well
Pu-242	1,4E–13	99	6,000	8.8E–13	Well
Am-241	1,6E–12	860	4,000	7.5E–13	LDF
Am-243	3,7E–12	1,033	4,000	5.5E–13	LDF
Cm-244	1,4E–13	113	5,500	4.4E–13	Well
Cm-245	1,7E–12	1,046	4,000	7.9E–13	LDF
Cm-246	1,0E–12	433	4,000	7.6E–13	LDF

Table 5-2. Landscape Dose Factor (LDF) values for a glacial period and greenhouse conditions at Forsmark expressed in units of Sv/y per Bq/y.

Radionuclide	LDF Glacial	LDF Greenhouse
Cl-36	1,40E–22	3,10E–16
Ca-41	7,10E–23	8,10E–16
Ni-59	1,20E–22	1,60E–16
Ni-63	2,40E–22	2,40E–16
Se-79	5,50E–20	2,80E–14
Sr-90	9,70E–21	9,00E–14
Zr-93	4,10E–22	5,40E–16
Nb-94	8,00E–22	1,50E–12
Tc-99	5,20E–21	4,00E–17
Pd-107	2,70E–24	6,50E–17
Ag-108 m	3,80E–21	9,40E–12
Sn-126	2,20E–20	4,10E–14
I-129	2,50E–19	5,90E–14
Cs-135	5,00E–21	7,60E–14
Cs-137	2,20E–20	3,10E–13
Sm-151	1,10E–23	5,00E–17
Ho-166 m	2,50E–22	2,40E–12
Pb-210	1,50E–19	1,00E–12
Ra-226	3,40E–18	6,80E–12
Th-229	4,90E–20	2,30E–12
Th-230	5,10E–20	8,10E–12
Th-232	2,30E–20	1,30E–12
Pa-231	2,60E–20	1,90E–13
U-233	2,60E–20	1,10E–14
U-234	2,50E–20	5,30E–14
U-235	2,40E–20	1,40E–14
U-236	2,40E–20	2,80E–15
U-238	2,30E–20	2,70E–15
Np-237	3,40E–20	1,00E–14
Pu-239	3,80E–20	2,90E–14
Pu-240	3,50E–20	2,60E–14
Pu-242	3,40E–20	3,00E–14
Am-241	6,50E–20	2,70E–13
Am-243	6,70E–20	1,40E–12
Cm-244	1,20E–20	7,80E–15
Cm-245	3,80E–20	2,30E–13
Cm-246	3,80E–20	1,20E–13

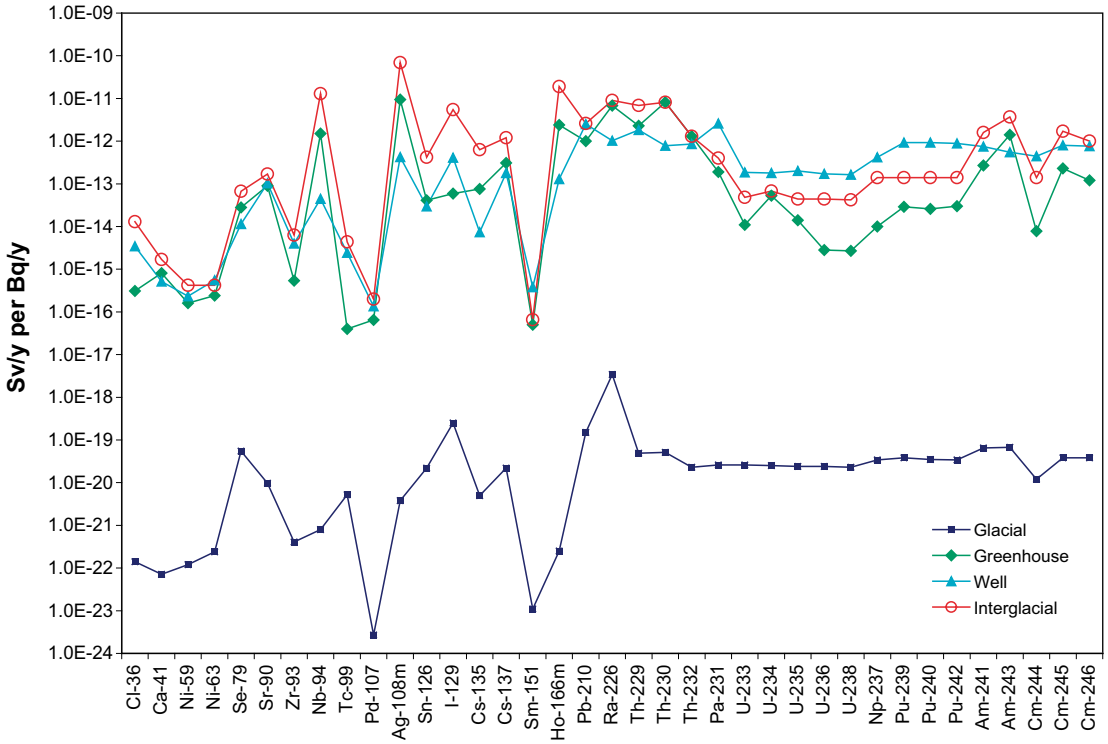

Figure 5-2. *The Landscape Dose Factors for the interglacial period, glacial period and greenhouse conditions and the Dose Conversion Factors for the well at Forsmark.*

5.3 Landscape Dose Factors for Laxemar

5.3.1 Landscape Dose Factors for the interglacial period

The values of the Landscape Dose Factors for the interglacial period are presented in Table 5-3, where Dose Conversion Factors for the well are also included. The values range from 2.0 10^{-16} for Sm-151 to 1.0 10^{-10} for Ag-108 m and Th-230, i.e. six orders of magnitude as for Forsmark. The maximum LDF values are observed at different times either during the Coastal or the Terrestrial Periods. The number of persons in the most exposed group also varies from radionuclide to radionuclide. As for Forsmark, the larger values of the number of people in the group are obtained for radionuclides with a predominant contribution of external exposure and/or inhalation to the dose rates: Nb-94, Ag-108 m, Ho-166 m, etc. For some radionuclides, uranium isotopes and actinides, the Dose Conversion Factors for the well were higher than the LDFs. In these cases, the well DCFs are used in the risk estimates for SR-Can.

5.3.2 Landscape Dose Factors for other climatic conditions

The LDF values obtained for the glacial period, the greenhouse variant and the two variants of permafrost conditions are presented in Table 5-4. The values for the Glacial Period are much lower than all other values. As for Forsmark, the values for greenhouse conditions were up-to about ten times lower than the values for the interglacial period (Figure 5-3). For most radionuclides, either the LDF value for the interglacial period or the DCF value for the well, were the highest among all calculated LDF values. Of the two calculated LDF values for permafrost conditions, the one with forest ecosystems showed about ten times higher values than the variant with mires.

Table 5-3. Landscape Dose Factor (LDF) values for an interglacial period at Laxemar expressed in units of Sv/y per Bq/y. N is the number of persons in the most exposed group, Year indicates the time when the maximum LDF value is observed, with positive values for the period AD and negative values for the period BC, DCF Well is the Dose Conversion Factor for the well and Maximum indicates which conversion factor has the higher value.

Radionuclide	LDF	N	Year	DCF Well	Maximum
Cl-36	8.1E–15	905	7,250 AD	3.7E–14	Well
Ca-41	5.6E–14	106	1,250 AD	5.5E–15	LDF
Ni-59	4.4E–15	147	750 AD	2.5E–15	LDF
Ni-63	3.8E–15	41	750 AD	5.9E–15	Well
Se-79	1.1E–12	28	750 AD	1.2E–13	LDF
Sr-90	8.0E–13	46	1,750 AD	1.1E–12	Well
Zr-93	2.9E–14	68	7,250 AD	4.3E–14	Well
Nb-94	2.1E–11	207	1,500 AD	4.7E–13	LDF
Tc-99	3.1E–15	520	750 AD	2.6E–14	Well
Pd-107	2.2E–15	133	1,250 AD	1.4E–15	LDF
Ag-108 m	1.0E–10	82	1,750 AD	4.5E–12	LDF
Sn-126	2.0E–12	35	2,250 AD	3.2E–13	LDF
I-129	1.6E–11	141	1,250 AD	4.4E–12	LDF
Cs-135	2.3E–12	18	1,750 BC	7.9E–14	LDF
Cs-137	4.1E–12	18	7,250 AD	1.9E–12	LDF
Sm-151	2.0E–16	221	750 AD	4.0E–15	Well
Ho-166 m	2.9E–11	100	1,500 AD	1.4E–12	LDF
Pb-210	5.3E–12	27	2,250 BC	2.7E–11	Well
Ra-226	4.7E–11	45	6,250 AD	1.1E–11	LDF
Th-229	3.2E–12	2,513	2,250 BC	2.0E–11	Well
Th-230	1.0E–10	60	6,250 AD	8.3E–12	LDF
Th-232	1.2E–12	2,513	2,250 BC	9.1E–12	Well
Pa-231	7.6E–12	556	8,250 AD	2.8E–11	Well
U-233	3.7E–13	140	750 AD	2.0E–12	Well
U-234	2.4E–12	78	6,250 AD	1.9E–12	LDF
U-235	3.2E–13	175	750 AD	2.1E–12	Well
U-236	3.4E–13	139	750 AD	1.8E–12	Well
U-238	3.2E–13	140	750 AD	1.8E–12	Well
Np-237	8.7E–13	135	750 AD	4.5E–12	Well
Pu-239	9.5E–13	241	750 AD	9.9E–12	Well
Pu-240	9.1E–13	234	750 AD	9.9E–12	Well
Pu-242	8.9E–13	258	750 AD	9.4E–12	Well
Am-241	6.3E–13	144	750 AD	8.0E–12	Well
Am-243	5.6E–12	198	1,750 AD	5.9E–12	Well
Cm-244	6.6E–14	1,116	2,250 BC	4.7E–12	Well
Cm-245	7.0E–13	337	750 AD	8.5E–12	Well
Cm-246	7.5E–13	215	750 AD	8.1E–12	Well

Table 5-4. Values obtained for Laxemar of the Landscape Dose Factors (LDFs) for a glacial period, greenhouse conditions and the two variants of permafrost conditions (expressed in units of Sv/y per Bq/y).

Radionuclide	LDF Glacial	LDF Greenhouse	LDF Permafrost Variant with forests	LDF Permafrost Variant with mires
Cl-36	6.3E–19	6.4E–15	1.3E–14	2.0E–15
Ca-41	9.9E–19	2.1E–15	2.1E–14	1.0E–15
Ni-59	1.2E–18	1.5E–15	4.6E–15	3.6E–16
Ni-63	7.7E–19	8.2E–16	3.2E–15	6.1E–16
Se-79	4.1E–16	6.2E–13	1.0E–12	1.9E–13
Sr-90	2.3E–17	1.3E–13	1.8E–12	1.6E–13
Zr-93	1.7E–18	2.7E–14	2.7E–14	6.0E–15
Nb-94	5.8E–18	1.3E–12	4.1E–12	3.2E–12
Tc-99	2.1E–17	2.8E–15	2.6E–15	7.0E–16
Pd-107	3.2E–20	3.8E–16	2.0E–15	1.5E–16
Ag-108 m	1.4E–17	4.5E–14	1.4E–11	1.3E–11
Sn-126	1.6E–16	1.3E–12	1.5E–12	4.0E–13
I-129	1.8E–15	2.1E–12	2.3E–12	5.7E–13
Cs-135	7.0E–17	2.1E–12	3.1E–12	1.8E–13
Cs-137	5.2E–17	3.1E–12	6.6E–12	1.8E–12
Sm-151	3.2E–20	2.0E–16	2.4E–16	6.5E–17
Ho-166 m	1.1E–18	6.0E–13	4.9E–12	4.5E–12
Pb-210	2.7E–16	2.6E–12	3.0E–12	2.8E–12
Ra-226	2.3E–14	9.9E–12	1.1E–10	1.4E–11
Th-229	1.9E–16	3.6E–12	2.9E–12	3.6E–12
Th-230	5.4E–15	2.2E–11	4.7E–10	1.9E–11
Th-232	9.1E–17	2.6E–12	1.8E–12	2.3E–12
Pa-231	1.1E–16	6.3E–12	7.6E–12	7.6E–13
U-233	3.5E–16	2.3E–13	1.7E–13	4.6E–14
U-234	3.6E–16	4.3E–13	9.2E–12	3.1E–14
U-235	3.3E–16	2.1E–13	1.5E–13	5.4E–14
U-236	3.3E–16	2.1E–13	1.6E–13	4.2E–14
U-238	3.1E–16	2.0E–13	1.5E–13	4.1E–14
Np-237	3.5E–16	7.2E–13	7.9E–13	2.1E–13
Pu-239	2.7E–16	1.1E–12	1.4E–12	3.4E–13
Pu-240	2.4E–16	1.0E–12	1.3E–12	3.3E–13
Pu-242	2.5E–16	1.0E–12	1.3E–12	3.2E–13
Am-241	2.3E–16	1.3E–13	5.0E–13	2.8E–13
Am-243	2.6E–16	3.0E–13	1.4E–12	2.1E–12
Cm-244	2.0E–17	1.7E–14	7.0E–14	6.5E–14
Cm-245	1.5E–16	8.4E–13	1.2E–12	4.1E–13
Cm-246	1.5E–16	7.3E–13	1.1E–12	3.4E–13

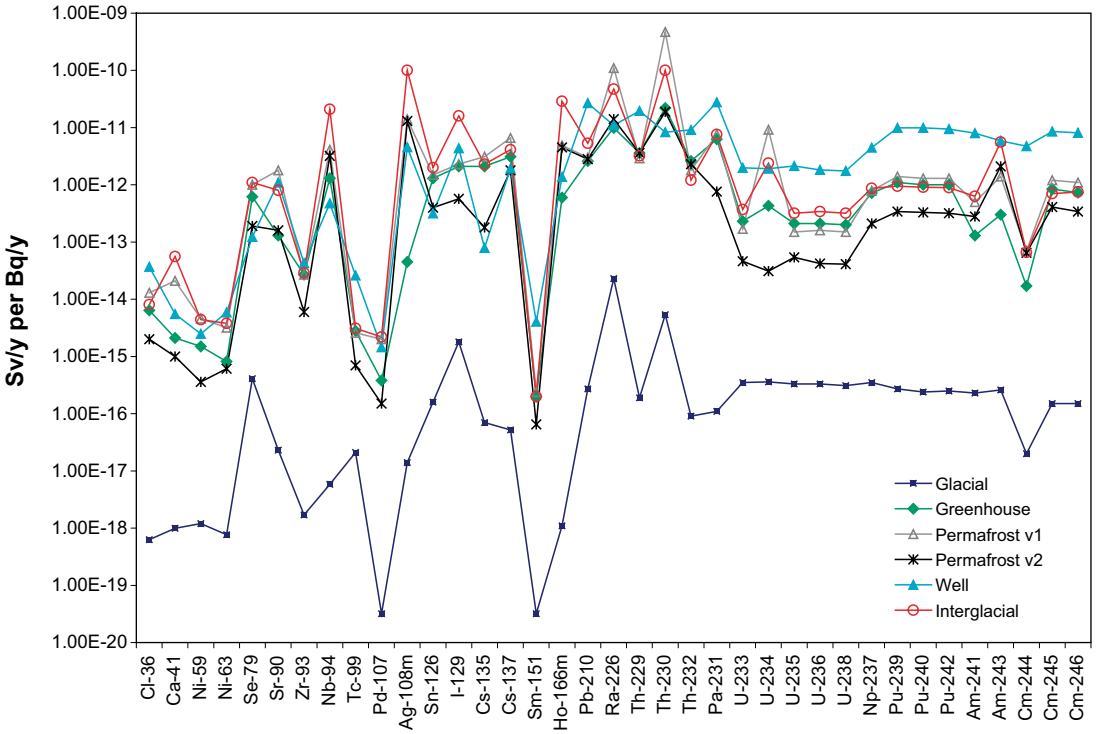

Figure 5-3. *Landscape Dose Factors for the interglacial period, glacial period, permafrost (two variants) conditions, greenhouse conditions and Dose Conversion Factors for the well at Laxemar.*

6 Discussion and conclusion

6.1 Sensitivity and uncertainty analysis

A sensitivity analysis of the ecosystem models was carried out to identify which parameters had the largest effect on the simulation endpoints of interest. The endpoints considered were the fraction of the release that is retained in the ecosystem, the activity concentrations in soil, water and sediments, and the dose rates from external exposure, inhalation, and ingestion of water and food; evaluated at different times after the start of the simulations. The simulations were carried out for constant unit input rate of radionuclides to the ecosystems. A detailed description of the sensitivity study is given in /Avila 2006a/. Some of the most relevant results, from the analysis of the uncertainties for the LDF values, are discussed below. For the marine ecosystems, the results are presented for an accumulation time of 10,000 years, which is close to the duration of the Sea Period at Forsmark. For other ecosystems, the results are presented for an accumulation time of 3,000 years, which is close to the assumed average lifetime of these ecosystems in the landscape models.

Sensitivity analysis method

The sensitivity analysis was carried out using the Morris method /Morris 1991/ implemented in the software package Eikos /Ekström and Broed 2005/. With this method it is possible to screen out parameters that have negligible effects and to rank the parameters by their effect on the endpoints of interest. It is also possible to identify which parameters have non-linear effects or are involved in interactions with other parameters.

The Morris method uses two sensitivity measures: the mean (μ) and the standard deviation (σ) of the elementary effects of the parameters. The elementary effects are obtained from simulations using "one factor a time" sampling for evaluating the impact of changing one parameter at a time. Both sensitivity measures have to be taken into account when interpreting the results. To facilitate this, the estimated mean and standard deviation can be displayed in the (σ, μ) plane (see examples in Figures 6-2 to 6-5).

The mean (μ) measures the effect that each single parameter has on the endpoint of interest and the sign of the effect. The standard deviation (σ) is a measure of non-linearity in the effects of the parameters and/or of parameter interactions. A parameter with a high absolute value of the mean and a low standard deviation will have a strong effect on the endpoint independently of the value of other parameters. The effect could either positive (if $\mu > 0$) or negative. On the other hand, a parameter with a low absolute value of the mean and a high standard deviation will have a low direct effect on the endpoint, but significant indirect effects through interactions with other parameters. For ranking the parameters, it is convenient to use a sensitivity index (SI) that combines both the mean and the standard deviation. The SI used in this study was the square root of the sum of the squared mean and standard deviation, normalised by the sum over all parameters and expressed in percent units.

6.1.1 Sensitivity analysis of the aquatic ecosystem models

Sensitivity analysis of the sea model

The parameters with the largest effect on the fraction of the releases retained in a sea ecosystem (Table 6-1) are the velocity of the upward water fluxes in the sea bottom (v_bottom), which has a negative effect and the fraction of accumulation bottoms (acc_bottom), with a positive effect. As the distribution coefficient increases there is a decrease in the effect of the parameter v_bottom and an increase in the effect of the parameter acc_bottom. There are strong interactions between the parameters and non-linearity in their effects. The effects of the distribution

coefficient for the suspended sediments on the retained fraction are negligible, whereas the distribution coefficients in the bottom sediments (K_d_sed) have positive effects that decrease with the increase of the K_d_sed. For Am-241, the effect of the K_d_sed is practically negligible because of its high value in combination with the relatively short half-life of this radionuclide.

The parameter v_bottom has a positive effect on the dose rates, while the parameter acc_bottom has a negative effect (Figure 6-1). The same type of dependency with the K_d_sed as for the retained fraction is observed. The effects of the K_d_sed on the dose rates are negative and weaker than the effects on the retained fraction. The bioaccumulation factors (BF_coast) have a positive effect on the dose rates, of approximately the same magnitude as the effects of the v_bottom and acc_bottom. Other parameters have a weak direct effect on the dose rates, which decreases as the distribution coefficients increase. For example, for Ra-226 (see Figure 6-1b) the estimated mean of all parameters except the acc_botttom and the BF_coast is close to zero.

It is worth noting that the parameter "retention time", which determines the residence time of the radionuclides in the water compartments has a negligible effect on the retained fractions and the dose rates.

Sensitivity analysis of the lake model

The catchment's area (area_catchment) and the time to sorption equilibrium (Tk) have a negative effect on the retained fraction of releases (Table 6-2). Note, however, that the Tk was varied within a very wide range of values (from 10^{-5} to 10^{-1} years). Judging from the high standard deviations, these parameters have either non-linear effects and/or strong interactions with other parameters. The area of the lake (lake_area), its mean depth (mean depth) and the distribution coefficient for the suspended sediments (K_d_lake) have a positive effect, especially for radionuclides with high K_d values. Note that the fraction of accumulation bottoms has negligible effects on the retained fraction. This parameter was varied in a very narrow range with values close to one, reflecting the assumptions made in the calculations for Laxemar. Other parameters identified as important (Table 6-2) affect the retained fractions mainly through interactions with other parameters.

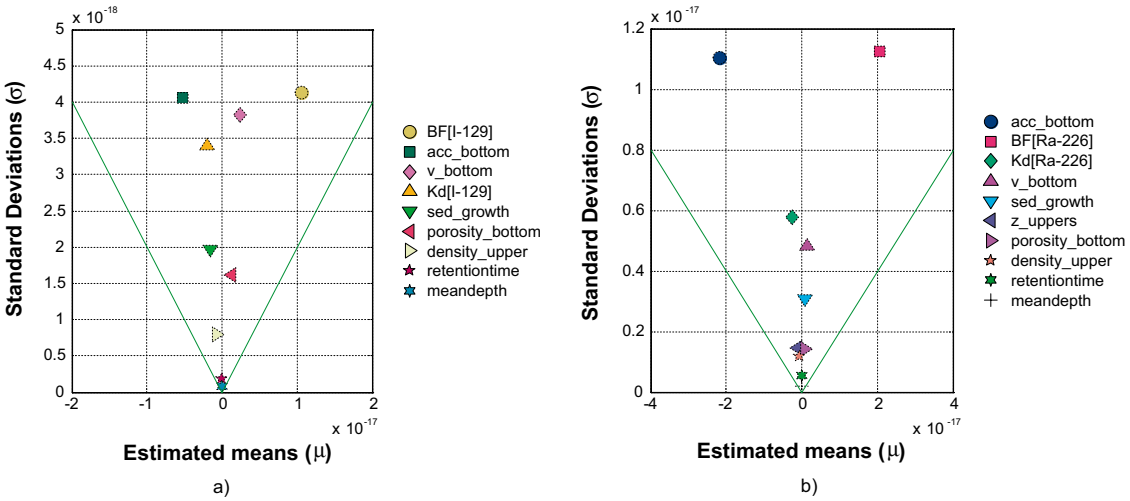

Figure 6-1. *Mean and standard deviation of the elementary effects of the model parameters on the dose rates from I-129 (a) and Ra-226 (b) at 10,000 years after the start of a continuous release to the sediments of a sea ecosystem.*

Table 6-1. Sensitivity Indexes, expressed in %, obtained with the Morris method as a combined measure of the effect of the parameters of the sea model on the fractions of the releases retained in the ecosystem (RF) and the total dose rates (Dose).

Parameter	Cl-36		Ni-59		Se-79		Tc-99		I-129		Cs-135		Ra-226		Pu-239		Am-241	
	RF	Dose	RF	Dose	RF	Dose	RF	Dose	RF	Dose	RF	Dose	RF	Dose	RF	Dose	RF	Dose
acc_bottom	29.1	15.2	61.9	36.0	67.4	46.9	27.7	13.5	34.7	20.2	54.6	35.1	56.0	35.9	56.6	37.8	65.0	39.1
v_bottom	23.3	13.9	9.9	5.8	7.5	3.8	24.3	10.7	19.7	14.0	11.4	8.0	10.2	7.4	11.6	7.5	0	0
porosity_bottom	12.3	6.3	6.9	2.8	4.9	2.7	12.6	6.7	12.1	7.7	7.1	4.9	4.1	2.4	5.1	3.0	0	0
sed_growth	11.3	6.6	5.6	3.2	5.5	2.9	11.6	5.9	10.7	6.4	8.2	6.5	7.2	4.7	5.6	3.9	18.8	13.1
density_upper	5.2	3.3	2.9	1.6	2.8	1.8	5.2	2.9	4.9	3.2	3.5	2.3	3.0	1.8	2.9	2.1	0	0
z_uppers	0	0	1.6	0	2.0	0	0	0	0	0	1.2	0	4.9	2.6	1.5	0	13.5	8.0
BFcoast		43.2	0	42.3	0	35.6	0	49.0	0	35.1	0	32.6	0	34.7	0	35.8	0	37.1
Kd_sed	18.2	10.0	11.2	6.8	9.8	4.7	18.1	9.5	17.3	12.2	13.9	9.2	14.6	9.2	16.6	8.3	1.3	0

Table 6-2. Sensitivity Indexes, expressed in %, obtained with the Morris method as a combined measure of the effect of the parameters of the lake model on the fractions of the releases retained in the ecosystem (RF) and the total dose rates (Dose).

Parameter	Cl-36		Ni-59		Se-79		Tc-99		I-129		Cs-135		Ra-226		Pu-239		Am-241	
	RF	Dose	RF	Dose	RF	Dose	RF	Dose	RF	Dose	RF	Dose	RF	Dose	RF	Dose	RF	Dose
Area catchment	20.5	55.4	19.3	24.1	20.5	31.4	8.8	39.7	22.9	42.2	18.2	32	18.4	25.2	14.8	33.4	21	35
Part conc	14.2	0	5.8	2.3	7.3	2.7	7.6	2.8	6	2.1	5.5	1.6	5.8	1.9	5.4	1.8	6.2	4.2
Lake area	10.4	0	16.6	24.8	15.5	10.5	6.1	2	6.9	2.8	14.7	10.4	17	21.4	18.2	25.1	14.5	16.3
Mean depth	8.8	0	9.7	3.8	11.4	7.5	5	0	4.5	1.2	12.8	5.6	11.3	3.9	13.6	1.6	13	6.1
V bottom	5.7	0	2.4	1.7	2.1		9	4.2	4.1	1.1	2.1	0	1.4	0	1.7	5.1	0	0
runoff	2.3	13.4	3.2	4.8	3.5	9.3	2.5	9.2	1.5	11.9	3.3	9.1	3.1	6.2	2.8	0	3.5	7.2
V sinking	1.9	0	7.2	0	8.3	1.3	7.1	3.3	6.8	1.6	7.1	1.9	6.8	0	6.1	0	7.7	0
Sed growth	0	0	3.4	2.4	0	0	6.2	0	2	0	3.1	0	4	0	2.3	0	0	0
BF_lake	0	28.6	0	21.8	0	17.1	0	25.8	0	23.5	0	16.5	0	11.7	0	9.9	0	13.2
Kd_lake	4.8	0	12	4.6	8.3	4.5	5.3	1.1	4.7	2.1	15.8	7.1	9.8	7.3	17.5	15.2	14	12.1
Kd_peat	0	0	2.2	0	1.2		12.8	1.8	6.2	1.4	2.7	0	4.5	9.9	2.8	0	0	0
Tk	29.9	1.4	16.5	7.9	20.1	12.9	29	8.2	33.6	9.8	13.4	14.3	16.5	10.9	13.6	5.2	19	5.2

The parameter (area_catchment) has a dominant negative effect on the dose rates (Figure 6-2), which is more accentuated for the most mobile radionuclides. For radionuclides with high K_d,the lake_area and the K_d_lake have also a moderate negative effect on the dose predictions. The parameter with the highest positive effect on the dose rates is the bioaccumulation factor (BF_lake), which is more pronounced for mobile radionuclides. Other parameters identified as important (Table 6-2), including the distribution coefficients, affect the dose rates mainly through interactions with other parameters.

6.1.2 Sensitivity analysis of the terrestrial ecosystem models

For the terrestrial ecosystems models, the results of the sensitivity analysis are presented only for the dose rates. For the forest and mire models, the dose rates are directly proportional to the retention fractions. Hence, the parameters that are important for the dose rates are also important for the retention fractions, with the exception of the transfer factors to biota. Agricultural systems seldom receive direct releases and, when they do receive releases will retain only a very small fraction.

Sensitivity analysis of the agricultural land model

For radionuclides that give exposure mainly by food ingestion (Cl-36, Ni-59, Se-79, I-129, Cs-135 and Ra-226), the concentration ratio for agricultural food (CRagriland) has the largest positive effect on the dose rates (see Table 6-3). For radionuclides with low concentration ratios (Pu-239 and Am-241), exposures by inhalation dominate and, therefore, the parameter with the highest positive effect is the dust concentration. Other parameters with a positive although lesser effect are the upward water fluxes in soil (Fsads and Fdsts). The parameters catchment area (area_cathment), area of agricultural land (area_agriland), depth of the deep soil (z_deeps), runoff and percolation have a negative effect. The effect of the distribution coefficient (K_d_soil) is complex. For some radionuclides (Cl-36, Tc-99, Se-79 and Ra-226) the effect is positive, whereas for others the effect is negative. This is illustrated in Figure 6-3 for I-129 and Ra-226. The strength of the effect of the K_d_soil also varies between radionuclides. There is no clear relationship between the sign of the effect and the K_d_soil values, which suggests that there are strong interactions with other parameters such as the concentration ratio for agricultural land (CRagriland).

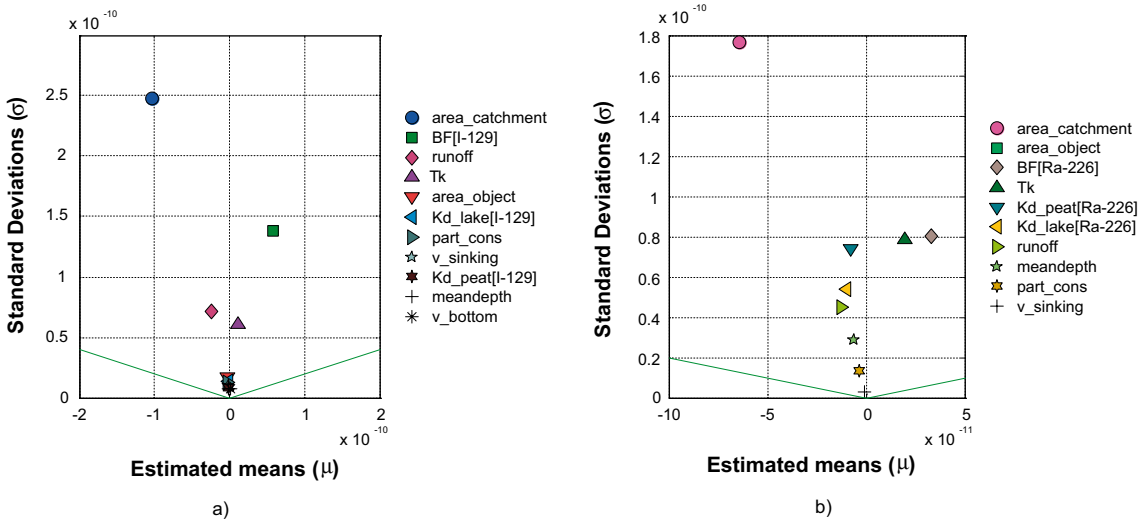

Figure 6-2. *Mean and standard deviation of the elementary effects of the model parameters on the dose rates from I-129 (a) and Ra-226 (b) at 3,000 years after the start of a continuous release to the sediments of a lake.*

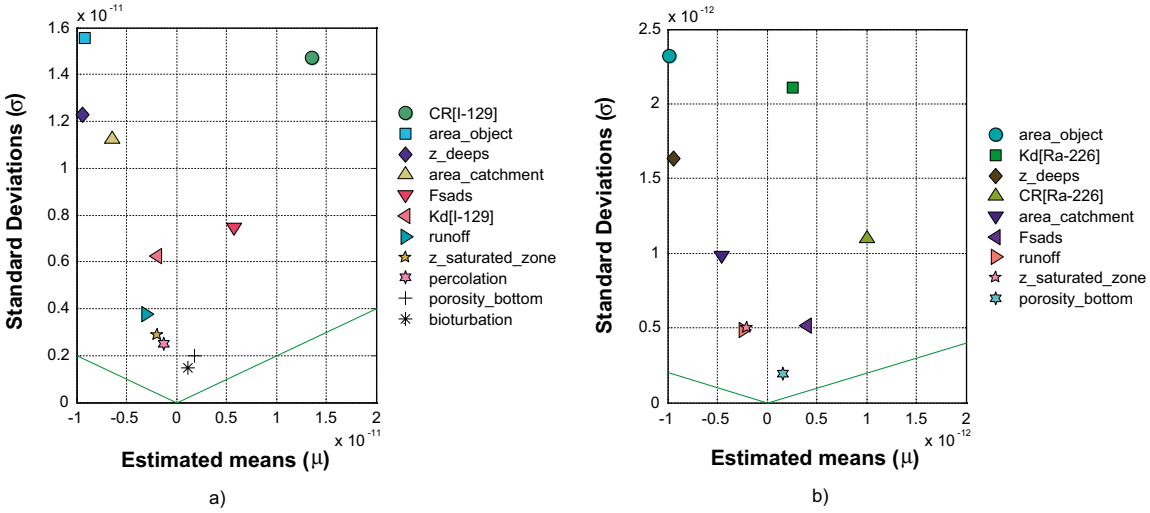

Figure 6-3. *Mean and standard deviation of the elementary effects of the model parameters on the dose rates from I-129 (a) and Ra-226 (b) at 3,000 years after the start of a continuous release to the saturated zone of an agricultural land.*

Sensitivity analysis of the forest model

The concentration ratio to forest food (CRforest), the distribution coefficient (K_d_forest_soil) and the dust concentration (for Pu-239) are the only parameters with a positive effect on dose rates in a forest ecosystem (Table 6-4 and Figure 6-4). The effects of these parameters are of approximately equal size and there seem to be interactions between them. The catchment area and the area of the forest have strong negative effect on the dose rates, whereas other important parameters (Table 6-4) seem to influence mainly through interactions.

Sensitivity analysis of the mire model

The effect of the parameters of the mire model (Table 6-5 and Figure 6-5) on the dose rates was similar to the effects observed for the forest ecosystems. The effect of the catchment's area was somewhat greater for the mire than for the forest.

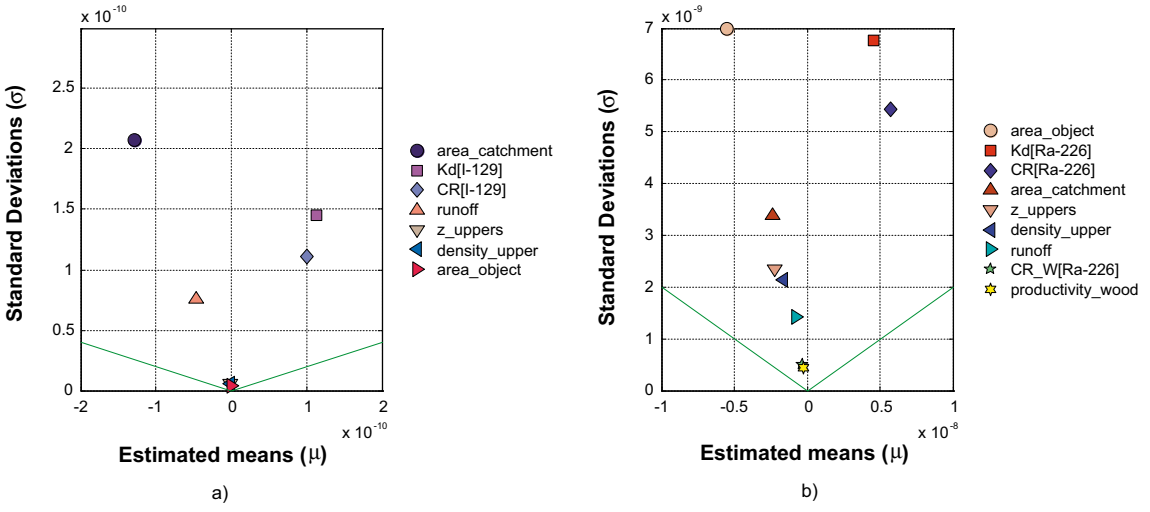

Figure 6-4. *Mean and standard deviation of the elementary effects of the model parameters on the dose rates from I-129 (a) and Ra-226 (b) at 3,000 years after the start of a continuous release to the rooting zone of the forest.*

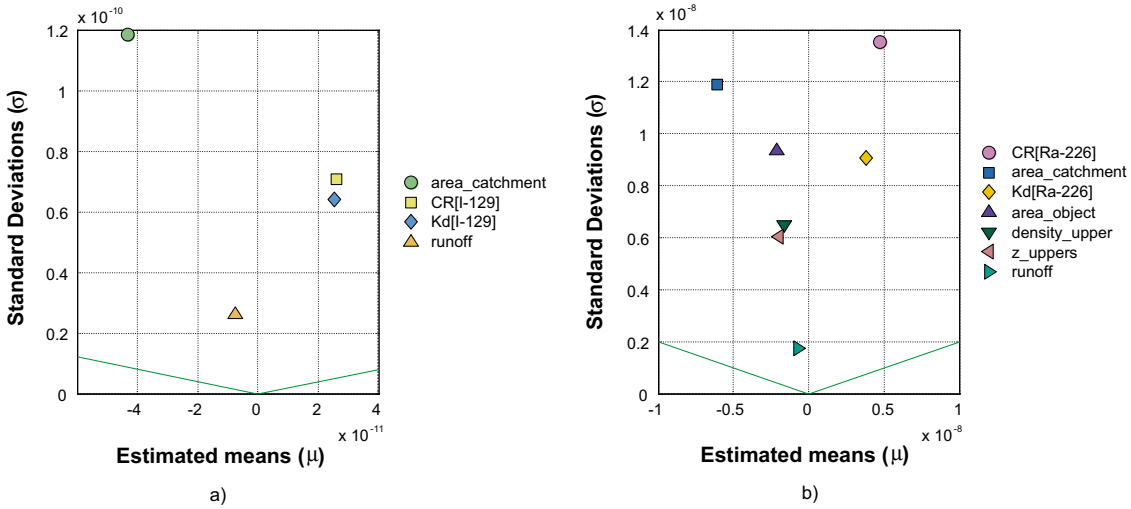

Figure 6-5. *Mean and standard deviation of the elementary effects of the model parameters on the dose ratess from I-129 (a) and Ra-226 (b) at 3,000 years after the start of a continuous release to a mire.*

Table 6-3. Sensitivity Indexes, expressed in %, obtained with the Morris method as a combined measure of the effect of the parameters of the agricultural land model on the total dose rates.

Parameter	Cl-36	Ni-59	Se-79	Tc-99	I-129	Cs-135	Ra-226	Pu-239	Am-241
area_agriland	0	14.7	12.3	0	17.8	26.0	21.4	17.4	12.5
z_deeps	0	14.7	7.5	0	15.2	20.1	16.0	17.8	21.2
area_catchment	28.2	11.1	17.8	22.2	12.8	7.5	9.2	0	8.1
Fsads	10.8	7.7	9.4	0	0	8.9	5.6	7.2	0
Fdsts	5.2	0	0	6.7	0	0	0	0	0
runoff	11.7	0	9.3	16.9	0	0	0	0	0
percolation	6.6	0		9.2	0	0	0	0	0
Dust concentration	0	0	0	0	0	0	0	15.1	7.3
CRagriland	17.7	22.4	15.4	17.0	19.7	9.2	18.0	0	0
Kd_soil	16.4	10.3	12.9	14.9	6.4	13.8	12.6	16.0	22.4

Table 6-4. Sensitivity Indexes, expressed in %, obtained with the Morris method as a combined measure of the effect of the parameters of the forest model on the total dose rates.

Parameter	Cl-36	Ni-59	Se-79	Tc-99	I-129	Cs-135	Ra-226	Pu-239	Am-241
area_catchment	29.1	13.1	11.2	34.8	35.7	5.3	10.8	5.2	0
area_forest	0	21.4	21.9	0	0	24.7	23.4	27.7	34.5
runoff	12.5	5.8	6.5	13.4	13.1	0	0	0	0
z-uppers	0	7.5	6.2	0	0	10.7	8.4	15.2	17.9
forest soil density	0	0	0	0	0	5.5	7.1	8.6	10.3
Dust concentration	0	0	0	0	0	0	0	15.6	0
CRforest	25.9	21.2	20.4	28.1	21.9	0	20.7	8.2	27.6
Kd_forest_soil	30.3	25.6	15.7	23.4	26.9	13.2	21.4	17.1	0
CRwood	0	0	0	0	0	7.7	0	0	0

Table 6-5. Sensitivity Indexes, expressed in %, obtained with the Morris method as a combined measure of the effect of the parameters of the mire model on the the total dose rates.

Parameter	Cl-36	Ni-59	Se-79	Tc-99	I-129	Cs-135	Ra-226	Pu-239	Am-241
area_catchment	38.4	36.9	24.7	47.7	42.4	40.0	21.5	31.0	0
area_mire	0	0	5.5	0	0	0	15.5	9.2	22.6
runoff	8.3	9.6	5.8	12.1	9.1	11.5	0	0	0
z-uppers	0	11.7	9.6	0	0	0	10.2	18.6	6.2
peat density	0	6.0	13.5	0	0	0	10.8	0	0
Dust concentration	0	0	0	0	0	0	0	10.1	0
CRmire	31.4	22.4	21.8	11.0	25.3	19.0	23.1	6.2	30.4
Kd_peat	21.9	12.3	19.0	29.2	23.2	23.8	15.8	18.2	32.1

6.1.3 Uncertainty in the LDF values

From the sensitivity analysis of the ecosystem models, the parameters with the highest impact on the fraction of the releases retained in the objects and the dose rates were identified. It is reasonable to expect that uncertainties in the LDF values will be determined by the uncertainty in these parameters. However, the influence of the parameters is not linear and depends on multiple parameter interactions. For the landscape model, interactions between objects have also to be taken into account. Hence, for elucidating the effects of the parameter uncertainties on the uncertainties in the LDF values, it is necessary to make sensitivity studies for the landscape models as a whole, similar to the studies reported above for the ecosystem models. Such studies have not yet been carried out to the needed extent.

Preliminary analyses have been done by varying important parameters one-at-a-time within their range of variation while keeping other parameters at their best estimate values. Example are shown in Figures 6-6 and 6-7 where the results for three simulation runs of the Laxemar landscape model are presented, with all K_d values in all landscape objects set at: i) the best estimate values, ii) the minimum values and iii) the maximum values.

The effect of the K_d on the maximum total dose rate was different in different periods, with practically no effect in some periods (for example the Sea Period) and pronounced effects in other periods, particularly in periods when ecosystem shifts occur. The effect of the K_d was also different for different radionuclides. For example, much larger variations were observed for Ra-226 than for I-129. Note that, in the case of Ra-226 in some periods, the effect of an increase in K_d can be even negative. The application of the method outlined in Chapter 5 for derivation of LDFs to these three cases yields the values in Table 6-6. It can be observed that the maximum LDF values are obtained at different time periods for the different cases and that the values differ by about one order of magnitude. Similar responses of the LDFvalues were observed when making one-at-a-time variations of other important parameters.

When evaluating the uncertainties in the LDF values, it should be taken into account that several conservative assumptions have been made in the dose calculations and for selection of the LDF values that are used in SR-Can. As was shown in Chapter 4, the estimated maximum dose rates were close to the maximum values of the latent dose rates. This means, that for a given retained fraction of the releases, the dose rates per unit release rate cannot be much higher that the LDF values. Several of the radionuclide-independent parameters that have the highest effect on the retained fractions, such as the area of the objects, the catchment areas, the run-off, depend on the topography of the sites, which is fairly predictable. During the Sea Period, the fraction of accumulation bottoms and the water velocity in the bottom sediments has the largest effect on the retained fraction of the releases. These parameters are more difficult to estimate. However, as was shown in Chapter 4, the accumulation during the Sea Period does not seem to have a significant impact on the maximum dose rates and the LDF values.

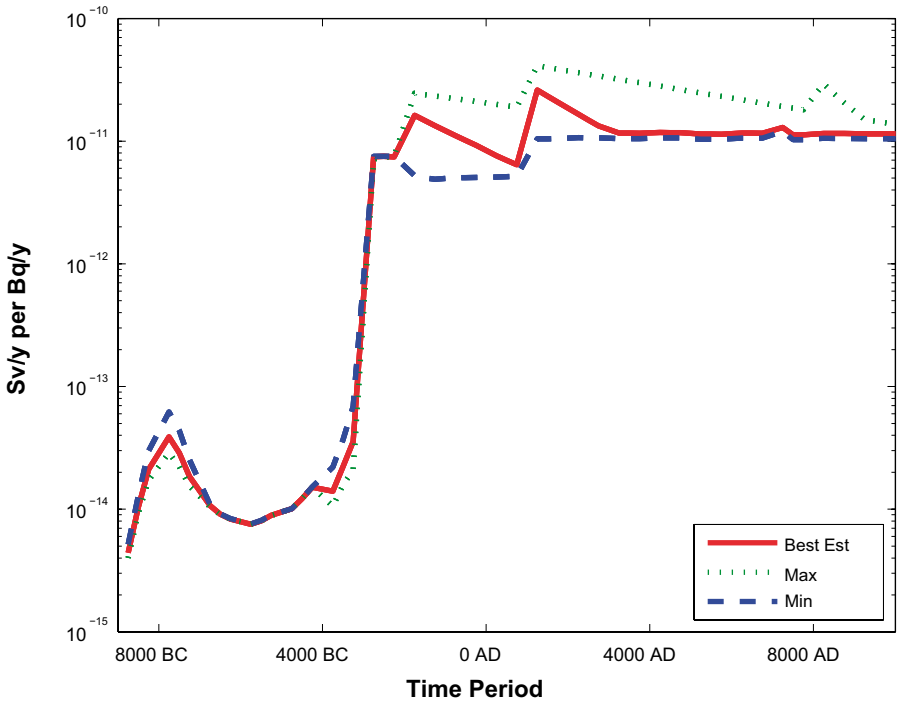

Figure 6-6. *Maximum values of the total dose rates for a continuous release rate of 1 Bq/y of I-129 to the Laxemar landscape assuming different Kd values in all objects (best estimate, maximum and minimum values).*

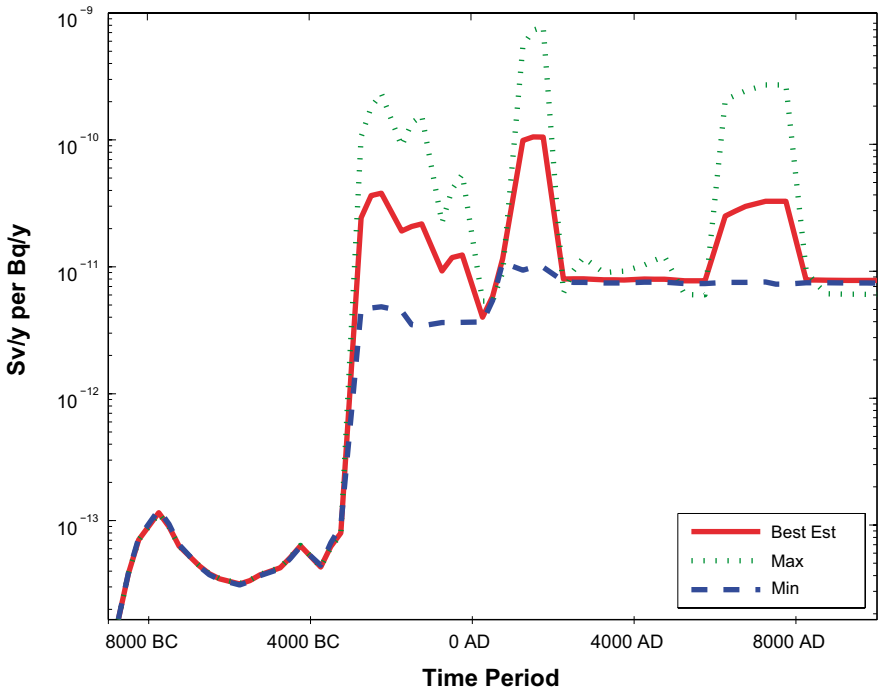

Figure 6-7. *Maximum values of the total dose rates for a continuous release rate of 1 Bq/y of Ra-226 to the Laxemar landscape assuming different Kd values in all objects (best estimate, maximum and minimum values).*

Table 6-6. Landscape Dose Factor values (Sv/y per Bq/y) for three study cases at Laxemar, assuming different sets of K_d values in all landscape objects: best estimate, minimum and maximum values. The number of people (N) and the period (Time AD) when the maximum is observed are also indicated.

Radionuclide	Case	LDF	N	Time AD
I-129	Best Est	1.6e–11	142	1,250
	Min	2.3e–12	179	7,250
	Max	2.7e–11	174	1,250
Ra-226	Best Est	2.6e–11	30	1,500
	Min	1.9e–12	127	750
	Max	8.3e–11	16	1,750

6.2 Comparison of results for Forsmark and Laxemar

The LDF values obtained for Laxemar were usually higher than the values for Forsmark (Figure 6-8). For most radionuclides the differences were within a factor of 10 and are, as explained in Section 6.1, within the range of uncertainty of the LDF values. For a few radionuclides (Ca-41, Se-79, Th-230, Pa-231 and U-234) more than a factor of 10 differences were observed. In the cases of Ca-41 and Pa-231, published data on the radionuclide-dependent parameters are lacking and the assumed values might be inconsistent. It should be noted that these radionuclides have shown negligible contributions to overall doses in previous safety assessments /SKB 1999, 2004/. The higher values for Se-79 at Laxemar might be explained by a large difference in distribution coefficients between ecosystems assumed for this radionuclide (see Figure 2-6), in combination with differences in the ecosystem types prevailing in Forsmark and Laxemar. Both U-234 and Th-230 have daughter radionuclides with important contributions to the Dose Factors. The radionuclides in the same decay chain may have the maximum dose rate values at different time and landscape objects, which may lead to additional differences between the LDF values, as these are taken as maximum values over the whole simulation period (see Chapter 5).

The differences in LDF values observed between Laxemar and Forsmark seem to be due to landscape differences between these sites. The area at Laxemar that can be potentially affected by the discharges is about ten times smaller than the potentially affected area at Forsmark. This is dictated by differences in the topographic conditions at the sites, which are rather well understood and predictable. The retention of radionuclides in both areas is similar, which in combination with a smaller area at Laxemar leads to higher concentrations and consequently higher dose rates at this site. Note that the capacity of the wells is lower in Laxemar than in Forsmark, which leads to lower Dose Conversion Factors for the well. The well capacity is influenced by the hydrology of the sites, which is strongly influenced by topography.

There are also important differences between Forsmark and Laxemar in the characteristics of the sea bottom sediments. It appears that accumulation bottoms, which favour radionuclide retention in sediments, are more predominant in Laxemar than in Forsmark.

The results of the sensitivity analysis confirm the explanations given above. Parameters related to the topography and hydrology of the sites have large effects on the dose rate predictions by affecting fluxes through the landscape objects (drainage areas, run-off) and radionuclide retention (fraction of accumulation bottoms).

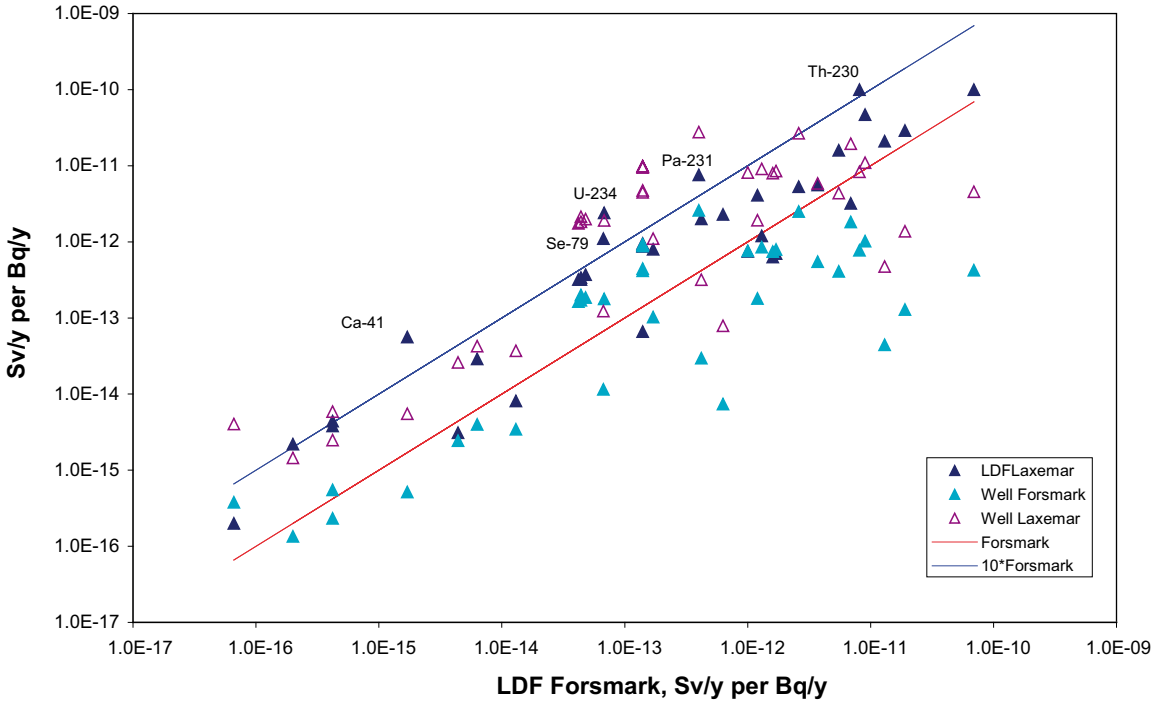

Figure 6-8. *Comparison of LDF values for Forsmark in the interglacial period with LDF values for Laxemar and the DCF for a well at Forsmark and Laxemar. The red line indicates perfect agreement with the LDF for Forsmark, whereas the blue line shows values that are exactly 10 times higher.*

When comparing the results obtained for Forsmark and Laxemar, it should be also taken into account that several conservative assumptions were introduced in the process of derivation of the LDF values, such as selecting the highest LDF value over all time periods, assuming that the whole radionuclide inventory that is accumulated in sea and lake sediments becomes available when these shift to terrestrial ecosystems, etc. The degree of conservative in these assumptions might be different for Laxemar and Forsmark. A more comprehensive comparison of the sites will need to be done on the basis of realistic assessments using the information being collected in the site investigation programmes.

6.3 Comparison of the results for different climatic conditions

The LDF values for the glacial period were substantially lower than all other calculated LDF values. This difference is easily explained by a higher dilution in the sea objects. This is consistent with the lower values observed for the Sea Period in the interglacial scenario. The observed differences in LDF values between the interglacial period and the permafrost and greenhouse conditions fall within the uncertainty ranges of the estimations. For the permafrost conditions two alternative cases were considered, one with mires and another with forests prevailing in the landscape. The differences between these cases were also within a factor of ten. The differences in LDF values observed for different climatic conditions are of the same order of magnitude as the differences observed between Laxemar and Forsmark, which, as discussed above, can consider being within the uncertainty ranges.

It should be noted that the landscape models used for other climatic conditions were not developed and justified in the same systematic way as for the interglacial period. Also, the same ecosystem models were used without taking into account possible effects of climatic changes on the processes and parameter values. Hence, there are larger conceptual uncertainties associated with these cases, requiring further examination.

6.4 Conclusion

In this report Landscape Dose Factors (LDFs) have been derived for the Forsmark and Laxemar sites using dynamic models of the transport and accumulation of radionuclides in the landscape. The LDFs estimate effective dose rates to the most exposed population group per unit release of activity from a HLW repository. The LDFs can be used in the SR-Can assessments for demonstrating compliance with the Swedish regulatory criteria. The methodology applied for derivation of the LDFs allows estimating the size of the potentially most exposed groups. This information can be used for selecting the appropriate risk criterion, following the recommendations given in the regulations.

The derivation of the LDFs was focused on the interglacial period within a glacial cycle, where the highest exposures are expected to occur. The values were derived for a hypothetical situation with releases starting from the beginning of the current interglacial period. It is assumed that these results are applicable to other interglacial periods as well. Further, it was established by variant calculations that assuming the start of releases to coincide with the beginning of an interglacial period constitutes the conservative calculation case.

Calculations of LDF values were also carried out for glacial and permafrost periods, as well as for greenhouse conditions. Results obtained for an interglacial period were found to be bounding for the other climatic regimes. Additionally, Dose Conversion Factors were calculated for the case of releases to a well assuming that the radioactive plume is completely intercepted by the well. For some radionuclides these Dose Conversion Factors were higher than the LDF values. In those cases, it is recommended to use the well DCF for the risk estimations.

A number of limitations of the approach that has been previously used (the EDF approach) for derivation of the Dose Conversion Factors, have been overcome in deriving the LDFs in the study presented here. In particular, the connection of the different ecosystems within the landscape is considered and the fluxes of radionuclides through these interconnected ecosystems are taken into account. This also allows estimation of the significance of simultaneous exposures to several ecosystems and other relevant interactions between ecosystems, such as the use of a lake for irrigation of agricultural lands.

A major improvement as compared to previous approaches relates to the fact that now temporal changes in the biosphere driven by land rise, ecosystem succession, climate change, etc are explicitly addressed. These changes usually are difficult to model when considering generic ecosystems in isolation, since the relevant processes act on a landscape scale. They can, however, be consistently taken into account based on the dynamic landscape model presented here using the data obtained from the site investigation programmes.

A further benefit of the dynamic landscape model lies in the fact that important exposure parameters, such as the size of exposed groups and drainage areas, can be consistently estimated within the landscape model and do not have to be treated as generic input parameters to the modelling, as in the case of considering isolated ecosystems.

The results of the simulations performed with the landscape models show that a few objects at both sites dominate the radiation exposure. It is not possible to choose any single object or ecosystem type that would provide a conservative estimate for all radionuclides. As a consequence, simpler models for deriving LDFs can be defined, but determining their detailed design in terms of landscapes can only be done in a reliable way by using the dynamic landscape model as basis.

A preliminary uncertainty analysis of the methods applied for derivation of the LDFs was carried out, based on sensitivity analyses of the ecosystem models and on studies of the effects of one-at-at-time variation of the parameters on the predictions with the landscape models. However, a more complete analysis of the uncertainties needs to be performed, taking also into account conceptual and scenario uncertainties. Some needed improvements of the models have already been identified. In particular, the models applied are not suitable for C-14, which is an important radionuclide. The work for adaptation of the models to C-14 has already started based on studies of the carbon cycling being carried out as part of the site investigation programmes. It is expected that this will result in a general improvement of the models for all radionuclides considered.

7 References

Avila R, 2006a. The ecosystem models used for dose assessments in SR-Can. SKB-R-06-81, Svensk Kärnbränslehantering AB.

Avila R, 2006b. Model of the long-term transfer of radionuclides in forests. SKB TR-06-08, Svensk Kärnbränslehantering AB.

Avila R, Bergström U, 2006. Methodology for calculation of doses to man and implementation in Pandora. SKB R-06-68, Svensk Kärnbränslehantering AB.

Bergström U, Nordlinder S, Aggeryd I, 1999. Models for dose assessments. Modules for various biosphere types**.** SKB-TR 99-14, Svensk Kärnbränslehantering AB

Bergström U, Barkefors C, 2004. Irrigation in dose assessments models. SKB R-04-26, Svensk Kärnbränslehantering AB.

BIOMASS, 2003. Reference biospheres for solid radioactive waste disposal. IAEA Biomass-6 (Vienna: IAEA).

Chen Q, Kowe R, Jones A, Oatway W, Mobbs S F, Watson S, 2004. Development and application of a generic biosphere tool for dose assessments. NRPB EA/13/2004 (Chilton: NRPB).

Ekström P-A, Broed R, 2006. Sensitivity Analysis Methods and a Biosphere. Test Case Implemented in Eikos. Posiva Working Report 2006-31.

Jones J, Vahlund F, Kautsky U, 2004. Tensit – a novel probabilistic simulation tool for safety assessments Tests and verifications using biosphere models. SKB TR-04-07, Svensk Kärnbränslehantering AB.

Kumblad L, Gilek M, Naeslund B, Kautsky U, 2003. An ecosystem model of the environmental transport and fate of carbon-14 in a bay of the Baltic sea, Sweden. Ecological modeling 166(2003): 193–210.

Morris M D, 1991. Factorial sampling plans for preliminary computational experiments. Technometrics 33 (2):239–245.

Sheppard SC, Sheppard MI, Bird GA, 1999. Critical load modelling: Cd, Cu, Ni, Pb, Zn and As emitted by smelters and refineries. Report for Environment Canada adressing CEPA PSL2 assessments (Ottawa).

SKB, 1999. Deep repository for spent fuel SR 97 - Post closure safety. SKB TR-99-06 Main Report volume I and II, Svensk Kärnbränslehantering AB.

SKB, 2004. Interim main report of the safety assessment SR-Can. SKB TR-04-11, Svensk Kärnbränslehantering AB.

SKB, 2006a. The Biosphere at Forsmark. SR-Can. SKB R-06-82, Svensk Kärnbränslehantering AB.

SKB, 2006b. The Biosphere at Laxemar. SR-Can. SKB R-06-83, Svensk Kärnbränslehantering AB.

SKB, 2006c. Climate and climate related conditions – report for the safety assessment SR-Can. SKB TR-06-23, Svensk Kärnbränslehantering AB.

SKB, 2006d. Long-term safety for KBS-3 repositories at Forsmark and Laxemar – a first evaluation. Main Report of the SR-Can project. SKB TR-06-09, Svensk Kärnbränslehantering AB.

SSI, 2005. Statens strålskyddsinstituts allmänna råd om tillämpning av föreskrifterna (SSI FS 1998:1) om skydd av människors hälsa och miljön vid slutligt omhändertagande av använt kärnbränsle och kärnavfall. SSI FS 2005:5, Statens strålkyddsinstitut.

Åstrand P-G, Jones J, Broed R, Avila R, 2005. Pandora technical description and user guide. Posiva Working Report 2005-64.

Appendix A

Parameter values used in the models

Table A-1. Parameter values used in the Coastal model. For Forsmark and Laxemar, the minimum and maximum values over all time periods and objects are shown. The best estimate is the average value over all landscape objects. Generic values are default values provided in the initial description of the models.

Parameter	Unit	Site	Best estimate	Min	Max
Area, *area_object*	m^2	Generic	1.12E+07	1.12E+07	1.12E+07
		Forsmark	2.26E+11	6.13E+05	4.53E+11
		Laxemar	3.52+E06	3.20E+05	6.72E+06
Mean depth, *meandepth*	m	Generic	9.50E+00	8.50E+00	1.05E+01
		Forsmark	7.26E+01	1.33E+00	1.44E+02
		Laxemar	1.74E+01	7.66E+00	2.72E+01
Suspended matter, *sea_part_cons*	kg/m^3	Generic	5.00E–03	2.50E–03	1.00E–02
		Forsmark	2.76E–04	1.3E–04	5.5E–04
		Laxemar	3.0E–04	1.1E–04	6.0E–04
Water retention time, *retentiontime*	year	Generic	2.11E–03	1.05E–03	4.22E–03
		Forsmark	1.32E+01	5.36E–04	2.64E+01
		Laxemar	4.1E–02	1.15E–03	8.90E–02
Fraction accumulation bottoms, *acc_bottom*		Generic	2.20E–01	0.00E+00	4.40E–01
		Forsmark	5.00E–01	0.00E+00	1.20E+00
		Laxemar	4.08E–01	9.56E–03	9.50E–01
Fine particles settling velocity, *sea_v_sinking*	m/year	Generic	3.65E+02	7.30E+01	7.30E+03
		Forsmark	6.00E+01	4.00E+00	1.17E+02
		Laxemar	6.02E+01	3.65E+00	1.17E+02
Half-time to reach sorption *equilibrium, Tk*	year	Generic	1.00E–03	1.00E–05	1.00E–01
		Forsmark	1.00E–03	1.00E–05	1.00E–01
		Laxemar	1.00E–03	1.00E–05	1.00E–01
Sediment growth rate, *sea_sed_growth*	m/year	Generic	1.00E–02	4.00E–03	2.00E–02
		Forsmark	1.00E–03	0.00E+00	1.00E–02
		Laxemar	6.45E–04	8.07E–05	1.21E–03
Depth of upper sediment, *z_uppers*	m	Generic	2.00E–02	5.00E–03	5.00E–02
		Forsmark	2.00E–02	5.00E–03	5.00E–02
		Laxemar	1.00E–01	5.13E–03	1.00E–01
Advection velocity, *sea_v_bottom*	m/year	Generic	–	–	–
		Forsmark	1.60E–02	1.31E–02	2.08E–02
		Laxemar	5.80E–02	3.00E–04	3.69E–01
Density, *sea_density_upper*	kg/m^3	Generic	–	–	–
		Forsmark	767	92	1,700
		Laxemar	1,550	700	1,800
Porosity, *sea_porosity_bottom*	–	Generic	–	–	–
		Forsmark	6.00E–01	2.50E–01	8.50E–01
		Laxemar	4.90E–01	1.00E–01	9.00E–01
Standard sediment density, *standardSedDensity*	kg/m^3	Generic	–	–	–
		Forsmark	1,867	1,600	2,100
		Laxemar	1,867	1,600	2,100
Standard sediment density, *standardSedDepth*	m	Generic	–	–	–
		Forsmark	1	–	–
		Laxemar	1	–	–

Table A-2. Parameter values used in the lake model. For Forsmark and Laxemar, the minimum and maximum values over all time periods and objects are shown. The best estimate is the average value over all landscape objects. Generic values are default values provided in the initial description of the models.

Parameter	Unit	Site	Best estimate	Min	Max
Area, *area_object*	m^2	Generic	1.06E+06	8.00E+05	1.25E+06
		Forsmark	1.51E+06	6.09E+04	2.96E+06
		Laxemar	3.27E+05	4.00E+02	6.54E+05
Area of watershed, *area_catchment*	m^2	Generic	–	–	–
		Forsmark	8.75E+08	1.95E+05	1.75E+09
		Laxemar	3.20E+07	6.53E+05	6.33E+07
Mean depth, *meandepth*	m	Generic	1.70E+00	1.40E+00	2.10E+00
		Forsmark	3.06E+00	1.65E–01	5.96E+00
		Laxemar	2.84E+00	6.99E–04	5.68E+00
Suspended matter, *lake_part_cons*	$kg/(m^3)$	Generic	2.00E–03	5.00E–04	5.00E–03
		Forsmark	5.90E–04	2.28E–04	1.64E–03
		Laxemar	6.30E–04	2.20E–04	8.60E–04
Water retention time, *rettime*	year	Generic	2.40E–01	1.70E–01	3.10E–01
		Forsmark			
		Laxemar			
Fraction accumulation bottoms, *lake_acc_bottom*		Generic	2.00E–01	0.00E+00	1.00E+00
		Forsmark	9.80E–01	5.00E–01	1.00E+00
		Laxemar	8.85E–01	7.80E–01	0.99E+00
Fine particle settling velocity, *lake_v_sinking*	m/year	Generic	1.83E+02	3.65E+01	3.60E+03
		Forsmark	1.83E+02	3.65E+01	3.60E+03
		Laxemar	1.83E+02	3.70 E+01	3.60E+03
Half–time to reach *sorption equilibrium, Tk*	year	Generic	1.00E–03	1.00E–05	1.00E–01
		Forsmark	1.00E–03	1.00E–05	1.00E–01
		Laxemar	1.00E–03	1.00E–05	1.00E–01
Sediment growth rate, *lake_sed_growth*	m/year	Generic	4.00E–03	1.00E–03	1.00E–02
		Forsmark	6.55E–04	3.50E–04	1.35E–03
		Laxemar	1.33E–03	4.44E–07	2.67E–03
Depth of sediment, *lake_z_uppers*	m	Generic	2.00E–02	5.00E–03	5.00E–02
		Forsmark	8.39E–02	0.00E+00	4.00E–01
		Laxemar	6.00E–02	2.00E–02	1.00E–01

Table A-3. Parameter values used in the forest model. For Forsmark and Laxemar, the minimum and maximum values over all time periods and objects are shown. The best estimate is the average value over all landscape objects. Generic values are default values provided in the initial description of the models.

Parameter	Unit	Site	Nominal	Min	Max
Yearly production of tree wood, *forest_productivity_wood*	kg (dw)/m^2/year	Generic	1.80E–01		
		Forsmark	2.69E–01	0.00E+00	1.43E+00
		Laxemar	2.65E–01	1.36E–02	7.94E–01
Yearly production of tree leaves, *forest_productivity_leaf*	kg (dw)/m^2/year	Generic	8.00E–02	5.00E–02	1.70E+00
		Forsmark	2.30E–01	0.00E+00	1.12E+00
		Laxemar	2.11E–01	5.00E–02	1.70E+00
Yearly production of understorey plants, *forest_productivity_understory*	kg (dw)/m^2/year	Generic	8.00E–02	2.00E–02	2.50E–01
		Forsmark	1.24E–01	4.36E–02	2.02E–01
		Laxemar	8.92E–02	2.00E–02	2.50E–01
Tree wood biomass	kg (dw)/m^2	Generic	5.10E+00	2.20E+00	5.50E+01
		Forsmark	8.21E+00	0.00E+00	4.33E+01
		Laxemar	5.05E+00	5.33E–02	1.90E+01
Tree leaf biomass	kg (dw)/m^2	Generic	5.00E–01	2.00E–01	7.00E+00
		Forsmark	3.99E–01	0.00E+00	2.11E+00
		Laxemar	6.11E–01	1.24E–03	2.21E+00
Understorey biomass	kg (dw)/m^2	Generic	8.00E–02	2.00E–02	2.50E–01
		Forsmark	1.17E–01	8.40E–02	1.53E–01
		Laxemar	6.03E–02	3.30E–02	2.82E–01
Yearly fractional loss of tree wood biomass, *forest_loss_wood*	1/year	Generic	4.00E–03		
		Forsmark	4.00E–03	2.00E–04	1.20E–02
		Laxemar	4.00E–03	–	–
Yearly fractional loss of tree leaf biomass for coniferous trees, *forest_loss_leaves*	1/year	Generic	2.50E–01		
		Forsmark	2.20E–01	1.00E–01	2.70E–01
		Laxemar	2.20E–01	–	–
Yearly fractional loss of understorey plants biomass, *forest_loss_understory*	1/year	Generic	1.00E+00		
		Forsmark	3.58E–01	5.91E–02	6.46E–01
		Laxemar	7.74E–01	3.80E–01	1.00E+00
Yearly fractional loss of litter biomass, *forest_loss_litter*	1/year	Generic	1.60E–01		
		Forsmark	4.00E–01	2.05E–02	1.20E+00
		Laxemar	4.00E–01	1.00E–01	7.00E–01

Table A-4. Parameter values used in the agricultural model. For Forsmark and Laxemar, the minimum and maximum values over all time periods and objects are shown. The best estimate is the average value over all landscape objects. Generic values are default values provided in the initial description of the models.

Parameter	Unit	Site	Best estimate	Min	Max
Runoff, *runoff*	m^3/m^2/year	Generic	2.50E–01	2.00E–01	3.00E–01
		Forsmark	2.26E–01	7.53E–02	6.78E–01
		Laxemar	1.54E–01	9.50E–02	1.88E–01
Depth of top soil, *Agricultural Land_z_uppers*	m	Generic	2.50E–01	2.00E–01	3.00E–01
		Forsmark	2.50E–01	2.00E–01	3.00E–01
		Laxemar	2.50E–01	2.00E–01	3.00E–01
Depth of deep soil, *z_deeps*	m	Generic	–	–	–
		Forsmark	8.83E+00	1.35E+00	1.63E+01
		Laxemar	5.50E+00	8.85E–01	1.01E+01
Depth of saturated zone, *Agricultural Land_z_saturated_zone*	m	Generic	3.00E+00	2.00E+00	4.00E+00
		Forsmark	1.00E+00		
		Laxemar	3.00E+00	2.00E+00	4.00E+00
Top soil porosity, *Agricultural Land_porosity_upper*	m^3/m^3	Generic	5.00E–01	4.00E–01	6.00E–01
		Forsmark	3.33E–01	2.60E–01	4.20E–01
		Laxemar	5.00E–01	4.00E–01	6.00E–01
Deep soil porosity, *Agricultural Land_porosity_bottom*	m^3/m^3	Generic	5.00E–01	4.00E–01	6.00E–01
		Forsmark	2.085E–01	1.40E–1	2.98E–01
		Laxemar	5.00E–01	4.00E–01	6.00E–01
Saturated zone porosity, *Agricultural Land_porosity_saturated_zone*	m^3/m^3	Generic	3.00E–01	2.50E–01	4.00E–01
		Forsmark	3.00E–01	2.50E–01	4.00E–01
		Laxemar	3.00E–01	2.50E–01	4.00E–01
Soil density, *Agricultural Land_density*	kg/m^3	Generic	2,650	2,600	2,700
		Forsmark	1,867	1,600	2,100
		Laxemar	2,650	2,600	2,700
Bioturbation, *Agricultural Land_bioturbation*	$kg/(m^2$/year	Generic	2.00E+00	1.00E+00	3.00E+00
		Forsmark	2.00E+00	1.00E+00	3.00E+00
		Laxemar	2.00E+00	1.00E+00	3.00E+00
Water transport from groundwater to deep soil, *Agricultural Land_Fsads*	m^3/m^2/year	Generic	2.00E–01	1.00E–01	3.00E–01
		Forsmark	1.97E–01	1.01E–02	5.90E–01
		Laxemar	2.00E–01	1.00E–01	3.00E–01
Water transport from deep soil to topsoil, *Agricultural Land_Fdsts*	m^3/m^2/year	Generic	1.00E–01	5.00E–02	2.00E–01
		Forsmark	5.70E–02	2.90E–03	1.71E–01
		Laxemar	1.00E–01	5.00E–02	2.00E–01
Water transport from deep soil to groundwater, *Agricultural Land_percolation*	m^3/m^2/year	Generic	2.00E–01	1.00E–01	3.00E–01
		Forsmark	5.97E–01	3.80E–01	8.50E–01
		Laxemar	2.00E–01	1.00E–01	3.00E–01
Area of agricultural land, *area_object*	m^2	Generic	5.30E+05	4.00E+05	6.25E+05
		Forsmark	1.31E+06	3.34E+04	2.59E+06
		Laxemar	2.09E+05	2.84E+04	3.89E+05
Drainage area, *area_catchment*	m^2	Generic	–	–	–
		Forsmark	1.14E+07	1.95E+05	2.26E+07
		Laxemar	1.84E+06	3.22E+05	3.35E+06
Half–time to reach sorption equilibrium, *Tk*	year	Generic	1.00E–03	1.00E–05	1.00E–01
		Forsmark	1.00E–03	1.00E–05	1.00E–01
		Laxemar	1.00E–03	1.00E–05	1.00E–01
Soil removal, *Agricultural Land_loss_soil*	m^3/m^2/year	Generic	5.00E–03	2.00E–03	2.00E–02
		Forsmark	5.00E–03	2.00E–03	2.00E–02
		Laxemar	5.00E–03	2.00E–03	2.00E–02

Table A-5. Parameter values used in the mire model. For Forsmark and Laxemar, the minimum and maximum values over all time periods and objects are shown. The best estimate is the average value over all landscape objects. Generic values are default values provided in the initial description of the models.

Parameter	Unit	Site	Best estimate	Min	Max
Runoff, *runoff*	m^3/m^2/year	Generic	2.50E–01	2.00E–01	3.00E–01
		Forsmark	2.26E–01	7.53E–02	6.78E–01
		Laxemar	1.54E–01	9.55E–02	1.88E–01
Density, *mire_density_upper*	kg (dw)/ m^3	Generic	1.00E+02	8.00E+01	1.20E+02
		Forsmark	1.00E+02	8.00E+01	1.20E+02
		Laxemar	1.00E+02	3.00E+01	1.90E+02
Porosity, *mire_porosity_upper*	m^3/m^3	Generic	9.00E–01	8.00E–01	9.50E–01
		Forsmark	8.90E–01	7.60E–01	9.50E–01
		Laxemar	9.26E–01	8.70E–01	9.80E–01
Peat depth, *z_uppers*	m	Generic	–	7.00E–01	2.10E+00
		Forsmark	8.72E–01	8.39E–02	1.66E+00
		Laxemar	9.13E–01	1.67E–01	1.66E+00
Mire area, *area_object*	m^2	Generic	–	2.40E+05	1.25E+00
		Forsmark	1.13E+06	1.83E+04	2.24E+06
		Laxemar	3.33E+05	1.64E+04	6.49E+05
Drainage area, *area_catchment*	m^2	Generic	–	–	–
		Forsmark	5.21E+07	1.95E+05	1.04E+08
		Laxemar	3.20E+07	6.53E+05	6.33E+07
Half–time to reach sorption equilibrium, *Tk*	year	Generic	1.00E–03	1.00E–05	1.00E–01
		Forsmark	1.00E–03	1.00E–05	1.00E–01
		Laxemar	1.00E–03	1.00E–05	1.00E–01